2020

An Oxidative Stress Response Mechanism By The Vibrio Cholerae Arcab Two-Component System

Yitian Zhou
University of Pennsylvania

An Oxidative Stress Response Mechanism By The Vibrio Cholerae Arcab Two-Component System

Abstract

Vibrio cholerae, the causative agent of the infectious disease, cholera, is a water-borne pathogen with a dynamic lifestyle across physical environments of different oxygen levels with various sources of oxidative stress. The anaerobic respiratory control (ArcB/A) two-component system is a global regulator that facilitates the transition between different electron transport strategies with respect to the redox environment. Upon sensing a more anoxic quinone pool at the inner membrane, the histidine kinase ArcB activates the response regulator ArcA's regulatory functions by phosphorylation. ArcA has been reported in Escherichia coli and Salmonella enterica to be important for oxidative stress resistance, yet the mechanism through which ArcA respond to this stress is unknown. Here we report ArcA's regulatory functions being partially retained in V. cholerae upon oxidative stress. This additional redox-sensing under oxidative stress is dependent on a cysteine residue, C173, in ArcA's C-terminal DNA-binding domain. C173 is crucial in sustaining in vitro oxidative stress challenges and during colonization of mouse intestines. Phosphorylation state analysis indicates that ArcA phosphorylation is compromised when V. cholerae is challenged by oxidative stress. In vitro biochemical assays reveal that C173- dependent oxidation initiates ArcA binding to DNA containing an ArcA-binding motif. C173- dependent oxidation also promotes ArcA-ArcA interaction, similar to the effect from a microaerobic induction of ArcA. ArcA C173 is conserved in various Gram-negative pathogens. In vitro oxidative stress challenges and human intestinal epithelial cell invasion experiments with S. enterica further underscore the importance of ArcA C173 for bacterial survival. This work uncovers a new post-translational modification, oxidation, in addition to phosphorylation, that serves as an activating signal for ArcA. The redox response from ArcA couples a stress response to other ArcA-mediated transitions for an adaptation to a new environment, demonstrating theintricacy of bacterial stress responses and their close association to basic energy metabolism.

Degree Type

Dissertation

Degree Name

Doctor of Philosophy (PhD)

Graduate Group

Biology

First Advisor

Jun Zhu

Second Advisor

Mark Goulian

Keywords

cysteine, redox sensing, stress response, transcriptional regulation, two-component system, Vibrio cholerae

Subject Categories

Biochemistry | Microbiology | Molecular Biology

AN OXIDATIVE STRESS RESPONSE MECHANISM BY THE VIBRIO CHOLERAE ARCAB TWO-COMPONENT SYSTEM

Yitian Zhou

A DISSERTATION

in

Biology

Presented to the Faculties of the University of Pennsylvania

in

Partial Fulfillment of the Requirements for the

Degree of Doctor of Philosophy

2021

Supervisor of Dissertation

_____

Jun (Jay) Zhu

Professor of Microbiology

Graduate Group Chairperson

_____

Brian Gregory, Associate Professor of Biology

Dissertation Committee

Mark Goulian, Charles and William L. Day Distinguished Professor in the Natural Sciences

Mechthild Pohlschröder, Professor of Biology

Sunny Shin, Associate Professor of Microbiology

Fevzi Daldal, Professor of Biology

ACKNOWLEDGMENT

I am greatly thankful for my advisor Dr. Jun (Jay) Zhu, for all the patience and guidance he offered for my project and my development as a researcher. He embodies a passionate and resilient scientist with the strongest work ethic imaginable. I am greatly appreciative of my thesis committee members, Drs. Mark Goulian, Mechthild (Mecky) Pohlschröder, Sunny Shin, and Fevzi Daldal, for their scientific insights as well as tremendous mental and material support.

Dr. Jane Schulte has lent me her keen scientific perspectives, calm demeanor, and company during writing sessions. Drs. Ann Stock and Rong Gao have kindly provided key insights for the structural predictions of ArcA. I thank Dr. Patricia Kiley for her work that has laid the foundation of ArcA functions and our encouraging conversations when she visited Penn.

I am fortunate to have incredible colleagues from the Zhu lab, Drs. Jiandong Chen, Qinqin Pu, Guijuan Hao, Yuning Wang, Hanghang Jiang, Jessie Larios Valencia, I-Ji Jung, Reyna Garcia, Tao Liu and Zachariah L. Lee, who bestowed their guidance and company. I am also indebted to the Goulian lab members, Drs. Manuela Roggiani, Srujana Samhita (Sam) Yadavalli, Jeffrey Carey, Annie Chen, and Josie Ni for valuable joint lab meeting discussions and generous training.

This work would not have been possible without the material and technical support from Drs. Stefan Steimle, Rahul Kohli, Igor Brodsky, Wei-Jun Qian, Hsin Yao Tang, Michael Cory, Charlie Mo Ye, Meghan Wynosky, Kushol Gupta, and Haoyang Zeng. I am grateful to Sheila Mayne for her coaching in academic writing, and Dr. Shelley Payne for her intricate work in *V. cholerae* iron metabolism. I want to express my gratitude for the friendship and kindness from Johnson Pavilion 2nd floor, especially from Marisa Egan, Narwar Naseer, Dr. Xin Liu, Mark Boyer, the rest of the Shin lab, Drs. Yonggang Pei, Wei Liu, and Ranran Wang. I appreciate the hard work from Sandra Wiggins, Don Pijak, Michael Ma, Rene Larraga, Craig Gary, Hussen Aleyu and Mike Leeke who sustained the operations of our facilities. I thank Drs. Christina Scheel and Margaret Race for motivating me in the pursuit of Ph.D.- level knowledge to tackle major challenges in the world.

I am sincerely grateful for my loving parents, Yulan Long and Geoff Hammond. They are my rock and my cheerleaders. The unconditional trust they have in me is truly empowering. The friendship and adventures shared with Kylen Ford, Xuxu Song, Qingqing Long, Run Jin, Chunmiao Wang, Changru Tu, Tianyuan Shi, Shilin Zhou, Chan Jin, and others have nourished my mental wellbeing. Colleen Gasiorowski and Dr. Robin Sherwood have built a sense of belonging for

biology graduate students like myself. I am lucky to have shared joyous bioball memories with fellow biology graduate students. I want to commend my cohort, Drs. Janani Saikumar, Alexandra Brown, Haoran Zhou, Alex Berry, Jean Rosario, and Un-sa Lee, for their accomplishment and our support for each other. Lastly, I credit Greg Yeutter for the immense multifaceted support throughout the duration of this thesis work. I am greatly motivated by the kindness and love of Greg and his family.

I want to acknowledge the mice that sacrificed their lives for this study and for science in general. Finally, I would like to dedicate this thesis to the amazing prokaryotes that inspired this work and keep inspiring me in my everyday human life. As demonstrated by this work and the bacteria signaling literature, prokaryotes are remarkable observers of the world with the wide scope of signals they perceive. They are not fixated on a specific form of signal like we are with visual signals. Consider the methods we use in this study, for example, almost all the experiments involve the experimenter converting a process to a visual readout, whether it is originally an invisible process like a post-translational modification on a protein, or a more abstract kind like the expression of a gene. To convince fellow humans, we resort to describing molecular processes in ways visible to that of a human eye, in forms of colorimetric or luminescent outputs, for example. Studying how bacteria perceive and respond to the environment with their minimal infrastructure is truly awe-inspiring. They are the pinnacle of a self-sufficient minimalist that embraces any challenge in life, and they unapologetically take advantage of exploitable resources when available. Although pathogens like *V. cholerae* continue to be a great threat to humanity, they are laudable opponents we can draw wisdom from. Furthermore, there are a vast variety of nonpathogenic prokaryotes, some of them with very attractive traits from even the most anthropocentric utilitarian perspective. I look forward to a world with more appreciation for these inspiring organisms.

ABSTRACT

AN OXIDATIVE STRESS RESPONSE MECHANISM BY THE VIBRIO CHOLERAE ARCAB TWO-COMPONENT SYSTEM

Yitian Zhou

Jun Zhu

Vibrio cholerae, the causative agent of the infectious disease, cholera, is a water-borne pathogen with a dynamic lifestyle across physical environments of different oxygen levels with various sources of oxidative stress. The anaerobic respiratory control (ArcB/A) two-component system is a global regulator that facilitates the transition between different electron transport strategies with respect to the redox environment. Upon sensing a more anoxic quinone pool at the inner membrane, the histidine kinase ArcB activates the response regulator ArcA's regulatory functions by phosphorylation. ArcA has been reported in *Escherichia coli* and *Salmonella enterica* to be important for oxidative stress resistance, yet the mechanism through which ArcA respond to this stress is unknown. Here we report ArcA's regulatory functions being partially retained in *V. cholerae* upon oxidative stress. This additional redox-sensing under oxidative stress is dependent on a cysteine residue, C173, in ArcA's C-terminal DNA-binding domain. C173 is crucial in sustaining *in vitro* oxidative stress challenges and during colonization of mouse intestines. Phosphorylation state analysis indicates that ArcA phosphorylation is compromised when *V. cholerae* is challenged by oxidative stress. *In vitro* biochemical assays reveal that C173-dependent oxidation initiates ArcA binding to DNA containing an ArcA-binding motif. C173-dependent oxidation also promotes ArcA-ArcA interaction, similar to the effect from a microaerobic induction of ArcA. ArcA C173 is conserved in various Gram-negative pathogens. *In vitro* oxidative stress challenges and human intestinal epithelial cell invasion experiments with *S. enterica* further underscore the importance of ArcA C173 for bacterial survival. This work uncovers a new post-translational modification, oxidation, in addition to phosphorylation, that serves as an activating signal for ArcA. The redox response from ArcA couples a stress response to other ArcA-mediated transitions for an adaptation to a new environment, demonstrating the intricacy of bacterial stress responses and their close association to basic energy metabolism.

TABLE OF CONTENTS

LIST OF TABLES

LIST OF ILLUSTRATIONS

CHAPTER 1: Introduction

Vibrio cholerae is a facultative anaerobic motile gram-negative bacterium, the causative agent of the infectious disease, cholera. Many aquatic environments with a relatively warm temperature above 15 ºC are suitable *V. cholerae* habitats[1,2]. Virulent *V. cholerae* infect mammalian hosts via the fecal-oral route. When a human host consumes food or water contaminated by the virulent *V. cholerae*, the pathogen occupies the intestinal tract by colonizing and penetrating the mucosal layer that covers the villi. Upon colonization, *V. cholerae* produces virulence factors, toxin co-regulated pili (TCP) and the cholera toxin (CT). TCP facilitates the aggregation of bacteria and the tethering of cells to the host intestinal mucus layer as microcolonies that help combat the shearing forces of peristalsis in the small intestine and improve colonization. CT is a secreted AB_5 multi-unit toxin. The pentameric subunit B binds to the enterocytes, that leads to endocytosis of the toxin, upon which subunit A becomes active and catalyzes the ADP-ribosylation of the host G protein. This in turn retains the G protein in a constant GTP-bound form, causing continual adenylyl cyclase activity and cAMP production in the host. The elevated cAMP levels inhibit sodium chloride absorption, promote chloride and bicarbonate secretion, and activate the cystic fibrosis transmembrane conductance regulator (CFTR) [3]. These events cause an extensive efflux of electrolytes and fluid from infected enterocytes, leading to diarrhea, which allows *V. cholerae* to exit the host and return to an aquatic environment.

V. cholerae gene regulation as seen in *V. cholerae* virulence regulation

As *V. cholerae* transition between very different physical environments, cellular processes and stress responses optimized for respective environments are dynamically regulated by many regulators. The network of regulators that modulate *V. cholerae* virulence demonstrates how environmental cues inform *V. cholerae* lifestyle decisions for optimal fitness.

To reach the primary colonization site, the small intestine, *V. cholerae* needs to endure the acid stress in the stomach and transition to a less oxygenated environment compared to aquatic reservoirs. Host signals reflecting this transition, such as changes in bile salt concentration [4,5], pH

[6,7], unsaturated fatty acids [8,9], bicarbonate [10], iron concentration [11,12], and oxygen levels [6], collectively inform *V. cholerae* virulence regulation (**Fig. 1**).

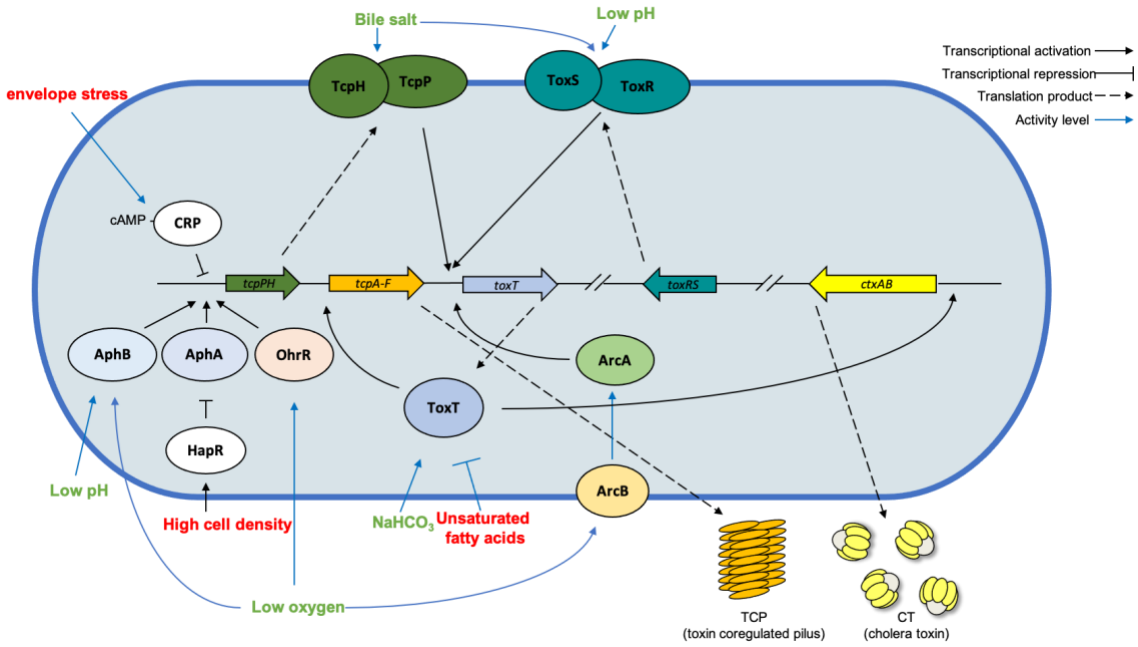

Figure 1: Signaling network of *V. cholerae* virulence regulation

A simplified schematic of *V. cholerae* virulence regulatory network. Green signals have a net stimulating effect on virulence; red signals have a net repressive effect on virulence. Relationships indicated can be direct or via intermediate factors not shown.

The membrane-bound transcription factor ToxR senses pH and bile salts that change its interaction dynamics with its stabilizing protein ToxS [7]. In an acidic pH environment or in the presence of bile salts, enhanced ToxR-ToxS interaction activates ToxR regulatory functions, facilitating an outer membrane porin composition for organic acid resistance while turning on the virulence activator gene *toxT* [13–16]. Another membrane-bound virulence activator TcpP, upon exposure to the bile salt taurocholate, transitions from a monomeric state to a transcriptionally active dimeric form with an intermolecular disulfide bond [17]. Similar to ToxS stabilizing ToxR, TcpH, encoded in the same operon as *tcpP*, provides protection against proteolysis for TcpP [18,19]. Activated by host signals, ToxR and TcpP collectively bind to the promoter region of *toxT* to initiate the transcription of the cytosolic master virulence activator, ToxT [20–22]. ToxT in turn enters

a positive feedback loop where it promotes its own expression all the while activating the expression of *ctxAB* and *tcpA*, which encode the two major virulence factors, CT and TCP, respectively. Further upstream in the regulatory cascade are cytosolic regulators AphB and AphA, which activate the transcription of the *tcpPH* operon collaboratively [23].

To activate *tcpPH* expression, AphB requires both low pH and low oxygen concentrations as stimulating inputs [24]. AphB is transcriptionally inactive at alkaline pH sensed by key residues in its ligand-binding pocket [25]. At low pH, AphB becomes active and also activates the expression of *cadC*, which encodes an activator for the lysine decarboxylation machinery that consumes protons to increase the cellular pH for acid tolerance [6]. Oxygen levels are sensed by AphB through the oxidation state of a cysteine residue, C235, in the C-terminal regulatory domain. Oxidation at C235 prevents AphB oligomerization, while a more anoxic environment leads to the reduction of this cysteine residue, facilitating AphB oligomerization necessary for *tcpPH* transcription [24]. Therefore, AphB ensures that virulence is only turned on when the bacteria have survived the acid barrier in the stomach and reached the microaerobic environment of the small intestine. To activate *tcpPH* expression, AphB binds cooperatively with AphA at the *tcpPH* promoter [23,26]. Since the expression of *aphA* is repressed by the quorum sensing regulator HapR [27], AphA serves as an indirect cell density sensor for virulence activation. At low cell densities, AphA levels are high, promoting virulence production; at high cell densities, AphA levels are reduced due to increased levels of HapR, therefore contributing to the inverse relationship between *V. cholerae* virulence and quorum sensing response.

Another regulator at the *tcpPH* promoter is cAMP-CRP [28], which inhibits the transcription of *tcpPH* when intracellular cyclic adenosine monophosphate (cAMP) is abundant. Envelope stress, usually signaled by a lack of environmental iron or efflux components, alters carbon uptake and utilization [11], increasing levels of intracellular cAMP that enhances the cAMP-CRP interaction. The resulting complex binds to the *tcpPH* promoter as a repressor [12]. Virulence repression

facilitated by cAMP-CRP allows for the prioritization of external stresses such as envelope stress or a lack of a preferred carbon source over virulence induction.

While high concentrations of bicarbonate in the upper small intestine enhance the activity of the virulence master activator ToxT [29], its proteolysis marks the termination of *V. cholerae* virulence [30]. Prior to exiting the host as *V. cholerae* reaches the lower intestines, the extracellular environment shifts from virulence-inducing to virulence-repressing due to increased pH and temperature, thereby breaking the ToxT-autoregulatory loop via degradation of ToxT.
By monitoring the extracellular pH, oxygen tension and host signals such as bile salts and bicarbonate, *V. cholerae* strategically turns on virulence only when the external signals indicate its presence at the primary colonization site.

The complex network of regulators for *V. cholerae* virulence illustrates the diverse measures of *V. cholerae* gene regulation in response to environmental inputs. Since running unnecessary or inappropriate programs is wasteful and harms the fitness of the bacteria, improper regulation often results in a fitness disadvantage compared to better adapted competitors. Besides virulence regulation, the modulation of other metabolic processes in *V. cholerae* also rely on regulators that promptly perceive external environmental cues and respond by assembling specific machineries to address the specific scenario.

***V. cholerae* two-component systems and the Arc two-component system**

When living in the aquatic environment, *V. cholerae* also need constant attendance to the numerous stresses no less stressful than those from a host. These adversities include nutrient scarcity, fluctuations of temperature and salinity, antibiotics secreted by other aquatic bacteria, and predatory behaviors such as protozoan grazing and vibriophage infections [31–34]. Some environmental *V. cholerae* may enter a metabolically quiescent state that is “viable but non-culturable” (VBNC) under stress. This dormant state might serve similar functions as do spores formed by spore-forming bacteria that allow the bacteria to persist until they can resume normal

metabolism when the situation permits. The lifestyle switch between these scenarios is rather high-stake as they often require global reconfiguration of multiple metabolic processes in a synchronized manner. Therefore, it is crucial for bacteria to correctly situate themselves by perceiving external cues, whether they are in or outside of a host. The perception of these signals by cellular sensors feed into programmed cellular circuits that yield a response tailored to maximize fitness in the environment reflected by those signals.

Two-component systems (TCSs) are used by *V. cholerae* and many other bacterial pathogens to perceive and respond to the environmental signals. In fact, TCSs are utilized by organisms across all kingdoms to modulate biological activities according to the perceived environment [35]. A bacterial TCS consists of two modular components: the membrane bound sensor histidine kinase (HK) that senses the external stimuli, and the cytosolic response regulator (RR) that responds to the message conveyed by the HK and performs regulatory functions, often transcriptionally. The chemical language used between the HK and the RR is phosphorylation. Upon encountering a positive signal through its sensing domain, the HK activates its ATPase activity, hydrolyzes the γ phosphate from an ATP and autophosphorylates on a histidine residue. When the phosphoryl group is subsequently transferred to an aspartate residue on the RR, the RR becomes active and produces a regulatory output, most often in the form of transcriptional regulation of genes in its regulon with the phosphorylation-dependent RR-promoter interaction dynamics.

V. cholerae encodes 52 RRs [36], many of which are involved in lifestyle switches in response to stressors. The PhoR/B TCS monitors periplasmic orthophosphate levels to facilitate dissemination at low phosphate concentrations [37]. The VprB/A TCS responds to host signals such as bile, acidic pH, and cationic antimicrobial peptides, and facilitates lipid A glycine modification to evade host immune response[38]. The CpxA/R TCS, triggered by envelope stress signaled by low extracellular iron or high extracellular chloride or copper [11,12,39], represses virulence and promotes efflux pump production to disgorge the stressor compounds [11,12,40].

The archetype of a TCS is a one-HK-one-RR pair which forms an exclusive one-to-one signaling pathway where the HK and RR are each phosphorylated and dephosphorylated sequentially. The specificity-determining residues in the HKs create subtle distinctions that minimize cross talks between different TCSs [41,42]. Nevertheless, there are many variations of the archetypical TCS architecture.

The *V. cholerae* VieSAB three-component system that modulate cellular c-di-GMP level, and therefore biofilm formation, is an example of a TCS variation with a built-in negative feedback by the third component. The *vieSAB* operon, repressed by the global repressor H-NS as well as the quorum sensing regulator HapR [43], encodes the HK VieS, the RR VieA, and a third component, VieB [44,45]. The VieS/A HK-RR pair, when activated by signals from the host environment such as contact to intestinal epithelial cells [46], positively regulate the expression of the *vieSAB* operon and *toxT*. The RR VieA, in addition to the N-terminal phosphorylation receiver domain and the C-terminal DNA-binding domain, has a EAL domain that hydrolyzes c-di-GMP, which in itself is necessary and sufficient in inducing *toxT* expression when cells are adhered to the host epithelium [46,47]. Therefore, phosphorylated VieA relays the host environment signal to coordinate two negatively associated cellular processes, enhancing pathogenesis while intervening biofilm maintenance. Consistent to its repressive effect on biofilm, the VieSAB system also contributes to promoting motility and flagellar synthesis [48,49]. The third component, VieB contains the conserved aspartate residue for phosphorylation yet lacks a DNA binding domain. Instead, it contains a structural motif that facilitate protein interactions. VieB binds to VieS and inhibits autophosphorylation of the HK, more efficiently so in its phosphorylated form [50]. At high levels of transcription of the *vieSAB* operon, as VieB accumulates, the signal transduction is cut off by inhibitory binding of VieB to VieS, resulting in a down regulation of the signal transduction system itself and the virulence.

Some TCSs combine the signal sensing and transcriptional regulation modules into one protein, therefore simplifying into one component. Aquatic *V. cholerae* is often found to be associated with exoskeletons of crustaceans and soft-shelled turtles [51–55]. These exoskeletons are rich in chitin, which are insoluble N-Acetylglucosamine (GlcNAc, or NAG) polymers. *V. cholerae* ChiS is an inner membrane-bound hybrid HK that monitors the oligosaccharide $(GlcNAc)_2$ that become more abundant in the periplasm when chitin is present in the extracellular environment [56]. When chitin is broken down into oligosaccharides such as $(GlcNAc)_2$ by secreted chitinases, these oligosaccharides enter the periplasmic space through outer membrane-bound porins such as chitoporins. Here, they are bound to chitin oligosaccharide-binding proteins (CBPs) that escort them to inner membrane-bound ABC type permeases for further import. Upon binding to $(GlcNac)_2$, CBPs are liberated from ChiS. In this CBP-free state, ChiS can change its own phosphorylation status by acting as a kinase or as a phosphatase [57]. Counter to the traditional TCS RR being regulatory active in the phosphorylated form, unphosphorylated ChiS activates the expression of the chitin utilization pathway genes by recruiting RNA polymerase through direct contact [56,58]. As a result, extracellular chitin detected by the HK ChiS, can be used as the sole source of carbon and nitrogen [57–59].

A phosphorelay is a variation of the archetypical TCS with additional phosphotransfer steps in between. In a phosphorelay, the HK and its cognate RR are still the start and the end of the phosphotransfer that activates the TCS, but the phosphoryl group is transitioned from the initial histidine on the HK to an aspartate on a RR-like shuttle domain. From there, it is subsequently transferred to another histidine phosphotransfer (Hpt) domain before eventually reaching the aspartate residue on the response regulator. The two additional domains, the RR-like shuttle domain and the Hpt domain, can either exist as part of the HK itself, making it a hybrid HK, or on their own as separate phosphotransfer shuttle proteins. The multistep relay gives rise to the potential problem of signal shutdown due to transferring of the phosphoryl group from the shuttle

aspartate to an incorrect histidine residue in the line, but it also gives more regulation opportunities in the signaling pathway.

The anoxic redox control, or the aerobic respiratory control (ArcB/A) two-component system is a phosphorelay in many Gram-negative facultative bacteria that regulates the transitions between different electron transport strategies with respect to the redox environment [60–62] (**Fig. 2**). As demonstrated in *E. coli*, the HK ArcB, located at the inner membrane (IM), directly monitors the redox state of menaquinone and ubiquinone dissolved within the lipid bilayer of the IM and autophosphorylates upon sensing a more reduced quinone pool [60(p),62,63]. Under reducing conditions, both of ArcB's cytosolic cysteine residues proximal to the IM are in the reduced state, activating ArcB kinase activities to autophosphorylate on His [292]. The phosphoryl group is subsequently relayed on the Asp[576] and His[717] on ArcB before eventually phosphorylating Asp[54] on ArcA, activating the response regulator. Upon phosphorylation, ArcA becomes active and regulates the expression of genes in the ArcA regulon [61,62], facilitating the transition from an aerobic to a more anaerobic lifestyle. Upon oxidizing conditions, the quinone pool oxidizes rapidly, inactivating ArcB's kinase activity by forming intermolecular disulfide bonds between ArcB cysteine residues [61,63]. At this point, the unphosphorylated ArcB turns into a phosphatase that dephosphorylates ArcA, inactivating the regulatory functions of ArcA. This bidirectional regulation of ArcA by ArcB through different phosphorylation states allows prompt signal transduction that most accurately reflects the extracellular redox environment, thus facilitating a precise and suitable choice between metabolism modes. Although these Arc TCS observations have not been made specifically in *V. cholerae*, and the *V. cholerae* ArcB only has one of the two cytosolic cysteine residues important for modulating kinase and phosphatase activities in the *E. coli* ArcB, the otherwise high homology between the *V. cholerae* and *E. coli* Arc proteins suggests possible similar oxygen sensing mechanisms.

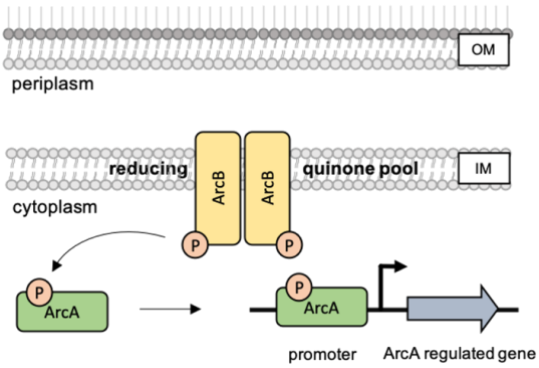

Figure 2: The Arc two-component system

A simplified pictorial view of the activation of the Arc TCS by a less oxygenated extracellular environment. The inner-membrane-bound histidine kinase ArcB autophosphorylates at H292 upon sensing a more reducing quinone pool. The phosphoryl group is relayed within ArcB in a H292-D576-H717 direction before phosphorylating the aspartate residue in the receiver domain of the response regulator ArcA. When phosphorylated, ArcA is activated for DNA-binding and regulation of the genes in the ArcA regulon.

While *V. cholerae* can survive a wide spectrum of oxygen levels, from fully aerobic to completely anaerobic, the differences on the proteomic level between *V. cholerae* under aerobiosis and anaerobiosis have revealed drastically different metabolic needs under these respective conditions [64]. For aerobic respiration, *V. cholerae* has three terminal oxidases, cbb3-oxidase, bd-oxidase I, and bd-oxidase II, that transport electrons from the quinol to O_2. When oxygen is not available, *V. cholerae* can perform anaerobic respiration using alternative terminal electron acceptors TMAO, fumarate, biotin sulfoxide (BSO), DMSO, or nitrate. The fumarate and nitrate reduction regulatory protein (Fnr) upregulates enzymes in the utilization pathways for alternative electron acceptors for anaerobic respiration. Although not specifically studied in *V. cholerae*, *V. cholerae* and *E. coli* Fnr homologs are 85.83% identical, suggesting possible function similarity. Unlike Fnr, the Arc TCS when activated transcriptionally represses carbon oxidation pathways that recycle redox carriers via respiration and drives the cell into using pathways that recycle redox carriers via fermentation, mostly by repressing genes in the TCA cycle to minimize the generation of NADH and promoting glycolysis to push metabolism toward fermentation [65]. *V. cholerae* is capable of fermentation of various carbon sources including glucose, sucrose, maltose, mannitol, lactose, dextrin, and starch [66,67]. Besides differences in proteins essential for

the respective energy metabolism, aerobiosis is associated with more carbohydrate transporters while anaerobiosis is associated with more stress response proteins and fewer motility proteins such as the flagellin B subunit. Aside from changed amounts and classes of proteins, there are also spatial rearrangements of existing proteins in response to oxygen levels. For example, some chemotaxis-related proteins localize to polar and lateral membrane regions in microaerobiosis [68]. The holistic reprograming of cell metabolism involved in lifestyle switches across oxygen levels is rather dramatic. The Arc TCS directly regulates 85 and affects the expression of genes from a total of 229 operons in *E. coli* and is predicted to directly regulate 47 operons in *V. cholerae* [65,69], establishing an unequivocable central role for the Arc TCS as a global regulator.

Decreased oxygen level is an important signal to *V. cholerae* not only because it signifies the need for a different collection of proteins but also because it is an activating signal for virulence through AphB. Intriguingly, a study by Sengupta and colleagues has suggested that *V. cholerae* ArcA activates the expression of virulence master activator *toxT* independently of ToxR and TcpP in the virulence regulatory network [70]. The ArcA-dependent *toxT* expression is seen in both aerobiosis and anaerobiosis but is more pronounced in the latter [70], suggesting an important role for ArcA in virulence and colonization under microaerobiosis.

The versatility of TCS-based signaling structures facilitates the sensing and processing of precise environmental signals to accurately inform the regulation of cellular processes. The modular structure offers many variations in the signaling pathway, providing opportunities for integration and coordination of environmental inputs for responses ranging from upregulation of a single pathway to holistic whole cell reprograming involving multiple metabolic pathways. Phosphorylation states of the components in these systems communicate the sensed signal and the extent of response execution. In fact, many other post translational modifications on transcriptional regulators are employed in regulating bacterial metabolic processes and stress responses, as seen in the case of oxidation-mediated regulation in bacterial ROS resistance.

V. cholerae ROS resistance thiol-based regulators

V. cholerae encounters unique challenges in the aquatic environment and in the host, but some stressors are present in both. Among these ubiquitous stressors are reactive oxygen species (ROS), oxygen containing molecules that are highly reactive due to their unpaired electron. In the environment, exogenous ROS sources include other microbes co-inhabiting a niche [71–73] or completely non-biological processes such as photochemical reactions [74,75]. In a host, ROS are produced by neutrophils, macrophages, and epithelial cells that use NADPH oxidases to reduce oxygen to superoxide anions and hydrogen peroxide [72]. ROS can be non-radicals, such as hydrogen peroxide and superoxide, or more reactive and damaging radicals, such as the hydroxyl radical, superoxide anion, and singlet oxygen that can be generated by non-radical species in the presence of transition metals such as iron and copper through Fenton chemistry. To avoid the Fenton reaction, *V. cholerae* iron uptake is tightly regulated to ensure sufficient iron for normal functions of iron-requiring proteins while avoiding reactive species damage [76]. Less prevalent but equally damaging are other classes of reactive molecules that damage cellular targets in manners similar to ROS. These species include reactive nitrogen species (RNS) generated from nitrogen metabolism; reactive electrophile species (RES) generated from quinones and aldehydes; and hypochloric acid (HOCl) generated by host myeloperoxidase in the presence of H_2O_2 and Cl^- [77].

Due to their reactive nature, ROS cause oxidative damage to lipids, nucleic acids, and proteins. Upon peroxidation, lipids, which are fundamental to cell membranes, degrade into cytotoxic aldehydes and hydrocarbons [78]. When in contact with nucleic acids, ROS can act on the sugar backbone, leading to single-strand breakage, or on the nucleobases, resulting in base degradation and the generation of free radicals that lead to DNA-protein cross-links [79–81]. Some of these damages can be amended by DNA repair enzymes such as those recruited in the SOS repair response [82,83], but the low fidelity of SOS polymerases such as DinB can cause mutations with major consequences [84]. In addition to the unintended cross-linking to DNA, proteins upon oxidative modification on amenable residues are subject to fragmentation, altered electrical

charges, and conformational changes [85,86]. Thus, in contrast to other stressors like nutrient scarcity and antibiotics, which only target specific metabolic processes and only act on actively metabolizing cells, reactive species attack both the blueprint and the building blocks of life, regardless of the metabolic state of the cells. This poses tremendous challenges for all living organisms. Despite self-harming consequences such as cancer [87], host cells use ROS as an effective weapon to eliminate pathogens.

To cope with this common stress, *V. cholerae* encode many mitigating enzymes targeting different ROS (**Fig. 2**). Superoxide dismutases such as the manganese-binding SodA convert superoxide into hydrogen peroxide and oxygen [88]. Catalases such as KatB and KatG detoxify peroxides into water and oxygen [89]. Peroxiredoxins such as PrxA and AphC target organic (alkyl) hydroperoxides [90]. DNA-binding proteins from starve cells (DPS) physically bind to DNA and sequester free iron to prevent ROS damage [88]. The virulence regulator ToxR, activated by the host environment, promotes a proper intracellular manganese level for ROS resistance [91]. *V. cholerae* even resorts to elevating mutation frequencies to diversify and enrich ROS resistance enhancing phenotypes, such as increased catalase and Vibrio polysaccharide production [92].

Although protein oxidation is generally undesirable as it often leads to misfolding or aggregation followed by removal and degradation, bacteria utilize oxidizable cysteine residues for protein functions [93]. Cysteine has a highly nucleophilic thiol side chain that tends to donate electrons, especially to other sulfhydryl groups, to form a disulfide bond. Making up only 1.3% of all reported proteins in the UniProt database, cysteine is a low occurrence residue commonly reserved only for its irreplaceable functions. For example, all *V. cholerae* c-type cytochromes rely on correct disulfide bond formation between their cysteine residues for maturation and heme-interaction [94]. In the case of heme nitric oxide/oxygen-binding (H-NOX) proteins, oxidation induces a conformational change through heme dissociation or disulfide bond formation at a zinc-binding motif encompassing four cysteine residues [95]. The resulting H-NOX binds to the HK in the

HnoK/B TCS, shutting down its kinase activity [96]. The RR HnoB contains an EAL domain that hydrolyzes c-di-GMP when phosphorylated, decreasing the positive signal for biofilm formation [97]. Therefore, the presence of oxidants causes H-NOX to inhibit the HnoK/B TCS, enhancing biofilm development.

Furthermore, reversible oxidation at cysteine residues is utilized to regulate redox stress response genes on a transcriptional level [98–100]. *V. cholerae* utilizes thiol-based transcription switches to adapt to different redox environments and their respective oxidative stress. As described previously, the AphB microaerobiosis induction of virulence is contingent on reduced C235 [24]. In fact, the non-redox sensing *aphB* mutant strain-with C235 mutated to a serine-is more susceptible to ROS [101]. AphB works closely with OhrR, another thiol-based transcription regulator that responds to redox changes sensed by its C23 and C128, in activating the transcription of the organic hydroperoxidase OhrA [101]. Oxidized OhrR falls off of the promoter of *ohrA* faster than oxidized AphB, derepressing the ROS resistance gene sequentially in regard to the amount of ROS present. Therefore, *ohrA* is transcribed as demanded by the severity of the imminent oxidative stress. Furthermore, the AphB OhrR duo exhibit the same differential kinetics when regulating the expression of the virulence regulator *tcpP*. Similar to C235 on AphB, C23 and C128 on OhrR in their reduced forms facilitate OhrR binding to the *tcpP* promoter, activating the transcription of the virulence activator. With multiple redox-sensing regulators, one responding more rapidly than the other, *V. cholerae* ensures a prudent initiation of virulence in a new redox environment [102].

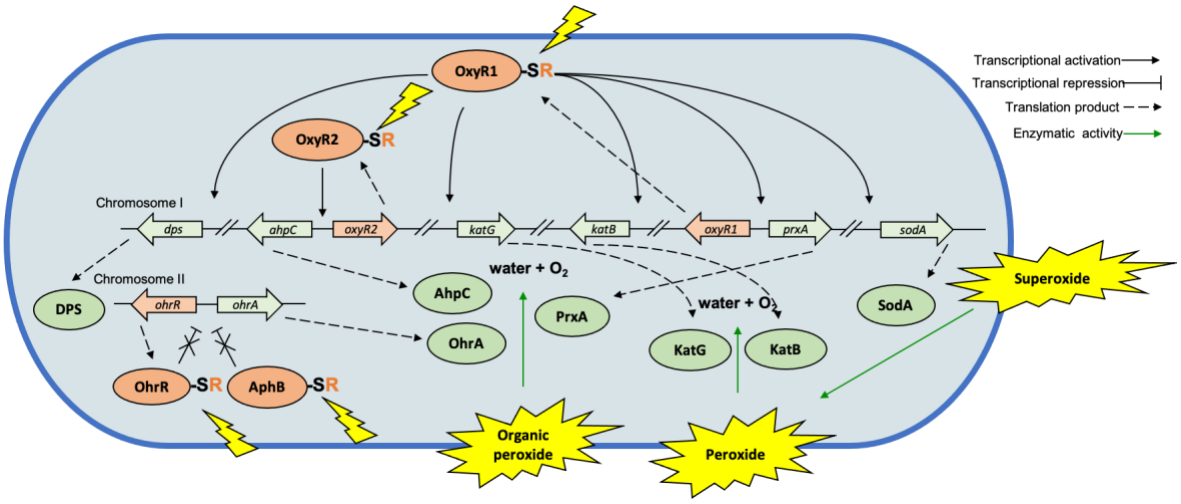

Figure 3: Thiol-based regulation of *V. cholerae* ROS resistance

A simplified schematic of the *V. cholerae* ROS regulatory network when challenged by ROS, with the transcriptional regulators in orange and the ROS resistance proteins in green. Extracellular ROS exposure reversibly oxidizes the thiols on cysteine residues in the thiol-based transcriptional regulators, activating their regulatory behaviors that result in the production of ROS resistance proteins, conferring ROS resistance. When oxidative stress is alleviated, reflected by reduced thiols on the regulator proteins, the transcriptional activation on the stress response proteins also pauses. Relationships indicated can be direct or via intermediate factors not shown.

Besides OhrA, many other major ROS resistance enzymes are specifically upregulated upon ROS exposure, which is detected by the ROS-sensing regulators OxyR1 and OxyR2 [88,90]. Upon oxidation, sulfenation at the conserved cysteine residue Cys199 on the *E. coli* OxyR is critical for activating its regulatory functions [103,104]. Two homologs of the *E. coli* OxyR, OxyR1 and OxyR2, both with the conserved redox-sensing cysteine residues, exist in the *V. cholerae* genome. OxyR1 responds to hydrogen peroxide and activates the expression of *prxA*, *katB*, *katG*, *sodA*, and *dps*, all of which contribute to ROS resistance [88]. OxyR2 responds to environmental oxidative stress and activates the transcription of itself and the divergently transcribed *ahpC*, both of which promote *V. cholerae's* transition from the oxygen-limiting gut to an oxygen-rich aquatic environment [90]. Both OxyR1 and OxyR2 activation rely on the oxidation of the conserved cysteine residues equivalent to the *E. coli* OxyR C199. OxyR's regulatory function becomes inactive when the C199 thiol oxidation is reduced by enzymes in its regulon, forming an autoregulatory negative feedback loop. Through the different regulation dynamics of OxyR1 and OxyR2 responding to

different oxidants, *V. cholerae* expresses ROS resistance enzymes adaptively and shut down the circuit when the oxidative stress is ameliorated.

V. cholerae stress responses exemplify the diverse strategies for bacterial survival across different physical environments. *V. cholerae* situate themselves by perceiving environmental cues that directly describe the circumstance, such as oligosaccharide levels, or resort to signals that stably correlate with the condition, such as an elevated bile salt level as a proxy to arrival at a colonization site. Following the perception of environmental signals, regulators act to adjust cellular functions such that the bacteria is equipped with metabolic machineries optimized for the current situation. The result is a streamlined process of stress exposure and stress response. Among these, the sensing of redox signals through oxidation states on cysteine thiols is especially critical as it modulate very common and dynamic processes. *V. cholerae* is not unique in employing this design in redox sensing, therefore the mechanism of *V. cholerae* thiol-based switches are instructive to a better understanding of bacterial redox sensing in general. There are still more thiol-based transcriptional regulators in *V. cholerae* that can inform us about the many events involved in bacterial ROS resistance. A universal stress for all living organisms regardless of the metabolic state, ROS is a potent weapon against pathogens with its wide-range damage to multiple cell components. More knowledge on bacterial ROS resistance will add to the mechanistic underpinning that devise and guide anti-microbial therapies and interventions.

CHAPTER 2: The Response Regulator ArcA Contains Redox-Sensing Cysteine residues

Introduction

Previous work from the Zhu lab on the *V. cholerae* virulence activator, AphB, which senses oxygen levels by C235 in the regulatory domain, demonstrated a thiol-based switch contingent on a single cysteine residue[105]. The reversible oxidation at C235 facilitated oxygen sensing by changing AphB oligomerization state, and thus its DNA-binding abilities and regulatory activities. This redox sensing is demonstrated to be important for both virulence induction as well as resistance to inorganic and organic hydroperoxides in *V. cholerae*[101].

Cysteine is one of the only two sulfur-containing amino acids. Unlike methionine with its sulfur in a relatively stable form of sulfide, cysteine contains a sulfhydryl chain, or a free thiol. With their highly reactive nucleophilic sulfhydryl side chains, cysteine residues are highly responsive to the redox environment and can undergo a number of modifications responding to reactive oxygen or nitrogen species and oxidation in general [10698]. Most commonly, cysteine sulfhydryl group can be reversibly oxidized to sulfenic acids (-SOH), further oxidized to sulfinic acids ($-SO_2H$), or irreversibly to sulfonic acids ($-SO_3H$) [99,107]. When another sulfhydryl group is in the physical proximity, an oxidizing environment facilitates the formation of disulfide bonds. Depending on the location of the other cysteine, the disulfide bond can be intra- or intermolecular. Other post-translational oxidation on cysteine sulfhydryl side chain also include S-nitrosylation (-SNO) and S-carbonylation [108,109].

To prevent undue oxidation on cysteine residues, low molecular weight (LMW) thiol and their oxidized forms act as redox buffers for the cellular redox environment. Under oxidative stress, LMW thiols absorb the impact of an oxidative assault by dimerizing amongst themselves, or by forming disulfide bonds with thiol-containing proteins, a cysteine oxidation termed S-thiolation[110] . The oxidized to reduced LMW thiol ratio increases upon extracellular oxidant exposure. Thiol reductases restore the LMW thiols to the reduced state, keeping the cysteine-containing cellular

proteins from the first line of oxidation. Glutathione (GSH), a cysteine-containing tripeptide (Glu-Cys-Gly), together with its oxidized form (GSSG), are used in many organisms including many Gram-negative bacteria[111]. In these GSH/GSSG buffered cells, cysteine containing proteins can be glutathionylated. Besides GSH, other LMW thiol buffers are used similarly in other bacteria[111]. Firmicutes such as *Bacillus* and *Staphylococcus* produce bacillithiol (BSH), *Actinomycetes* produce mycothiol (MSH), while Archaea and some Gram-positive bacteria use coenzyme A (CoASH) as thiol-redox buffers.

The oxidation-dependent thiol group post-translational modifications often lead to an altered oligomerization state or conformation of the transcriptional regulator. These changes in turn affect the regulator's regulatory activity, thus modulating the expression of the downstream genes upon oxidizing environmental cues, which usually involve adapting the bacterium to lifestyles suitable to the new redox environment [112,113].

The MarR family regulator BifR in *Burkholderia thailandensis* is demonstrated to use an intermolecular disulfide bond to change its oligomerization state [114]. Upon oxidation, an intermolecular disulfide bond forms between two BifR dimers via C104, enhancing the binding of BifR to the promoters of the BifR regulon. The enhanced binding further represses the expression of genes involved in biofilm formation and phenazine synthesis. For a soil microbe like *B. thailandensis*, it is critical to reserve the biofilm lifestyle to the most appropriate surroundings, and phenazine production to only when environmental oxygen is limited. The redox sensing through C104 facilitates accurate adaptation that is critical for the fitness of the bacteria.

An intramolecular disulfide bond can form between two cysteine residues on the same regulatory protein. In oxidizing conditions, the quorum sensing TCS response regulator, AgrA in the Gram-positive bacterium *Staphylococcus aureus*, forms a disulfide bond between C136 and C238 in its DNA binding domain[115]. The formation of the disulfide bond changes the conformation of AgrA,

lifting it off of the promoter of the *bsaA* gene which encodes a glutathione peroxidase. As a result, the presence of oxidative stress turned on bacterial resistance to oxidative stress. The intrinsic thiol switch in AgrA enables its response to redox signals in addition to the autoinducer peptide-based quorum sensing signals, demonstrating the versatile and complex nature of two-component systems and bacterial signal transduction.

Oxidation to sulfenic acid can also change the conformation of a regulator to facilitate transcriptional regulation in response oxidation. RitR in *Streptococcus pneumoniae*, a TCS RR, has a cysteine residue (C128) in its linker domain. This redox reactive cysteine residue senses the cellular redox state, changing the accessibility of the DNA-binding domain to interact with the promoter regions of the RitR regulon[116]. When C128 is oxidized to the sulfenic (-SOH), sulfinic (-SO_2H), or sulfonic (-SO_3H) forms, the linker region undergoes a "helical unravelling" which activates RitR. The activated RitR form dimers and the DNA-binding domain is unfolded from the regulatory domain to be available for DNA-binding. This results in the repression of genes such as *piu* that activates iron uptake [116,117], as well as the activation of genes that are involved in ROS remediation. As a consequence, the oxidative stress triggers the cell to prevent Fenton chemistry and to enhance ROS resistance.

Although not a transcriptional regulation as seen in the aforementioned examples, glutathionylation (-SG) changing the behavior of a regulator protein is seen with *E. coli* DnaK. DnaK catalyzes ATP hydrolysis and directly interacts with a number of bacterial heat shock response regulator proteins [118]. Glutathionylation on DnaK's only cysteine residue (C15) in its nucleotide-binding ATPase domain reduces its ATPase activity. Under oxidative stress, the lack of available ATP and the decreased ATP hydrolysis activity result in the release of σ32, triggering the bacterial heat shock response [119]. Although this modulation is on a protein level, S-glutathionylation on C15 plays a key role in changing the catalytic activity of DnaK, which has a

direct impact on the behavior of the transcriptional regulator, σ32. The oxidation of C15 on DnaK effectively regulates the heat shock response under oxidative stress.

These examples showed the critical roles cysteine residues play in perceiving redox changes in the immediate extracellular environment and relaying these signals to the cell. As a result, the cell subsequently undergoes transcriptional reform to adapt to the new environment. As a bacterium with a complex life cycle that involves adaptation to different redox environments as well as oxidative stress, *V. cholerae* and its thiol-based switches for transcriptional regulation are important subjects in deepening our understanding of bacterial stress responses. The importance of the AphB C235 for regulating both virulence and ROS resistance, and the prevalence of thiol-based regulators in bacterial stress response motivated a proteomic identification of *V. cholerae* reversibly oxidizable cysteine residues.

Results

Many *V. cholerae* proteins contain reversible thiol-oxidation

To identify more possible thiol-based regulators, we performed a mass spectrometry-based proteomic profiling of *V. cholerae* proteins that contain cysteine residues receptive to reversible oxidation modifications. Cells were grown under virulence inducing conditions to the mid-log phase when they were challenged by sublethal concentrations of cumene hydroperoxide (CHP), an organic peroxide that *V. cholerae* might encounter in a mammalian gut. The CHP exposure allowed for ROS-mediated oxidation on amenable cysteine residues inside of *V. cholerae* cells. The cell lysates were then processed such that the intracellularly oxidized thiols were labeled by a 57Da carbamidomethyl group (**Fig. 4A**). The LC MS/MS result revealed 26 proteins with 37 unique cysteine residues as labeled. Among these are proteins involved in the translation machinery and energy metabolism (**Appendix: Table 1**). ROS-dependent oxidation on ribosomal proteins was previously seen in *E. coli* [120]. Thioredoxin, a major regulator for redox homeostasis, was also detected. However, this screen did not identify AphB which contains an oxidizable cysteine residue, C235 [105]. This suggests that this approach, with the growth condition tested,

does not exhaustively detect all possible cysteine oxidation. Among the proteins that contain reversibly oxidized thiols, we see a transcriptional regulator ArcA, the response regulator of the Arc TCS. ArcA is consisted of an N-terminal receiver domain, which contains the highly conserved phosphorylation site D54, and a C-terminal DNA-binding domain, which contains two cysteine residues C173 and C233. The proteomic profiling revealed both ArcA cysteine residues in an oxidized state upon CHP exposure under the virulence inducing growth condition (**Fig. 4B and Table 1**).

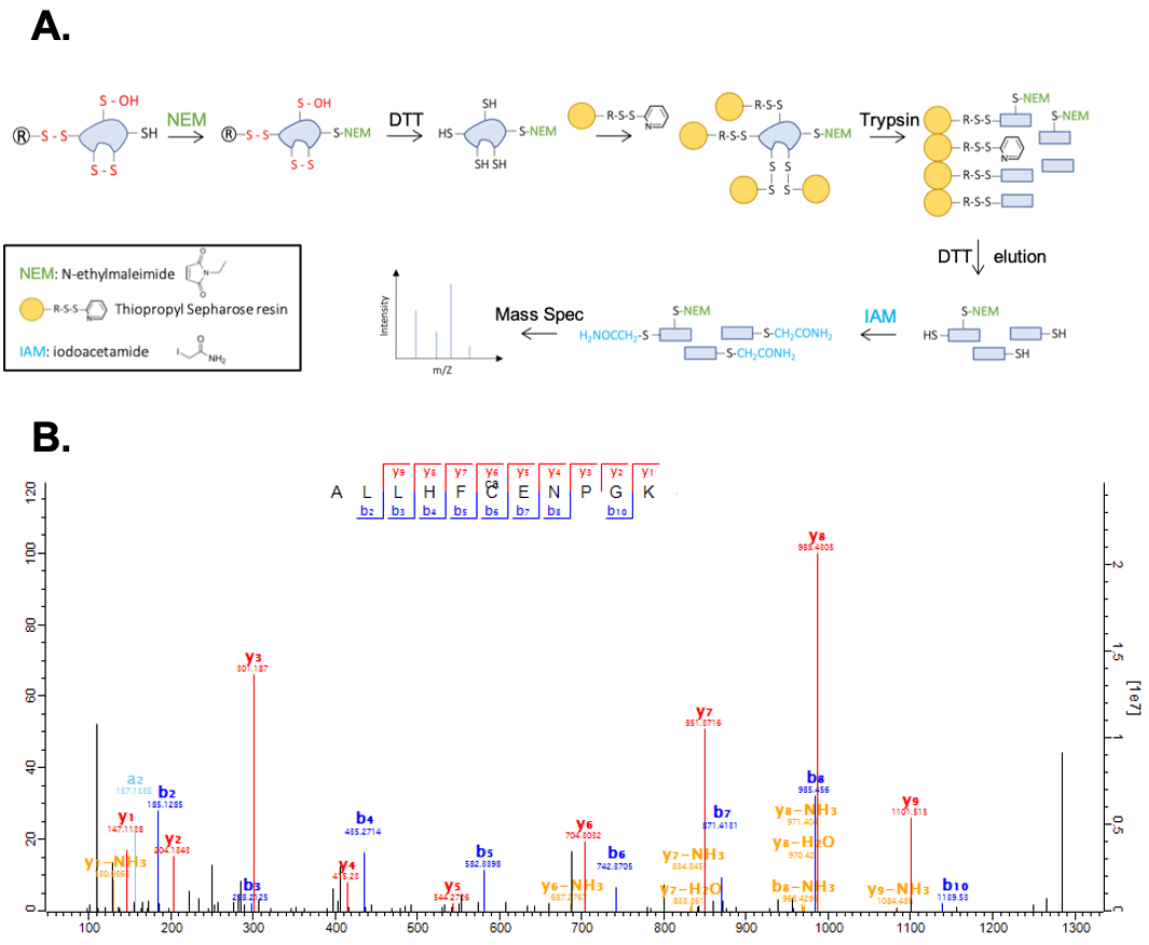

Figure 4 Proteomic detection of *V. cholerae* reversible thiol oxidation

A. A schematic of the thiol labeling protocol used to detect reversible oxidation on cysteine residues in *V.* cholerae after being challenged by ROS under virulence inducing conditions. Whole cell lysate is treated as shown prior to analysis by LC MS/MS to identify reversibly oxidized cysteine residues. **B.** A spectrum arising from a peptide from ArcA containing C173. Evidence for oxidation is observed by the 160 Da difference between species b5, b6 and y5, y6. For reference, the monoisotopic mass change for cysteine is 103 Da, and for carbamidomethyl modification, 57 Da.

An *arcA*^{C233S} mutant has similar basic metabolic defects to that of a Δ*arcA* mutant

To investigate the roles of ArcA cysteine residues in *V. cholerae* physiology, we generated a Δ*arcA* mutant (VC2368) by inserting a kanamycin resistance cassette with its own constitutive promoter in the opposite orientation of the *arcA* gene in *V. cholerae* C6706 (**Fig. 5A**). For complementation, we integrated the *arcA* gene with its native promoter at the *lacZ* locus (VC2338) on the large chromosome (chromosome I) in a Δ*arcA* background. To elucidate the role of the ArcA cysteine residues, we constructed variants of ArcA with each one or both of its cysteine residues mutated to a serine, the amino acid that closest resembles cysteine with an oxygen in place of the sulfur atom on the side chain. The hydroxyl side chain is sterically similar to the cysteine sulfhydryl albeit insusceptible to the thiol-based oxidation modifications due to the lack of the reactive sulfhydryl side chain (**Fig. 5A**). Similar to the wild type (WT) form of *arcA*, cysteine variants, *arcA*^{C173S}, *arcA*^{C233S}, *arcA*^{C173SC233S}, and the phosphorylation variant *arcA*^{D54A}, where the aspartate at the phosphorylation site is mutated to an unphosphorylatable alanine, were introduced to Δ*arcA* at the chromosomal *lacZ* locus with the native *arcA* promoter. A Δ*arcB* mutant (VC2369) was also constructed by inserting a spectinomycin resistance cassette (*spc*) with its own constitutive promoter in the *arcB* gene (**Fig. 5B**).

Δ*arcA* mutants exhibited slower growth in LB with 200rpm aeration and form smaller colonies on a 1.5% LB agar plate (**Fig. 5C and 5D**). While *arcA*^{WT} and *arcA*^{C173S} at the *lacZ* locus complemented growth and the small colony phenotype, *arcA*^{C233S}, *arcA*^{C173SC233S}, *arcA*^{D54A}, and Δ*arcB* mutants showed similar growth defects and colony morphologies to Δ*arcA* mutants (**Fig. 5C and 5D**). One of the first characterized phenotypes of a Δ*arcA* mutant is its sensitivity to certain dyes such as toluidine blue (TB)[121]. We tested the survival of the aforementioned strains on 1.5% LB agar plates containing a final concentration of 1μg/ml TB. Consistent with previous literature, a Δ*arcA* mutant is at least 3 logs more sensitive to TB compared to WT (**Fig. 5E**). Again, while *arcA*^{WT} and *arcA*^{C173S} at the *lacZ* locus restored TB survival in Δ*arcA* mutants, *arcA*^{C233S}, *arcA*^{C173SC233S}, *arcA*^{D54A}, and Δ*arcB* mutants showed sensitivity to the dye similar to

Δ*arcA* mutants. TB exerts oxidative stress in the presence of light [122]; however, *E. coli* Δ*arcA* mutants are still sensitive to TB in the dark, suggesting alternative modes of action [123]. Nonetheless, the results in our study show that C233 is essential in basic ArcA functions.

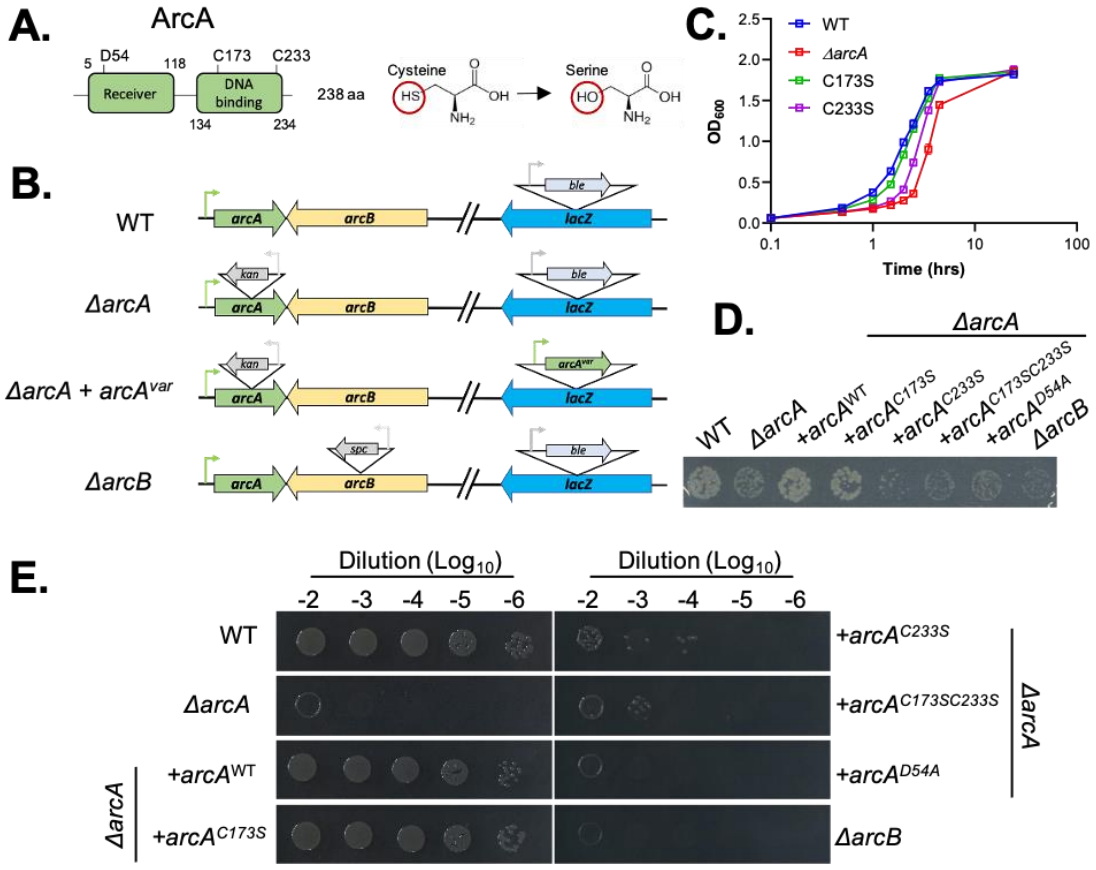

Figure 5: *V. cholerae* ArcA C233 affects basic ArcA functions

A. A schematic showing the ranges of ArcA N-terminal receiver domain and C-terminal DNA-binding domain highlighting the phosphorylation site (D54) and cysteine residues (C173 and C233); A cysteine and a serine with their side chains highlighted by red circles. **B**. A pictorial view of *arcA* and *arcB* chromosomal deletion, and the chromosomal complementation of *arcA* variants with a native *arcA* promoter in a *ΔarcA* mutant. **C.** Growth curves of respective strains in liquid LB media with 200rpm shaking for aeration with an optical density at 600nm as cell density readout. **D.** Colony morphology of respective strains on an 1.5% LB agar plate at 10E5 dilution of an OD_{600}=1 cell resuspension. **E.** Colony morphology of respective strains on 1.5% LB agar plate containing 1μg/ml toluidine blue.

ArcA cysteine residues are reversibly oxidized under ROS stress

To confirm that the ArcA cysteine residues are oxidized under ROS stress, a similar thiol labeling approach is used on whole cell lysates expressing His_6-tagged ArcA variant proteins (**Fig. 6A**).

Oxidized thiols were labeled by a 0.5kDa 4-acetamido-4'-maleimidylstillbene-2,2'-disulfonic acid, or AMS (**Fig. 6B**), visualized by a 0.5kDa shift in size in their SDS-PAGE migration patterns.

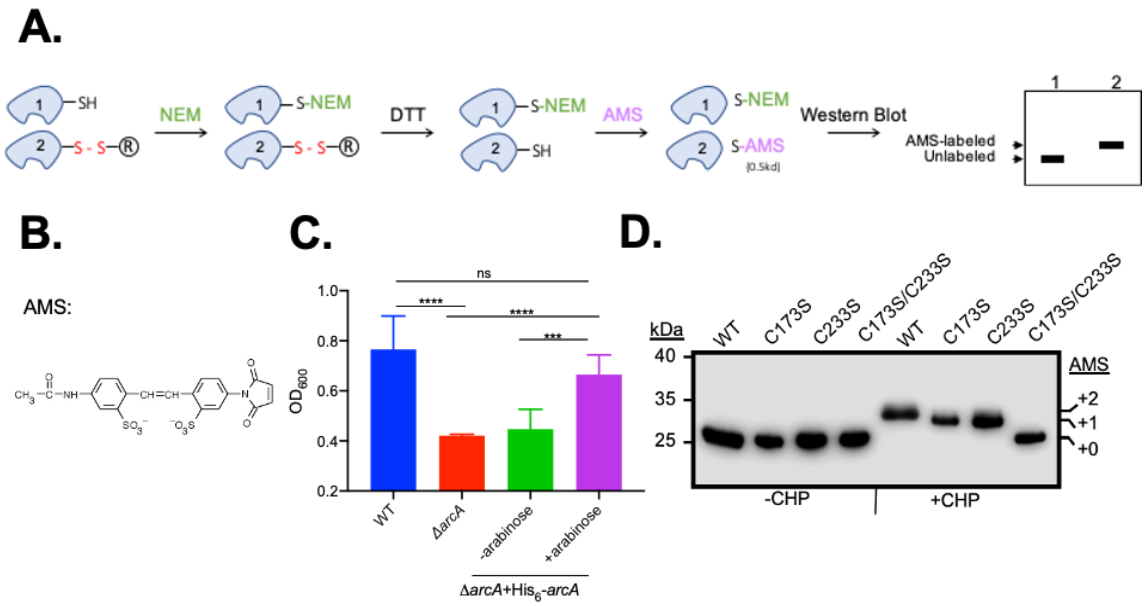

Figure 6: ArcA cysteine residues can be reversibly oxidized

A. A pictorial view of the protocol used to label reversibly oxidized cysteine residues on His_6-tagged ArcA variant proteins expressed in *V. cholerae* for visualization by SDS-PAGE analysis followed by western blot against His_6-tag. **B.** The 0.5kd 4-acetamido-4'-maleimidylstillbene-2,2'-disulfonic (AMS) used to label reduced thiols. **C.** A single timepoint OD_{600} reading indicating cell densities in respective strains during log-phase aerobic growth in LB media, N=6. The growth defect of *ΔarcA* are ameliorated with His_6-tagged ArcA on a plasmid when the expression is induced by including arabinose in the media. **D.** Anti-His western blot of *V. cholerae* cell lysates containing His_6-tagged $ArcA^{WT}$, $ArcA^{C173S}$, $ArcA^{C233S}$, or $ArcA^{C173SC233S}$ that underwent mock or CHP treatment prior to AMS labeling protocol shown in A.

We used *V. cholerae* C6706 WT to over express ArcA on a pET41 plasmid with an N-terminal His_6-tag under the control of a T7 promoter. Since *V. cholerae* does not encode a T7 RNA polymerase, we introduced an arabinose inducible T7 RNA polymerase on a plasmid (pTara). To test the functionality of over expressed His_6-tagged ArcA in *V. cholerae*, we introduced the same plasmids to Δ*arcA* mutants that are kanamycin sensitive. The resulting strain showed similar growth to *V. cholerae* C6706 WT in aerobic growth in liquid LB when 0.1% arabinose was included in the growth media, suggesting complementation to a Δ*arcA* growth defect with its functional production of His_6-ArcA from the pTara based T7 RNA polymerase (**Fig. 6C**). In

addition to His_6-$ArcA^{WT}$, His_6-$ArcA^{C173S}$, His_6-$ArcA^{C233S}$, or His_6-$ArcA^{C173SC233S}$ on a pET41 plasmid were also introduced to a *V. cholerae* C6706 WT with a pTara plasmid.

Same virulence-inducing growth conditions used in the proteomic profiling were imposed to grow the His_6-ArcA variant overexpression cultures followed by mock or CHP treatment before subsequent thiol-labeling by the 0.5kDa ASM. A western blot analysis of these ASM labeled samples showed only one band corresponding to the unlabeled His_6-ArcA size (28kDa) in all the mock treated samples, suggesting no thiol oxidation under this growth condition (**Fig. 6D**). Upon CHP exposure, the His_6-$ArcA^{C173SC233S}$ sample migrated to the same position as the untreated samples, suggesting an absence of oxidized cysteine residues. In contrast, both His_6-$ArcA^{C173S}$ and His_6-$ArcA^{C233S}$ yielded a band that is slightly higher than the unlabeled protein, signifying one oxidized thiol (**Fig. 6D**). Since His_6-$ArcA^{C173S}$ and His_6-$ArcA^{C233S}$ each only contains one cysteine residue, their respective labeled bands suggest the other cysteine residue can be oxidized upon ROS exposure. The His_6-$ArcA^{WT}$ sample showed an even higher shift compared to the single cysteine variants, suggesting more than one cysteine residues in an oxidized state under ROS exposure. Taken together, our results show that ArcA cysteine residues, both C173 and C233, are oxidized on the sulfhydryl side chains upon ROS exposure.

C173 is important for *V. cholerae* ROS resistance *in vitro*

Since both ArcA cysteine residues, C173 and C233, are reversibly oxidized under ROS exposure, we want to test ArcA's role in *V. cholerae* ROS resistance, with special focus on the characterization of the ArcA cysteine residues. Previous studies in *E. coli* and *Salmonella* have suggested critical roles for ArcA in conferring ROS resistance in these pathogens that transition between environments of different oxygen levels in their lifetime[124–126]. We first subjected the *V. cholerae* C6706 cells grown to mid-log phase under microaerobic conditions to 1hr of either mock or 350μM H_2O_2 treatment. Survival rates were calculated by CFU of H_2O_2-treated over mock-

treated cultures of respective strains. A Δ*arcA* mutant is about 2 logs more sensitive to H_2O_2 compared to WT. Consistent to the growth and TB sensitivity defect phenotypes, we see complementation of the Δ*arcA* mutant H_2O_2 sensitivity when $arcA^{WT}$ and $arcA^{C173S}$ were put back on the chromosome (**Fig. 7A**). Correspondingly, the $arcA^{C233S}$ and the $arcA^{C173SC233S}$ mutants showed survival rates more similar to Δ*arcA* mutants than to WT (**Fig. 7A**), further supporting that the C233S mutation have compromised basic ArcA functions.

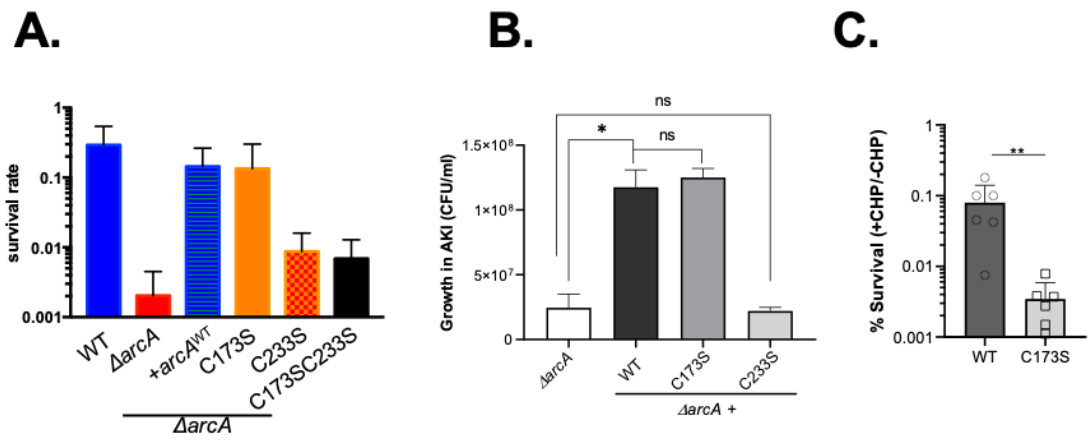

Figure 7: ArcA-dependent sensitivity to *in vitro* ROS exposure

A. Survival rates of *ΔarcA* mutants and ArcA variant complementation strains when exposed to H_2O_2 during log-phase under a microaerobic growth condition. N=9 for each strain. **B.** CFU quantification of cells grown in the virulence inducing condition in AKI media showing similar growth between WT and $arcA^{C173S}$ mutants. *ΔarcA* mutants and $arcA^{C233S}$ mutants have growth defects at this growth condition with an inoculum of 1:300. **C**. Survival rates for WT and $arcA^{C173S}$ mutants when exposed to CHP under virulence inducing condition in AKI media. n=6.

Although $arcA^{C173S}$ mutants showed similar level of survival to WT under H_2O_2 challenge and very similar growth under virulence-inducing AKI media under microaerobic conditions (**Fig. 7B**), when challenged by cumene hydroperoxide (CHP), the organic hydroperoxide used in the proteomic identification experiment, $arcA^{C173S}$ mutants showed ~30-fold lower survival compared to WT, suggesting a crucial role for C173 in ArcA-mediated resistance to organic ROS (**Fig. 7C**). Since the growth, colony morphology and even susceptibility to H_2O_2 of an $arcA^{C173S}$ mutant are unaffected under ArcA-activating conditions, we concluded that the $ArcA^{C173S}$ can carry out ArcA functions, except for those pertaining organic ROS resistance. Considering ArcA C173 is oxidized

upon ROS exposure and *V. cholerae* showed a C173-dependent resistance to CHP, we hypothesize C173 is specifically important for redox sensing and cell response to organic hydroperoxide.

V. cholerae colonization of ROS-rich mouse guts require C173

ArcA has been demonstrated to be important in *E. coli* colonization in an adult mouse model as well as in an infant rabbit model [127,128]. An infant mouse model is commonly used to study basic *V. cholerae* colonization machinery[129]. Suckling mice have yet developed the many defense mechanisms, such as antimicrobial peptide synthesis and immune responses[130]. This simplified host environment takes away challenges *V. cholerae* may face in a real colonization, but the fundamental colonization ability of a *V. cholerae* strain can be examined in a minimal context. To investigate the roles of the ArcA cysteine residues in *V. cholerae* colonization of a mammalian host, we used the infant mouse model to test the colonization of *arcA* single cysteine variant mutants in competition with *V. cholerae* C6706 WT. A 1:1 mix of *arcA* cysteine mutant and WT were perorally administered to the infant mouse. 12hrs post infection, *V. cholerae* CFU in the small intestine were enumerated on LB agar plates containing 40μg/ml of X-gal. Since the *arcA* cysteine variant sequences were put back onto the chromosome at the *lacZ* locus (VC2338), *arcA* cysteine variants form white colonies on agar plates containing X-gal while the WT C6706 with functional *lacZ* gene encoding a β-galactosidase form blue colonies. The competitive index was calculated as the ratio of mutant to wild-type colonies normalized to the input ratio in the inoculum that was used to infect the mice. A competitive index of 1 suggests no particular difference in the ability to colonize between the two strains. Although $arcA^{C173S}$ mutants did not show any disadvantage compared to WT, $arcA^{C233S}$ mutants showed a colonization defect with at least a log poorer colonization than WT, similar to that seen with Δ*arcA* mutants (**Fig. 8A**). This again underlines the important role of C233 in normal ArcA functions, as a point mutation at this residue compromises *V. cholerae* basic colonization.

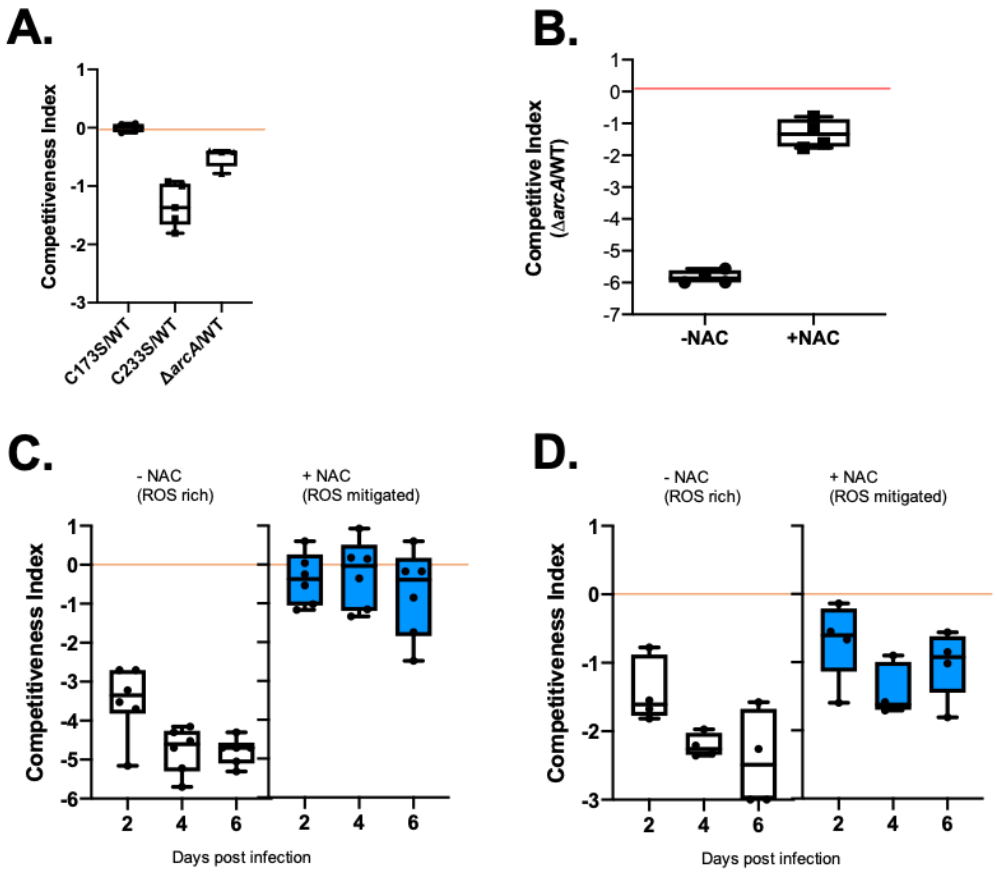

Figure 8: Colonization of an ROS rich mouse gut require C173

A. Competitive indices (log scale) of the mutant/WT in an infant mouse model, N=5. Individual values are shown with a five-number summary box plot. The red line indicates a competitive index of 1, signifying no difference. *arcA*^{C173S} mutants fall on the line when competed against WT, suggesting no colonization disadvantage. *arcA*^{C233S} mutants and *ΔarcA* mutants fall below the line, showing inferior colonization abilities when co-colonizing infant mouse guts with WT. **B.** Competitive indices of *ΔarcA* mutants/WT in two cohorts of adult CD-1 mice, one without including the ROS chelator N-acetyl cysteine (NAC) in the drinking water, representing a normal ROS level, and the other with NAC in the drinking water to mitigate gut ROS, N=5, data from 6 dpi. *ΔarcA* mutants showed a less severe colonization disadvantage compared to WT in the ROS-mitigated guts. **C.** *arcA*^{C173S}/WT competitive indices in adult mice with normal ROS level (-NAC) and in adult mice with mitigated levels of gut ROS (+NAC), N=5. The colonization defect of *arcA*^{C173S} mutants is only seen in an ROS-rich cohort. **D.** *arcA*^{C233S}/WT competitive indices in adult mice with normal ROS level (-NAC) and in adult mice with mitigated levels of gut ROS (+NAC). The colonization defect of *rcA*^{C233S} mutants are not ameliorated by ROS-chelation.

Since *arcA*^{C173S} mutants are able to colonize an infant mouse gut as well as WT, *arcA*^{C173S} mutants present an opportunity to investigate the role of the cysteine residue in more complex colonization conditions, such as in an ROS-rich gut in an adult mouse model. The Zhu lab has previously developed an infection protocol for adult CD-1 mice with the ROS scavenger, N-acetyl

cysteine (NAC) [101]. We showed that without NAC included in the drinking water, the mouse gut is an ROS-rich environment, but ROS was effectively removed in the NAC-treated mouse guts. We used this infection model to test the colonization of *arcA*^{C173S} mutants in competition with WT in normal ROS-rich guts as well as in the ROS-mitigated guts. A 1:1 mix of *V. cholerae* C6706 WT with functional *lacZ* gene encoding a β-galactosidase and *arcA*^{C173S} mutant with *lacZ* disrupted by the *arcA*^{C173S} sequence were intragastrically introduced to two groups of mice, one without NAC treatment, and one with NAC in their drinking water. Fecal pellets were collected 2 and 4 days after inoculation for CFU enumeration on LB agar plates containing X-gal where WT and *arcA*^{C173S} mutants form blue and white colonies, respectively. A final data point from day 6 was collected when the mice were sacrificed for enumeration of CFUs from homogenized small intestines. In the untreated mice with the ROS-rich guts, *arcA*^{C173S} mutants showed a severe colonization defect as indicated by the low competitive indices (**Fig. 8C**). *arcA*^{C173S} mutants showed 3 logs lower colonization compared to WT from day 2 and progressively decreased to 4-5 logs at 4 days post infection, which was maintained throughout the rest of the infection until the conclusion of the experiment at day 6. In contrast, *arcA*^{C173S} mutants showed comparable colonization abilities to WT throughout the course of the 6-day infection period in the ROS-mitigated group, as indicated by competitive indices around 1 (**Fig. 8C**). This result mirrored the *in vitro* observations where *arcA*^{C173S} mutants had a significantly lower survival rate compared to WT when treated with CHP (**Fig. 7C**) but showed no apparent defect in the absence of extracellular ROS stress (**Fig. 7B, 5C, 5D and 5E**).

When *arcA*^{C233S} mutants were competed against WT in adult CD-1 mouse colonization, in line with the infant mouse experiment results, *arcA*^{C233S} mutants have a colonization defect (**Fig. 8D**). Although *arcA*^{C233S} mutants are not as strongly disadvantaged as *arcA*^{C173S} mutants in a normal adult mouse gut, the addition of NAC in the mouse drinking water failed to fully alleviate the colonization disadvantage, only slightly improving *arcA*^{C233S} mutant colonization with competitive indices under 1 (**Fig. 8D**), similar to that seen with Δ*arcA* mutants (**Fig. 8B**).

The growth experiment, the *in vitro* CHP challenge, and the *in vivo* colonization experiment suggest that while ArcA^{C233S} lost many of the essential ArcA functions, ArcA^{C173S} can carry out most, if not all, of ArcA functions, except for when ROS is present.

C173 affects ArcA transcriptional regulator activity during ROS exposure

Since ArcA is active as a transcriptional regulator, we wanted to test if C173 plays a role in the proper functioning of ArcA regulatory activities in the context of ROS exposure. In order to do this, we need to use a gene within the ArcA regulon as a reporter of ArcA activities. *sdhC* encodes a succinate dehydrogenase which is part of the TCA cycle. It is known to be directly repressed by phosphorylated ArcA in *E. coli* [65]. A Vibrionaceae ArcA binding position weight matrix was reported from a comparative genomic analysis [69]. When used to generate a sequence logo, the resulting Vibrionaceae ArcA binding motif, GTTAATTAAATGTTA (**Fig. 9A**), highly resembles that of the reported *E. coli* ArcA box [65], containing two direct repeats with a center-to-center distance of approximately 10bp. We scanned the *V. cholerae* O1 biotype El tor genome with this motif and confirmed an ArcA box (GTTGAATAAATGTTA) 73bp upstream of the *V. cholerae sdhC* gene (VC2091). Therefore, we examined the transcription profile of *sdhC* in WT (*lacZ*-), Δ*arcA* mutants (*lacZ*-), and *arcA^{C173S}* mutants under ArcA activating conditions, in the absence or in the presence of CHP. Using a transcriptional fusion of the *sdhC* promoter to a promoterless *lacZ* gene on a plasmid (pAH6), we quantified the transcription of *sdhC* by β-galactosidase activities. Since the assay subject mid-log phase cells to a 1hr CHP treatment, the viable CFU in the culture is not best reflected by OD_{600}. Instead, viable CFU at the time of assay were determined by serial diluting the cultures and subsequently spotting 5μl of each dilution on an LB agar plate. Accordingly, instead of using OD_{600} to normalize the β-galactosidase activity for Miller Unit calculations, β-galactosidase activity was quantified in special units (SU) that result from normalizing OD_{420} signals from β-galactosidase activity against every 10E6 CFU. To ensure the consistency of CHP treatment, as considerable stochasticity is often seen with ROS treatments, and to ensure adequate number of viable cells post CHP treatment for meaningful levels of

enzymatic activities, CHP-treated samples that have a 10%-20% survival rate as calculated by CFU in CHP treated/control of the respective strain were analyzed for β-galactosidase activity levels.

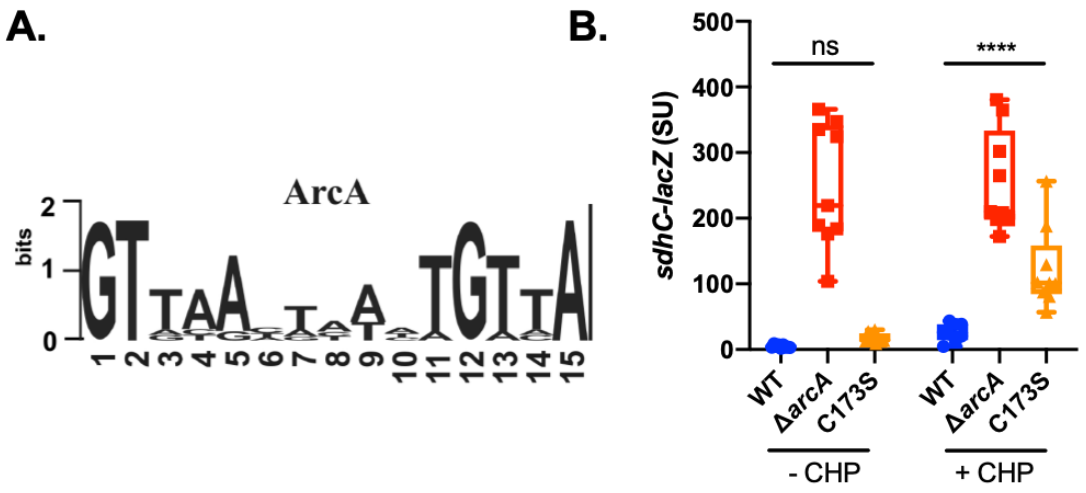

Figure 9: ArcA^{C173S} variant failed to repress *sdhC* expression in the presence of ROS

A. The Vibrionaceae ArcA binding box logo constructed based on reported predicted position weight matrix (Ravcheev et al., 2007). **B.** The expression of *sdhC* as quantified by β-galactosidase activities in special units (SU) normalized by per million CFU, n=9 from 3 independent experiments.

Indeed, *V. cholerae* ArcA represses the expression of *sdhC* under the microaerobic virulence inducing condition we tested, as shown by the much higher levels of β-galactosidase activity in the absence or in the presence of CHP in Δ*arcA* mutants compared to WT (**Fig. 9B**). In the absence of ROS, *arcA^{C173S}* mutants showed similarly low levels of *sdhC* expression compared to WT, suggesting repression activities on the *sdhC* promoter from ArcA^{C173S} (**Fig. 9B**). When challenged by CHP, ArcA repression on the *sdhC* promoter is slightly lifted, as seen in the slight increase in *sdhC* expression in WT under CHP treatment compared to untreated WT; nonetheless, much of the repression is retained (**Fig. 9B**). However, *arcA^{C173S}* mutants when challenged by CHP, had approximately 5-fold higher *sdhC* expression compared to WT under the same condition, suggesting an ROS-mediated weaker repression on the *sdhC* promoter from ArcA^{C173S} compared to ArcA^{WT} (**Fig. 9B**). This ROS-dependent and C173-dependent ArcA

regulation of *sdhC* expression supports our hypothesis that C173 is a redox sensing cysteine key to ArcA regulatory functions.

Collectively, we identified *V. cholerae* ArcA as a protein containing reversibly oxidizable cysteine residues. Both ArcA cysteine residues, C173 and C233, are in the C-terminal DNA binding domain and can be reversibly oxidized in the presence of ROS, suggesting possible redox-sensing roles for both. C233, in addition, is instrumental in basic ArcA functions, possibly by maintaining proper critical conformations for the enzyme, as a point mutation at this residue results a strain with phenotypes highly comparable to that of Δ*arcA* mutants. C173's role is not evident under normal conditions, but when *V. cholerae* are exposed to ROS, C173 plays a critical part in maintaining ArcA functions as seen in the C173-dependent *in vitro* ROS resistance, the C173-dependent colonization of ROS-rich mouse guts, and the C173-dependent *sdhC* repression during ROS exposure.

CHAPTER 3: Biochemical studies of ArcA activities

Introduction

Response regulators (RRs) are defined by the presence of a receiver (REC) domain. A REC domain has a primary sequence encoding five consecutive β-sheet-α-helix elements joined by linker sequences. These secondary structures are spatially arranged such that the five α helices surround the five parallel β sheets in the 21345-topology in the middle. The highly conserved phosphorylation site is located at the C terminus of β3. The RRs are categorized into subfamilies based on the presence, functions, and structural similarities in their C-terminal effector domains. While some RRs have enzymatic output domains, as seen in the *V. cholerae* VieA, VieB and HnoB, most RRs contain a DNA-binding effector domain. The structure of these DNA-binding (DBD) domains further categorizes RRs into three major subfamilies: the OmpR/PhoB, NarL/FixJ, and NtrC/DctD subfamilies encompassing the majority of bacterial RRs that deliver an transcriptional response to signal perception[131].

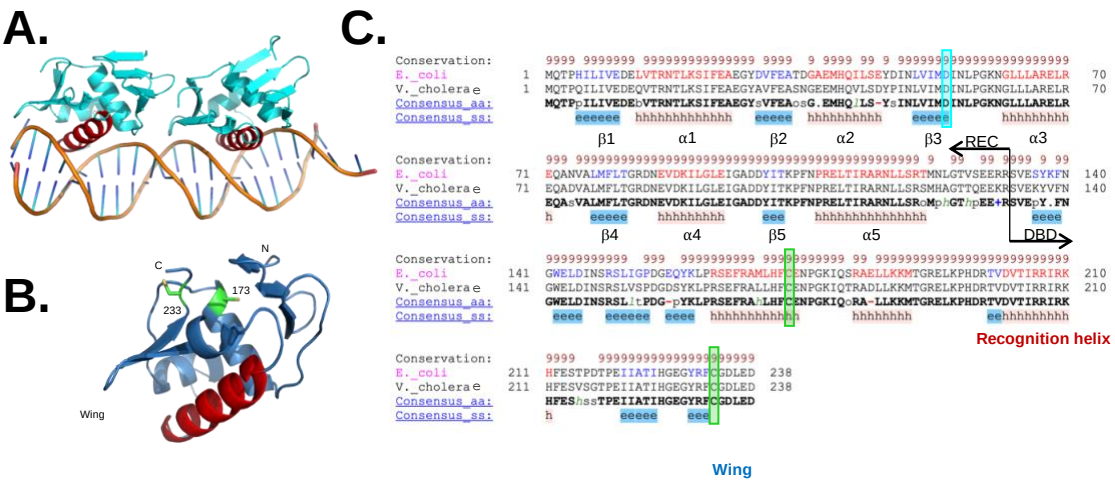

Figure 10: ArcA is a PhoB/OmpR family response regulator

A. Crystal structure of two truncated *E. coli* PhoB C-terminal DNA-binding domains bound to DNA with their respective recognition helix colored in red. **B.** Homology model of ArcA C-terminal DNA-binding domain constructed based on one of the PhoB protomers bound to DNA (PDB ID: 1GXP). The N and C termini of the domain and the wing motif are labeled. The recognition helix that would interact with the major groove DNA is colored red. The two cysteine residues are highlighted in green with side chains shown as sticks. **C.** An alignment of *E. coli* and *V. cholerae* ArcA amino acid sequence and predicted secondary structure generated by PROMALS3D. β sheet sequences are marked in blue and α helix sequences in red. The receiver (REC) and DNA-binding (DBD) domains are indicated. The phosphorylation site D54 is highlighted in cyan, the cysteine residues C173 and C233 are highlighted in green.

ArcA contains a C-terminal winged-helix DBD domain characteristic to a PhoB/OmpR subfamily RR, the most abundant RR subfamily widely distributed in all bacterial phyla. This family of RRs usually have their REC and DBD domains tightly packed in the absence of phosphorylation, conferring an inactive state of the regulator. The α1-α5 and the α4-β5-α5 faces in the REC domain contain residues that facilitate salt bridge formations and hydrophobic interactions [132–134]. These non-covalent interactions allow the RR protomers to exist in an equilibrium of monomers and dimers. Phosphorylation at the conserved aspartate residue in the REC domain opens up the REC-DBD interface, driving the monomer-dimer equilibrium toward the dimer form through interactions in the α4-β5-α5 face, facilitating an active conformation of the RR for DNA binding[135]. The active conformation allows proper alignment of the DBD domains, forming a structure that allow the recognition helices to interact with the direct repeat motif on target DNA sequences (**Fig. 10A**). This active conformation promotes RR-DNA binding and subsequently activation or repression of genes regulated by the RR. As seen in the PhoB/OmpR family response regulator RitR in *S. pneumoniae*, the redox state at C128 in the linker region between the N-terminal REC domain and the C-terminal DBD domain modulates the conformation of the RitR monomer. Oxidation at C128 disrupts the REC-DBD packing, making the DBD available for dimerization and DNA binding, therefore activating RitR regulatory function[116]. It is worth noting that this process is independent of phosphorylation. The RitR REC domain does not contain a phosphorylation site, oxidation at the C128 position is sufficient to relay the external signal to activate the RR for its transcriptional activities[136].

E. coli ArcA is shown to oligomerize upon phosphorylation to up to octamers *in vitro*[137]. The binding motif of ArcA box in *E. coli* is an 18bp sequence motif with two direct repeat elements [138]. Some promoters in the *E. coli* ArcA regulon have up to five direct repeat elements in the ArcA binding region, further supporting the model where ArcA's regulatory activities are active with a collaborative binding of multiple ArcA monomers at the promoter sequence [65,139]. The *V. cholerae* ArcA contains a typical PhoB/OmpR family winged-helix C-terminal DNA-binding domain (**Fig.**

10B). The cysteine residues C173 and C233 flank the wing-helix motif, with C233 in a mobile region where it could adopt a position to interact with C173 (**Fig. 10B and 10C**). The *V. cholerae* ArcA is 88% identical to the *E. coli* ArcA, with important secondary structures fully conserved (**Fig. 10C**). The predicted Vibrionaceae ArcA box also contains two direct repeats (**Fig. 9A**), suggesting the possibility of a head-to-tail tandem docking of two ArcA protomers at the binding sequence. It is highly plausible that ArcA is in proximity of other ArcA monomers when activated, whether this ArcA-ArcA interaction happens simultaneously at the promoter sequence when individual ArcA monomers bind to the ArcA box, or forms prior to localizing to the promoter.

Here we investigated with biochemical assays, the effect of oxidation on ArcA's ability to be phosphorylated, to bind to DNA, and to interact with other ArcA monomers, with special attention to the role of C173 in these processes.

Results

ROS exposure abolishes ArcA phosphorylation in *V. cholerae*

As ArcA's regulatory function appear to be largely retained during ROS insults (**Fig.9B**), we want to test the effect of oxidative stress on ArcA phosphorylation, the known mechanism to achieve an active ArcA conformation for regulatory functions. *V. cholerae* C6706 WT with a pTara plasmid encoding the T7 RNA polymerase that over expresses His_6-$ArcA^{WT}$ under the control of a T7 promoter on a pET41 plasmid were grown under microaerobic conditions in the absence or in the presence of CHP for 3hrs following 2hrs of protein induction. Cell lysates were then immediately loaded onto a freshly made manganese-based phos-tag SDS-polyacrylamide gel for electrophoresis followed by an anti-His western blot to visualize ArcA phosphorylation. *V. cholerae* C6706 Δ*arcB* mutants hosting the same plasmids for $ArcA^{WT}$ expression and *V. cholerae* C6706 WT expressing His_6-$ArcA^{D54A}$, the phosphorylation deficient ArcA variant, were also examined as controls. Phosphorylated proteins have higher affinities to the positively charged manganese cations immobilized to the SDS-polyacrylamide gel by the phos-tag reagents, therefore migrating slower compared to their unphosphorylated counterparts [140]. In the

absence of CHP, *V. cholerae* C6706 WT expressing His_6-$ArcA^{WT}$ appeared as two bands, with the majority being phosphorylated (**Fig. 11A**). Although less in Δ*arcB* mutants grown under the same microaerobic conditions, ArcA is still phosphorylated in the absence of its cognate kinase ArcB (**Fig. 11A**). This suggests that ArcA can be phosphorylated by alternative kinases or small molecule donors, expanding ArcA activation beyond the ArcB-specific phosphorylation. *V. cholerae* C6706 WT expressing His_6-$ArcA^{D54A}$ appeared as a single band corresponding to the unphosphorylated species, indicating ArcA phosphorylation absolutely requires D54 as the reception site (**Fig. 11A**). In the presence of CHP, however, *V. cholerae* C6706 WT expressing His_6-$ArcA^{WT}$ no longer have phosphorylated ArcA, appearing as a single band similar to the His_6-$ArcA^{D54A}$ sample (**Fig. 11A**). This suggests that an extracellular ROS exposure abolishes existing phosphorylation or prevents phosphorylation altogether for the cytosolic ArcA.

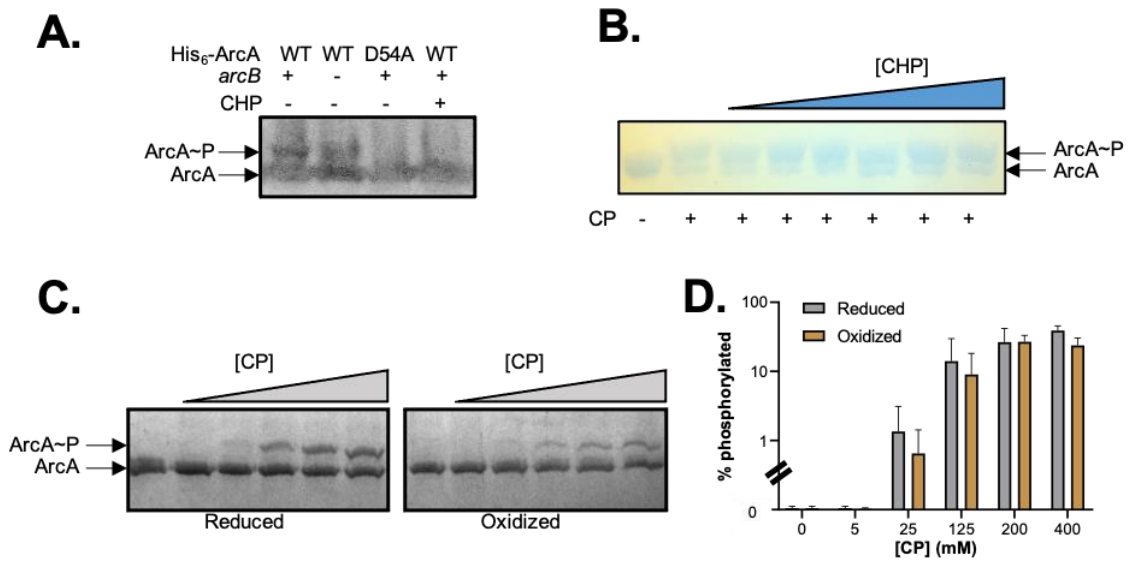

Figure 11: Oxidation does not aid phosphorylation.

A. A Mn-based phos-tag gel followed by western blot showing the effect of ROS exposure on *V. cholerae* cells over expressing His_6-tagged ArcA variants. His_6-$ArcA^{WT}$ is phosphorylated under microaerobic growth in WT, and less so in Δ*arcB* mutants. $ArcA^{D54A}$ cannot be phosphorylated in WT under the same growth conditions. $ArcA^{WT}$ phosphorylation is abolished in the presence of extracellular CHP. **B.** *In vitro* phosphorylated $ArcA^{WT}$ were subsequently exposed to 0, 2, 10, 20, 40, 60 or 80μM of CHP to test the effect of oxidation on phosphorylation. CHP did not affect existing phosphorylation on His_6-$ArcA^{WT}$ in the *in vitro* condition tested. **C.** Reduced or oxidized (by GSSG) His_6-$ArcA^{WT}$ were subsequently phosphorylated by increasing concentrations of carbamoyl phosphate (CP) to test the susceptibility for phosphorylation with regard to oxidation state. No effect was seen. **D.** Quantification of the band intensities in phos-tag electrophoresis analyses similar to the one shown in C. by FIJI or Biorad for the ratio of phosphorylated/unphosphorylated ArcA from three independent experiments.

This observation challenges that of *sdhC* expression where ArcA function is retained in the presence of ROS (**Fig. 9B**). We then tested with purified $ArcA^{WT}$ if oxidation dephosphorylates phosphorylated ArcA. ArcA phosphorylated by small molecule donor carbamoyl phosphate (CP) were exposed to a gradient of CHP concentrations from 0 to 80μM final concentrations and analyzed on a Mn-based phos-tag SDS-polyacrylamide gel followed by Coomassie staining to visualize the phosphorylation state. It appears that up to 80μM of CHP does not dephosphorylate existing ArcA phosphorylation, as all the CHP-challenged phosphorylated samples showed very similar migration patterns to an unchallenged phosphorylated $ArcA^{WT}$ (**Fig. 11B**).

Similarly, we characterized oxidation's effect on ArcA susceptibility for phosphorylation. Although phosphorylation state characterization of ROS-treated cell lysate suggest a negative effect from oxidation to phosphorylation (**Fig. 11A**), oxidation may facilitate unpacking of the N-terminal REC domain and the C-terminal DBD domain for a more permissive phosphorylation, as supported by a recent characterization of *Salmonella* ArcA showing that an ROS exposure increased ArcA phosphorylation [141]. Purified *V. cholerae* $ArcA^{WT}$ first underwent mock or oxidation treatment preceding to an incubation with a gradient of CP from 0 to up to 400mM and analyzed on a Mn-based phos-tag SDS-polyacrylamide gel followed by Coomassie staining for visualization. A larger population of the phosphorylated species at a lower CP concentration would indicate more receptivity for phosphorylation. However, for the *in vitro* conditions tested, oxidation of ArcA does not have an effect either way, neither preventing nor promoting phosphorylation (**Fig. 11C**). The ratios of the phosphorylated and unphosphorylated species in the mock and the oxidation treated $ArcA^{WT}$ are very comparable in all the CP concentrations tested. We can see that ArcA phosphorylation is saturated in this *in vitro* condition beyond 200mM, as increasing the CP concentration from 200mM to 400mM did not further increase the percentage of phosphorylated $ArcA^{WT}$ (**Fig. 11C and 11D**). Taken together, we see that oxidation subsequent to

phosphorylation does not nullify phosphorylation. Conversely, there is a lack of preference for ArcA oxidation state with respect to phosphorylation. These *in vitro* results lead us to believe that oxidation may not be directly coupled to phosphorylation and may be impacting ArcA activities in alternative ways.

Phosphorylation and C173-dependent oxidation promote ArcA-DNA binding

Since $ArcA^{WT}$ seems to retain its regulatory activity under ROS stress as seen in the example of *sdhC* repression (**Fig. 9B**), yet ArcA phosphorylation is compromised under ROS exposure in *V. cholerae* cells (**Fig. 11A**), we reasoned that oxidation inflicted by extracellular ROS act in place of phosphorylation in inducing a functionally active conformation in ArcA.

To test this, we performed electrophoretic mobility shift assays (EMSAs) using purified $ArcA^{WT}$, $ArcA^{C173S}$, and $ArcA^{D54A}$ proteins with the *sdhC* promoter. Each ArcA variant protein was tested for their ability to form protein-DNA complexes under three conditions: reduced without phosphorylation, reduced with phosphorylation, or oxidized without phosphorylation. $ArcA^{WT}$ forms a protein-DNA complex when phosphorylated or oxidized, but not in its mock-phosphorylation treated reduced form, suggesting an activating effect from either phosphorylation or oxidation (**Fig. 12A**). Without the suspected redox-sensing cysteine residue, C173, $ArcA^{C173S}$ still binds to DNA when phosphorylated, but oxidation no longer have an activating effect for DNA binding. Without the phosphorylation site D54, $ArcA^{D54A}$ does not respond to phosphorylation, but forms a protein-DNA complex when oxidized (**Fig. 12A**). Taken together, these data demonstrate that ArcA binding and repression of the *sdhC* promoter can be activated via a C173-reliant oxidation, independent of a D54-reliant phosphorylation.

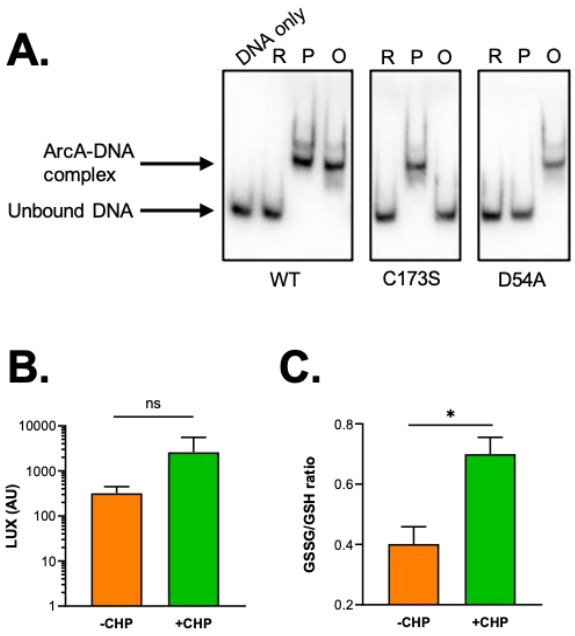

Figure 12: C173-dependent oxidation activates ArcA DNA-binding

A. EMSA migration patterns of purified ArcA proteins with a *V. cholerae sdhC* promoter. Purified tag-less $ArcA^{WT}$, $ArcA^{C173S}$, and $ArcA^{D54A}$ were treated *in vitro* such that they were in a reduced unphosphorylated (R), reduced phosphorylated (P), or oxidized unphosphorylated (O) state prior to incubation with *sdhC* promoter DNA. The protein-DNA mix were separated on a native gel at 4°C degrees prior to development and imaging on a Typhoon phosphorimager. $ArcA^{WT}$ forms a complex with the *sdhC* promoter when phosphorylated or when oxidized (by GSSG). $ArcA^{C173S}$ binds upon being phosphorylated but no longer respond to oxidation. $ArcA^{D54A}$ binds upon being oxidized but no longer respond to phosphorylation. **B.** The total intracellular glutathione content (GSH+GSSG) of *V. cholerae* C6706 WT grown under virulence inducing conditions in the absence or in the presence of CHP in the media as quantified by a luminescent readout from a GSH/GSSG-Glo assay (Promega). **C.** The intracellular GSSG/GSH ratio of *V. cholerae* C6706 WT grown under virulence inducing conditions in the absence or in the presence of CHP as calculated based on the luminescent readout from a GSH/GSSG-Glo assay. Data collected from three independent experiments.

Redox-sensing regulators are known to have preferential responsiveness to oxidants, many only respond to specific oxidants [99]. RitR, the PhoB/OmpR family RR with demonstrated cysteine-mediated redox sensing, dimerizes only upon H_2O_2 exposure, but remains as monomers when exposed to other oxidants such as CHP [116]. Conforming to this convention, the oxidation activation of ArcA is specific to the oxidant, oxidized glutathione (GSSG). No protein-DNA complex is formed from oxidation imposed by $CuSO_4$, $CuCl_2$, CHP, or H_2O_2. Indeed, upon extracellular CHP exposure to *V. cholerae* WT C6706, although the total glutathione level only slightly increased, the GSSG/GSH ratio almost doubled, increasing from approximately 0.37 without CHP to about 0.73 with CHP (**Fig. 12B and 12C**). The intracellular GSSG/GSH ratio

increase under extracellular ROS exposure provides more GSSG acting as a direct oxidant for the cytosolic ArcA, which activate ArcA for DNA binding.

C173-dependnet oxidation enhance ArcA-ArcA interaction

To further investigate the activating effect of oxidation on ArcA, we examined how oxidation affects ArcA-ArcA interactions. *E. coli* ArcA form dimers upon phosphorylation, and *in vitro* phosphorylation can lead to the formation of higher orders of oligomers such as a ArcA-P tetramer or an ArcA-P-ArcA hybrid octamer [134,137137]. The predicted Vibrionaceae ArcA binding motif, with two direct repeat elements (**Fig. 9A**), is highly similar to the *E. coli* ArcA box [65]. The high homology between the *V. cholerae* and *E. coli* ArcA sequences (**Fig. 10C**) and similar binding site architectures with more than one recognition element suggest possible cooperative occupancy of multiple *V. cholerae* ArcA monomers at promoters of ArcA regulated genes. In other words, ArcA-ArcA interaction can be crucial in activating *V. cholerae* ArcA regulatory activities. We hypothesized that oxidation promotes ArcA-ArcA interaction, leading to activation.

To quantify the interaction of *V. cholerae* ArcA, we utilized a bacterial two-hybrid system (BacTH) for detection of protein-protein interaction [142]. We constructed translational fusions of *V. cholerae* ArcA variants with T25 and T18, two fragments of the catalytic domain of the *Bordetella pertussis* adenylate cyclase (CyaA) that require physical proximity to produce cyclic adenosine monophosphate (cAMP). A plasmid carrying T25 - $ArcA^{var}$ and another for T18 - $ArcA^{var}$ with ArcA variants translationally fused to the C-termini of the catalytic domains, are introduced combinatorically to a *E. coli* BTH101 (Δ*cyaA*) background where the native adenylate cyclase is disrupted. By appending the T25 and T18 domains to the N-termini of ArcA variants, the interference from the additional domain to behaviors of ArcA cysteine residues, both in the C-terminal of ArcA, is minimized. In this experimental design, interactions between the proteins fused to the T25 and the T18 domains bring the two fragments together, generating varying amounts of cAMP that activates the transcription of the chromosomal *lacZ* gene in BTH101, resulting in quantifiable β-galactosidase activities that reflect the level of ArcA interactions.

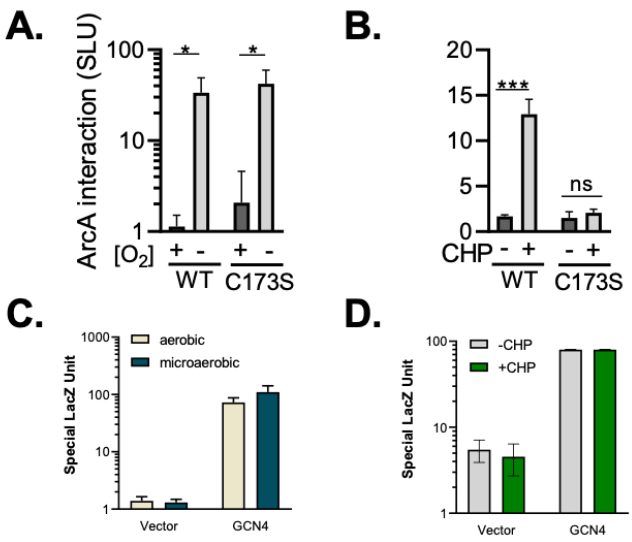

Figure 13: CHP exposure induces ArcA-ArcA interactions

A. Quantification of ArcA^{WT}-ArcA^{WT} or ArcA^{WT}-ArcA^{C173S} under aerobic or microaerobic growth by a bacterial two hybrid system (BacTH) by β-galactosidase activities normalized to OD_{600} with adjustments in reaction volume and shown in special lacZ units (SLU), N=6. ArcA interaction is promoted by microaerobic growth for either interaction pairs. **B.** BacTH experiment showing ArcA^{WT}-ArcA^{WT} or ArcA^{WT}-ArcA^{C173S} under aerobic growth in the absence or in the presence of CHP in the growth media. ArcA interaction is promoted by CHP exposure in a C173-dependent manner. **C and D** show the behaviors of the positive control (with leucine zipper containing small peptides GCN4 as interacting partners) and the negative control (empty vector carrying only the sequences encoding the T18 and T25 catalytic domains), under the respective conditions. The dynamic range shown and respective signals from the positive and negative controls validates the BacTH assays in the conditions tested.

Mirroring the *in vitro* conditions used in the EMSA experiments, we examined the interactions between *V. cholerae* ArcA variants with the *E. coli* BacTH system under three corresponding conditions: aerobic growth for reduced without phosphorylation, microaerobic growth for reduced with phosphorylation, or aerobic growth with CHP exposure for oxidation without phosphorylation. The BacTH system has an adequate dynamic range as indicated by the signal differences across all the conditions tested between the positive control carrying the leucine zipper domains from a yeast transcription factor (GCN4) and the negative control with standalone T18 or T25 domains of CyaA (**Fig. 13C and 13D**). ArcA^{WT}-ArcA^{WT} interaction in aerobically grown cells is almost comparable to negative control, indicating little ArcA-ArcA interaction under the non-stimulating condition. In comparison, cells grown microaerobically showed much higher ArcA^{WT}-ArcA^{WT} interactions, consistent with the assumption that ArcA becomes phosphorylated under low

oxygen conditions, and that phosphorylation promotes ArcA-ArcA interaction (**Fig. 13A**). When one of the interacting partners have a C173S mutation, the basal level of ArcA-ArcA is slightly increased under aerobic conditions, but a microaerobic condition induces a much higher level of $ArcA^{WT}$-$ArcA^{C173S}$ interactions, similar to that of microaerobic $ArcA^{WT}$-$ArcA^{WT}$ interaction (**Fig. 13A**). This corroborates the EMSA result that a C173S mutation does not affect ArcA's response to phosphorylation (**Fig. 12A**), in this case phosphorylation-dependent enhanced interaction as a response to low oxygen. Elevated interactions between $ArcA^{WT}$-$ArcA^{WT}$ were seen when aerobically grown cells were exposed to CHP (**Fig. 13B**), as signified by the approximately 7-fold increase in β-galactosidase activities compared to the untreated cells. However, when one of the interacting partners have a C173S mutation, CHP exposure no longer increase $ArcA^{WT}$-$ArcA^{C173S}$ interactions (**Fig. 13B**). Conforming with the EMSA data, where either phosphorylation or oxidation have an activating effect for ArcA-DNA binding activity (**Fig. 12A**), the BacTH experiments showed that either a microaerobic growth condition or an exposure to CHP under a non-stimulating aerobic growth condition promote ArcA-ArcA protein interactions. The ROS-dependent interaction relies on an intact C173 residue, echoing our previous conclusion that phosphorylation and C173-dependent oxidation are two post-translational modifications capable of activating ArcA regulatory functions.

Phosphorylation, but not oxidation, decreases *V. cholerae* ArcA solubility

Considering ArcA dimerizes upon phosphorylation in *E. coli*, and that both phosphorylation and oxidation promote *V. cholerae* ArcA-ArcA interactions, we hypothesize that these post translational modifications have similar effects on the oligomeric state of *V. cholerae* $ArcA^{WT}$. Hoping to determine the oligomeric states of ArcA under these conditions, we attempted an analysis of purified $ArcA^{WT}$ by size exclusion chromatography (SEC). $ArcA^{WT}$ phosphorylated by carbamoyl phosphate or oxidized by GSSG showed DNA-binding activities in EMSAs 6hrs after the *in vitro* reactions, suggesting the presence of DNA-binding active species throughout the 1-hour duration of the SEC. Immediately subsequent to the respective reactions with the same starting concentrations of $ArcA^{WT}$, phosphorylated, oxidized or mock treated $ArcA^{WT}$ were spun at

17,000 rcf for 30min at 4°C to exclude any insoluble species arisen during respective reactions. *E. coli* ArcA has been reported to fall out of solution upon phosphorylation in solution analysis[134]. Similarly, we see a significant decrease of soluble ArcA after phosphorylation reaction, with only around 10% of starting protein content in the supernatant (**Fig. 14A**). Solubility is calculated as a percentage of the protein content in the supernatant after a spin over that of an unspun sample as determined by Bradford assays. In contrast, oxidation by GSSG does not change the solubility of ArcA, as oxidized ArcA showed similar solubilities to mock treated ArcA at approximately 50% even after a second spin of the supernatant at an ultracentrifugal speed of 100,000 rcf for 30min at 4°C (**Fig. 14A**).

The soluble $ArcA^{WT}$ of respective reactions, in this case the supernatants derived from the 17,000 rcf centrifugation, were filtered through a 0.22um filter and subject to SEC to determine the oligomeric states resulting from phosphorylation or oxidation. A Superose 6 Increase 10/300 column with a bed volume of 24ml was coupled to an AKTA pure system at 4°C to separate soluble $ArcA^{WT}$ subsequent to the aforementioned treatments. An 8.4ml void volume was determined based on the blue dextran (2000kDa) elution volume. Calibration runs with urease, BSA and carbonic anhydrase resulted a Kav/Mw plot with a R^2 of 0.9899, establishing a correlation between the elution volume and the molecular weight (**Fig. 14B**). Among these, the 29kDa carbonic anhydrase eluting at 18.75ml serves as an important point of reference as it is very close in size to an His_6-ArcA monomer which is around 28kDa. The eluent from the column was collected in 0.5ml fractions and protein concentrations in fractions with positive OD_{280} readings were determined by Bradford assays.

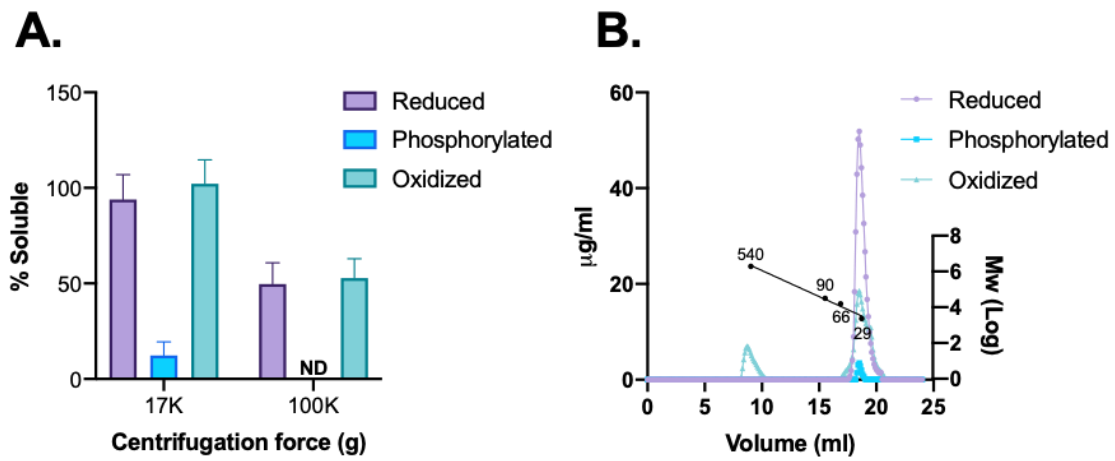

Figure 14: Size-exclusion chromatography analysis of *V. cholerae* ArcA oligomeric state

A. Solubility of reduced unphosphorylated, reduced phosphorylated, or oxidized unphosphorylated ArcA^{WT} after 30min of centrifugation at respective centrifugal forces. Solubility were calculated as the percentage of protein concentrations in the supernatant divided by that in the unspun reaction, N=4. **B.** The chromatographs of elution pattern of reduced (lavender), phosphorylated (blue), or oxidized ArcA^{WT} (turquoise) on an AKTA pure system with a Superose 6 Increase 10/300 column at a 0.5ml/min flow rate. The following molecular weight standards were used for calibration of the size-exclusion column (R^2=0.9899): blue dextran (2000kDa), urease hexamer (540kDa), urease monomer (90kDa), BSA (66kDa), and carbonic anhydrase (29kDa). Loading concentrations of 5.6uM were used for reduced and oxidized ArcA^{WT}, and 0.5uM for phosphorylated ArcA^{WT}.

As expected, the total area under the curve from the chromatograph for the phosphorylated ArcA^{WT} sample is much lower compared to the other two conditions, suggesting protein falling out of solution into the pellet prior to loading the supernatant onto the column (**Fig. 14A and 14B**). The peak elution volume of 18.5ml corresponds to that of an ArcA monomer, suggesting the small soluble fraction of phosphorylated ArcAWT as monomers (**Fig. 14B**). Mock-phosphorylation treated reduced ArcA^{WT} also eluted at 18.5ml, indicating a monomeric state of the protein in a reduced unphosphorylated state (**Fig. 14B**). Oxidized ArcA^{WT}, however, showed two peaks on the chromatograph, first eluting at 8.7ml then again at the 18.5ml (**Fig. 14B**). Since the first elution happened at the void volume, oxidized ArcA^{WT} is likely in an equilibrium between being in a very high order oligomers and being monomers.

Unfortunately, further solution studies such as analytical ultracentrifugation do not apply to analyzing ArcA oligomeric state due to the low solubility of phosphorylated ArcA seen here and

previous studies with *E. coli* ArcA[134]. Without phosphorylated ArcA as a meaningful reference for an active ArcA oligomeric state, it is difficult to draw conclusions from solution analysis of oxidized ArcA alone should any interesting results arise. Although a dramatic effect from an artificial *in vitro* oxidation condition, the observations from the SEC analysis show that oxidation is capable of inducing a change of the $ArcA^{WT}$ oligomeric state from monomeric under reduced condition to higher orders. These results strongly support our hypothesis that oxidation promotes ArcA-ArcA interaction critical in activating ArcA.

Oxidation facilitates the formation of an intramolecular disulfide bond

To further elucidate the nature of this increased ArcA-ArcA interaction that is required to activate ArcA, we examined the non-reducing SDS-PAGE migration patterns of *V. cholerae* C6706 WT hosting His_6-tagged ArcA variants with or without CHP and the reducing agent 2-mercaptoethanol (BME) in the growth media. Cells carrying His_6-tagged $ArcA^{WT}$, $ArcA^{C173S}$, $ArcA^{C233S}$, or $ArcA^{C173SC233S}$ were grown under ArcA-stimulating conditions where protein expression was induced and subsequently challenged with different combinations of CHP and BME.

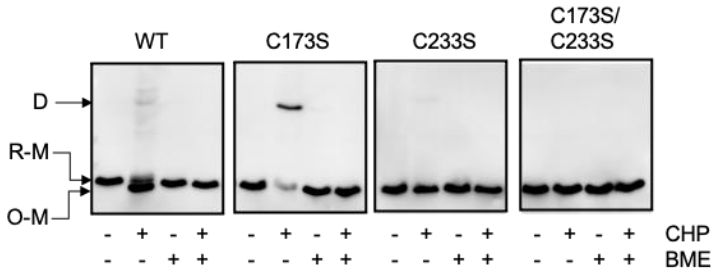

Figure 15: Non-reducing SDS-PAGE analysis for ArcA variants in *V. cholerae*

V. cholerae C6706 WT containing overexpressed His_6-tagged ArcA variants were grown under virulence inducing conditions and induced for protein expression under mock, CHP, BME, or a combination of CHP and BME included in the growth media. Cell lysates were separated on a non-reducing 12% SDS-polyacrylamide gel and His_6-tagged proteins are detected. Extracellular CHP exposure leads to the formation of an intramolecular disulfide bond in ArcA. Without C173, ArcA is prone to dimerizing via C233.

All ArcA variants migrated as a single band to the molecular weight position corresponding to an ArcA monomer in the absence of CHP (**Fig. 15**), suggesting an intracellular environment similar to the reduced conditions from the SEC experiment (**Fig. 14B**). The $ArcA^{WT}$ protein when

exposed to CHP, mostly migrated to a slightly lower position on the non-reducing gel, suggesting the formation of an intramolecular disulfide bond between C173 and C233, as these are the only two cystine residues within ArcA^{WT} (**Fig. 15**). A small fraction of ArcA^{WT} formed dimer under CHP challenge, suggesting the formation of intermolecular covalent bonds. The ArcA^{C173S} protein, unable to form an intramolecular disulfide bond with only an intact C233, mostly migrated to the dimer position when treated by CHP (**Fig. 15**). This suggests that in the absence of C173, when challenged by extracellular CHP, ArcA is prone to dimerize via a C233-dependent intermolecular disulfide bond. Indeed, the ArcA^{C233S} protein, with only an intact C173, formed much less dimer when exposed to CHP (**Fig. 15**). The dimers seen in the ArcA^{WT}, ArcA^{C173S} and ArcA^{C233S} samples when CHP is present are all cysteine-mediated, as the ArcA^{C173SC233S} was unable to form any dimer under the same CHP treatment. These disulfide bonds, inter- or intramolecular, are oxidation-dependent, as the inclusion of reducing agent BME along with CHP in the growth media abrogated these species in all of the ArcA variants (**Fig. 15**).

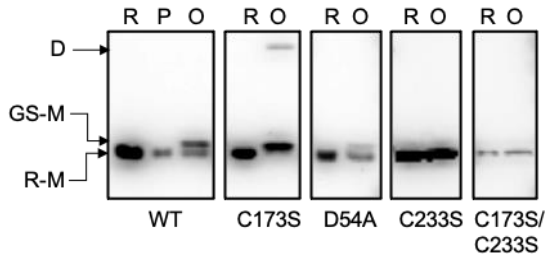

Figure 16: Non-reducing SDS-PAGE analysis of *in vitro* treated purified ArcA variants

Purified ArcA variant proteins were treated *in vitro* by 30μM GSSG or 20mM carbamoyl phosphate prior to non-reducing SDS-PAGE analysis. R denotes mock treated protein in a reduced unphosphorylated state, P denotes phosphorylated protein resulted from *in vitro* phosphorylation in a reduced state by carbamoyl phosphate, and O indicates oxidized unphosphorylated protein resulted from *in vitro* oxidation by GSSG. C233 is susceptible to various oxidation modifications while C173 plays an occluding role in preventing some of the C233 oxidation.

The role of C173 was further validated using *in vitro* oxidation of ArcA variants by GSSG. Purified His_6-ArcA variants were compared under reduced unphosphorylated or oxidized unphosphorylated conditions, with the reduced phosphorylated ArcA^{WT} as an active conformation migration pattern control. Phosphorylated ArcA^{WT} migrated to the exact same location as the

unphosphorylated ArcA^{WT}, at the predicted His$_6$-ArcA size, 28kDa, suggesting a non-covalent nature of the phosphorylation-derived ArcA active conformation (**Fig. 16**). This is in agreement to the structural analysis in *E. coli* that demonstrated ArcA monomers interact through several key residues in the N-terminal REC domain via a hydrophobic patch and salt bridges [134]. When oxidized by GSSG, in addition to the same band seen in the reduced and phosphorylated states, a band with slightly higher molecular weight appeared (**Fig. 16**). As mentioned earlier, glutathione can form disulfide bonds with cysteine-containing proteins, appending a glutathione tripeptide to the protein. This minor shift in oxidized ArcA^{WT} suggests possible glutathionylation when oxidized by GSSG, with a considerable fraction of ArcA^{WT} remaining at the original 28kDa position (**Fig. 16**). ArcA^{D54A} exhibited the same migration pattern as ArcA^{WT}, suggesting similar partial glutathionylation when oxidized by GSSG independent of the integrity of the phosphorylation reception site (**Fig. 16**). When ArcA^{C173S} was subject to the same oxidation, however, none remained at the original size (**Fig. 16**). Instead, ArcA^{C173S} appeared either as a slightly higher position band or as dimers, suggesting ArcA^{C173S} being fully glutathionylated and partially dimerized via its only remaining cysteine residue, C233. This further suggests an occluding role for C173 in preventing some unsought oxidation modifications at C233 to preserve the active ArcA species that migrates to the original position of ArcA. The lack of the suspected glutathionylation band or the dimer band in oxidized ArcA^{C233S} and ArcA^{C173SC233S} mutant samples further corroborated the conclusion that glutathionylation seen in *in vitro* oxidized ArcA^{WT}, ArcA^{D54A}, and ArcA^{C173S}, and dimerization seen in oxidized ArcA^{C173S} act through C233. The absence of the suspected glutathionylated species and the dimer band in the ArcA^{C173SC233S} mutant sample in the presence of CHP further suggest that the formation of those species is cysteine mediated (**Fig. 16**).

Located at the far C-terminus of ArcA and bioinformatically predicted to be exposed, C233 can be particularly vulnerable to unsolicited oxidation that confers an unfavorable conformation of ArcA

for its regulatory functions. Based on the results from the non-reducing SDS-PAGE, C173 is critical in defending C233 from over-oxidation, likely through the formation of an intramolecular disulfide bond, which at the same time, converts ArcA to an active form under oxidation. C173-C173 intermolecular disulfide bond is possible but unlikely, as indicated by the insignificant amount of dimer formed by $ArcA^{C233S}$ under CHP challenge in *V. cholerae* cells and a lack of dimer in *in vitro* oxidized $ArcA^{C233S}$ samples (**Fig. 15 and Fig. 16**). In the absence of C173, ArcA is inclined to form an intermolecular disulfide via the far C-terminal C233, an unanticipated observation as a disulfide bond dimer of $ArcA^{C173S}$ upon oxidation was not reflected in BacTH experiments (**Fig. 13B**). It is possible that with the C233-C233 intermolecular disulfide bond at the far C-termini of $ArcA^{C173S}$ fused to the C-termini of T25 and T18 domains, the catalytic domains are held together in unfavorable special arrangements or are still too distanced from each other to be catalytically active in producing cAMP for β-galactosidase expression.

Taken together, an extracellular ROS exposure from CHP compromises ArcA phosphorylation in *V. cholerae* cells grown under ArcA-stimulating conditions and increases the intracellular GSSG/GSH ratio that allows GSSG to act as a direct oxidant for cytosolic proteins. Oxidation of ArcA induces the formation of an intramolecular disulfide bond that activates ArcA-DNA binding activities and promotes ArcA-ArcA interactions.

CHAPTER 4: Summary and future directions

The importance of the AphB thiol-based switch for transcriptional regulation of virulence as well as ROS resistance motivated the identification of more reversibly oxidizable thiol-containing proteins in *V. cholerae*. We performed a proteomic mass spectrometry analysis on samples of *V. cholerae* cells challenged with cumene hydroperoxide under virulence inducing growth conditions, subsequently labeled by iodoacetamide targeted at reversibly oxidized cysteine residues. Among the identified proteins is ArcA, the response regulator in the ArcAB two-component system, a global regulator for energy metabolism transition from an aerobic to a more anaerobic lifestyle. In chapter 2, we show that both cysteine residues on ArcA, C173 and C233, are in the DNA-binding domain of the response regulator and amenable to reversible oxidation. C233 is likely crucial in providing structural integrity to ArcA, as a mutation at this residue renders severe defects in growth, infant mouse colonization, sensitivity to the toluidine blue dye and hydrogen peroxide. C173 shows redox reactive properties that is critical in maintaining ArcA functions under ROS stress. A C173S mutation compromises *V. cholerae*'s ability to sustain cumene hydroperoxide exposure *in vitro* and to colonize ROS-rich mouse guts, possibly due to obstructed ArcA regulatory functions owing to a failure to respond via the C173 residue. In chapter 3, we present biochemical evidence of an oxidation-dependent activation mechanism of ArcA regulatory function. We show that an extracellular ROS exposure abolishes ArcA phosphorylation in *V. cholerae* that are grown microaerobically under a virulence inducing condition and increases the intracellular oxidized to reduced glutathione ratio (GSSG/GSH). Either D54-dependent phosphorylation or C173-dependent oxidation promotes ArcA-DNA binding. ArcA-ArcA interaction is high under an ArcA stimulating condition of microaerobic growth or in the presence of ROS under a non-stimulating aerobic growth condition. Oxidation of ArcA promotes a transition of ArcA monomers into higher order oligomeric states.

Working model of ArcA activation

The current knowledge suggests the following working model for an oxidative stress response mechanism by the *V. cholerae* ArcB/A two-component system. In the reducing cytosolic space without phosphorylation, the REC and DBD domains of ArcA are closely associated to one

another in a conformation that inhibits dimerization for active DNA-binding, typical to a PhoB/OmpR subfamily response regulator. Under a microaerobic growth condition, phosphorylation at the D54 residue disrupts the REC-DBD interface, allowing for dimerization of ArcA, possibly via the α4-β5-α5 faces in the REC domain. The resulting formation of ArcA dimers are capable of DNA-binding and transcriptional regulation. In the presence of extracellular ROS, ArcA phosphorylation is abolished in *V. cholerae* either by inhibited phosphorylation from possible kinases and phosphoryl donors, or by enhanced phosphatase activities. The cytosolic space transiently becomes more oxidative, facilitating the formation of an intramolecular disulfide bond between C173 and C233 within an ArcA monomer. The intramolecular disulfide bond likely increases the association constant, promoting ArcA-ArcA interactions and collaborative binding at the promoters of ArcA-regulated genes (**Fig. 17**). This ROS-induced conformation, although different from the phosphorylation-mediated conformation, allows ArcA to bind to DNA, which retains its transcriptional regulatory functions under ROS exposure.

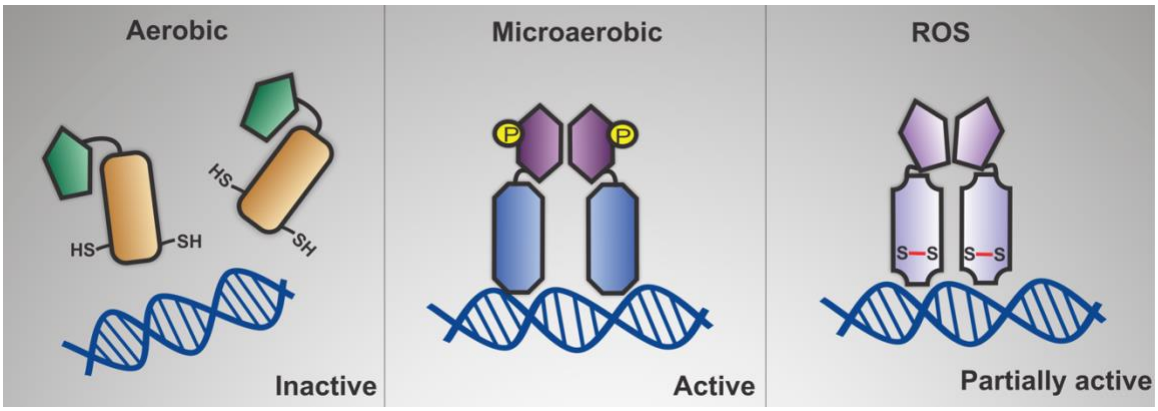

Figure 17: Working model for ArcA activation in *V. cholerae*

A pictorial representation of ArcA activation in *V. cholerae*. The N-terminal receiver domain (REC) (green in the aerobic panel) and the C-terminal DNA-binding domain (DBD) (orange in the aerobic panel) are linked by a flexible linker region. The cysteine residues sulfhydryl sidechains (-SH) in the DBD are indicated. ArcA in the reduced unphosphorylated state is in an inactive form as monomers. A microaerobic environment facilitates phosphorylation at the D54 residue in the REC domain, facilitating ArcA-ArcA interaction through non-covalent interactions such as hydrophobic interactions and salt bridges mediated by the α4-β5-α5 faces in the REC domain, resulting an active conformation in the DBD domain that allows DNA binding. When challenged by ROS, the cysteine residues C173 and C233 in the DBD domain form an intramolecular disulfide bond, introducing a conformational change that promotes ArcA-ArcA interaction and DNA-binding. Shapes are not drawn to scale, relative positions and orientation of domains are simply illustrative, not to strictly reflect reality.

ArcA cysteine residues are conserved across different bacterial species

The ArcB/A TCS is a major oxygen-sensing signal transduction system, regulating lifestyle transitions in many facultative anaerobic proteobacteria. *V. cholerae* have the *arcA* (VC2368) and *arcB* (VC2369) genes next to each other in a tail-to-tail arrangement on chromosome I. Most other bacteria including *E. coli* have a carbon source-responsive (Cre) two-component system (*creABCD*) operon immediately downstream to the *arcA* gene, with their *arcB* in a totally different genetic neighborhood [143] (**Fig. 18**). This close association of *arcB* and *arcA* in *V. cholerae* is suggestive of either a higher co-evolution pressure for these individual components in the ArcAB TCS in *V. cholerae* or a co-selection for the Cre TCS with ArcA in other bacteria for yet to be identified reasons, possibly attributing to the collaborative nature of the two TCSs in carbon metabolism necessary for the lifestyle of the bacteria in question.

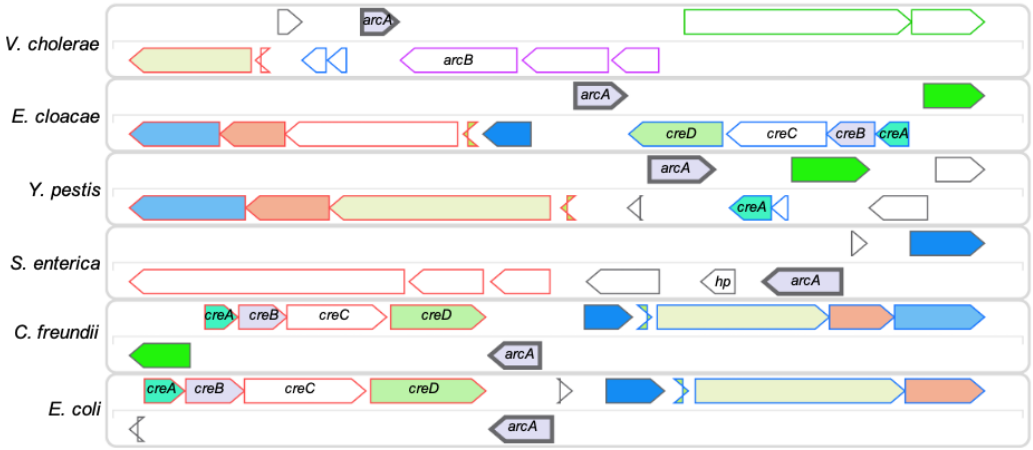

Figure 18: Genetic neighborhood for *arcA* in *V. cholerae* compared to that in other bacteria

The genetic neighborhood of *arcA* in *V. cholerae* compared to other bacteria. Schematic generated by Tree-based Exploration of Neighborhoods and Domains (TREND) based on ArcA homolog sequences. Genes immediately downstream of *arcA* are labeled. *V. cholerae arcA* is upstream to *arcB* while in many other bacteria including *E. coli*, *arcA* is upstream to a *cre* operon that encodes a two-component system regulating carbon catabolism.

Nevertheless, C173 and C233 are conserved in many ArcA homologs across different bacteria, including many human pathogens such as *E. coli*, *Salmonella*, and *Klebsiella* (**Fig. 19**). Similar to *V. cholerae* ArcA cysteine residues, the two cysteine residues at the conserved locations in the DNA-binding domain are often the only cysteine residues in these ArcA homologs. The

conservation at C173 is more relaxed in bacteria that do not have a part of their life cycle in a host environment, as seen in the example of the environmental bacterium, *Shewanella oneidensis*. Although environmental microbes such as *S. oneidensis* also encounter ROS[75], the type of source oxidant they encounter might be different from those for a pathogen present in a host environment[75]. The nuances between different oxidants and ArcA oxidant specificity seen in our *in vitro* H_2O_2 and CHP challenges (**Fig. 7A and 7C**) and EMSA results suggest an ArcA cysteine-mediated resistance particularly equipped for host environment ROS. The high conservation of both cysteine residues in these facultative anaerobic bacteria, many pathogens, suggest possible similar important functions for ArcA cysteine residues in these other bacteria.

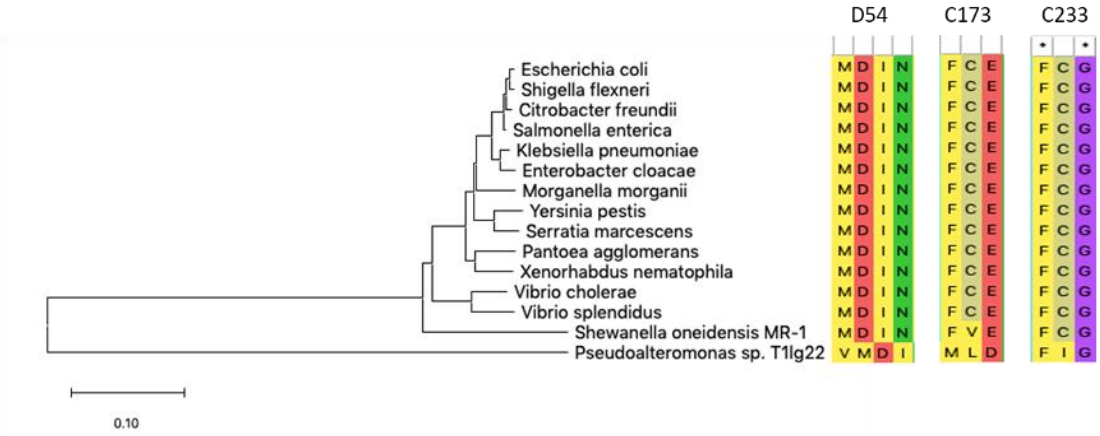

Figure 19: Key ArcA residues are conserved in different bacteria

A rootless phylogenetic tree constructed in MEGA5 based on ArcA homolog sequences from different bacteria using the neighbor-joining algorithm. The alignment around the phosphorylation site D54 and the two cysteine residues C173 and C233 are shown. *Pseudoalteromonas sp.* ArcA that is 66% identical to *V. cholerae* ArcA is used as the outgroup. The scale bar 0.1 indicates 10% diversity in amino acid sequence.

To test the generalizability of the cysteine dependent maintenance of ArcA functions, especially bacterial fitness under ROS exposure, we constructed Δ*arcA* mutants in *Salmonella enterica* serovar Typhimurium SL1344. Resembling Δ*arcA* mutants in *E. coli* and *V. cholerae*, SL1344 Δ*arcA* mutants also have a small colony morphology. $arcA^{WT}$ or $arcA^{C173S}$ with a native *Salmonella arcA* promoter is supplied to SL1344 Δ*arcA* mutants on a plasmid (pACYC117). SL1344 cells grown under a microaerobic virulence inducing condition to the mid-log phase were

challenged by CHP. Similar to what is seen in *V. cholerae*, SL1344 *arcA*^{C173S} mutants showed a similar survival defect to that of SL1344 Δ*arcA* mutants, which are more sensitive to CHP compared to SL1344 WT or the complementation strain (**Fig. 20A**). Analogous to *V. cholerae* *arcA*^{C173S} mutants having a disadvantage colonizing ROS-rich mouse guts, SL1344 *arcA*^{C173S} mutants showed a defect when infecting immortalized human colerectal adenocarcinoma cells Caco-2. After virulence induction for the expression of type III secretion system in *Salmonella* pathogenicity island-1 in LB supplemented with NaCl under microaerobic growth[144], SL1344 cells were introduced to Caco-2 cells at a multiplicity of infection (moi) of 20. Although having similar uptake by Caco-2 cells initially at 30 minutes post infection, SL1344 Δ*arcA* mutants showed a defect in intracellular replication 4hrs post infection (**Fig. 20B**).

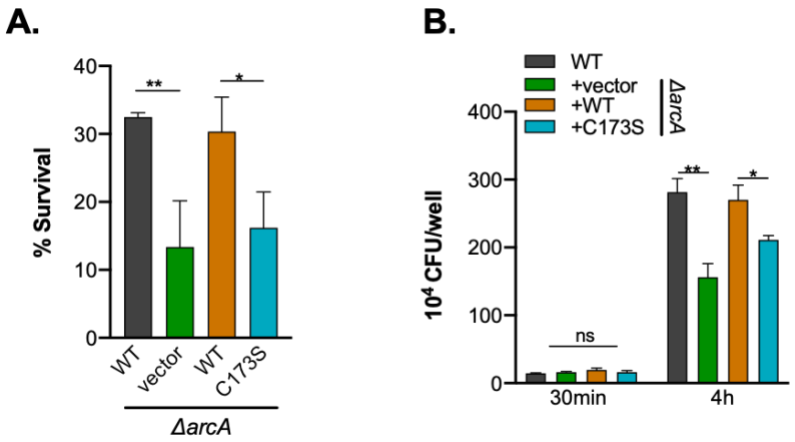

Figure 20: ArcA C173 is important for *S. enterica* ROS resistance and intracellular infection

A. Percentage survival of *in vitro* CHP challenge to *S.* Typhimurium SL1344 WT, *ΔarcA* mutants, the complementation strain, and *arcA*^{C173S} mutants, calculated by CFU remained in CHP challenged cells divided by that from unchallenged cells. Data collected from three biological repeats. *ΔarcA and arcA*^{C173S} mutants are more sensitive to extracellular CHP exposure than WT and the complementation strain. **B.** Recovered intracellular bacterial CFU from Caco-2 cells infected by SL1344 WT, *ΔarcA* mutants, the complementation strain, and *arcA*^{C173S} mutants. Data collected from three independent infections. *ΔarcA and arcA*^{C173S} mutants are defective in intracellular replication than WT and the complementation strain.

Although less dramatic compared to the *V. cholerae* results, preliminary results with SL1344 *in vitro* CHP challenge and Caco-2 infection suggest a role for ArcA C173 in mediating *Salmonella* survival in the presence of ROS. As *Salmonella* invade epithelial cells and grow intracellularly,

they are physically closer to the host NADPH oxidases, one of the major sources of host-derived ROS. Thus, *Salmonella*'s lifestyle require that they endure an even more challenging oxidative stress environment compared to that faced by an extracellular pathogen like *V. cholerae*. It is likely that *Salmonella* is more resourceful and diverse in ROS resistance strategies, thus limiting the observable ArcA-dependent net effect. These data along with the high conservation of cysteine residues across different ArcA homologs suggest important roles for these reversibly oxidizable thiols beyond *V. cholerae*, the model organism used in this study.

DBD cysteine residues are unique to ArcA in the PhoB/OmpR family RRs

While C173 and C233 are conserved in ArcA homologs across different bacteria, these conservations at their respective locations in the DBD are unique to ArcA in the PhoB/OmpR family response regulators (**Fig. 21**).

```
CLUSTAL O(1.2.4) multiple sequence alignment


ArcAe          SRTMNLGTVSEERRSVESYKFNGWELDINSRSLIGPDGEQYKLPRSEFRAMLHFCENPGK  60
ArcAv          SRSMHAGTTQEEKRSVEKYVFNGWELDINSRSLVSPDGDSYKLPRSEFRALLHFCENPGK  60
PhoP_5ed4      ----------------VRLTFADIELDEETH-EVWKAGQPVSLSPTEFTLLRYFVINAGT  43
KdpE_4KNY      ---------SATTAPDPLVKFSDVTVDLAAR-VIHRGEEEVHLTPIEFRLLAVLLNNAGK  50
PmrA_4S04      ------------NQGDNEISVGNLRLNVTRR-LVWLGETALDLTPKEYALLSRLMMKAGS  47
RstA_4NHJ      --------AMGTLTPHKTISFGSLTIDPVNR-QVMLGGENVALSTADFDMLWELATHAGQ  51
BaeR_4B04      ----------PQRELQQQDAESPLIIDEGRF-QASWRGKMLDLTPAEFRLLKTLSHEPGK  49
RitR_5u8K      ----------SLMK--VPRTYRNLRIDVEHH-TVYRGEEMIALTRREYDLLATLMG-SKK  46
PhoB_1GXP      ----------SPMAVEEVIEMQGLSLDPTSH-RVMAGEEPLEMGPTEFKLLHFFMTHPER  49
                                          ::              :   ::  :  :

ArcAe          IQSRAELLKKMTGRELKPHDRTVDVTIRRIRKHFESTPDTPEIIATIHGEGYRFCGDLED  120
ArcAv          IQTRADLLKKMTGRELKPHDRTVDVTIRRIRKHFESVSGTPEIIATIHGEGYRFCGDLED  120
PhoP_5ed4      VLSKPKILDHVWRYDFGGDVNVVESYVSYLRRKIDT--GEKRLLHTLRGVGYVLREPR--  99
KdpE_4KNY      VLTQRQLLNQVWGPNAVEHSHYLRIYMGHLRQKLEQDPARPRHFITETGIGYRFML----  106
PmrA_4S04      PVHREILYNDIYSGDNEPATNTLEVHIHNLREKIGK-----SRIRTVRGFGYMLANNDDT  102
RstA_4NHJ      IMDRDALLKNLRGVTYDGMDRSVDVAISRLRKKLLDNATEPYRIKTVRNKGYLFAPHAWD  111
BaeR_4B04      VFSREQLLNHLYDDYRVVTDRTIDSHIKNLRRKLESLDAEQSFIRAVYGVGYRWEADACR  109
RitR_5u8K      VLTREQLLESVWKYESATETNIVDVYIRYLRSKLDV-KGQKSYIKTVRGVGYTMQEG---  102
PhoB_1GXP      VYSREQLLNHVWGTNVYVEDRTVDVHIRRLRKALEP-GGHDRMVQTVRGTGYRFSTRF--  106
                  :  : . :         . :   :  :*  :         . :  . **
```

Figure 21: ArcA cysteine residues are unique in the PhoB/OmpR subfamily RRs

An alignment of the DNA-binding domains of representative PhoB/OmpR subfamily response regulators with the residue at the C173 position highlighted in red and the C233 position residue highlighted in blue.

Other regulators in the same family may contain redox-sensing cysteine residues, as seen in the example of *S. pneumoniae* RitR that regulates iron transport and nasopharyngeal colonization via

the oxidation states of a cysteine residue in the linker region joining the N-terminal REC and C-terminal DBD[116]. BaeR, the only other RR in this subfamily containing a far C-terminal cysteine in the DBD domain (**Fig. 21**), is reported to regulate efflux pumps and the transcription of the superoxide dismutase gene *sodA* in *Salmonella* [145]. The exclusivity of C173 and C233 in the DBD in ArcA, a regulator for oxygen sensing and shift between different electron transport strategies, presents the opportunity to couple the transition into microaerobiosis to ROS resistance, synchronizing two processes pivotal to a successful colonization in a mammalian host.

ArcA in conferring *V. cholerae* ROS resistance

C173 is important for the production of the ROS resistance protein OhrA

With *arcA*^{C173S} mutants showing higher sensitivity to CHP (**Fig. 7C**), we investigated conceivable mechanisms through which ArcA facilitate ROS resistance, particularly, if C173-mediated redox sensing is involved in conferring resistance to organic ROS.

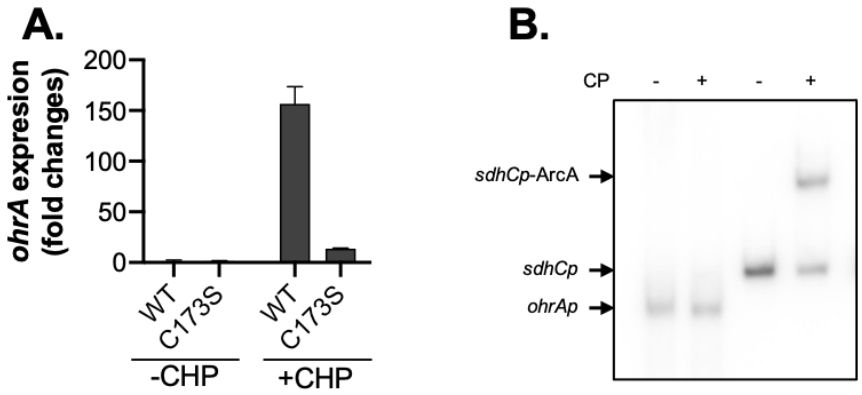

Figure 22: ArcA promotes *ohrA* expression under CHP exposure

A. The expression of *ohrA* as quantified by qPCR, determined by number of cycles with threshold fluorescence signal reflecting *ohrA* transcripts. Regions on the 16S sequence were used as internal references to calculate delta cycle threshold (dCt). The average of untreated samples was used to calculate ddCt, and the linear fold change is calculated as 2^(-ddCt). **B.** A gel shift assay (EMSA) of unphosphorylated and phosphorylated ArcA^{WT} with the *ohrA* promoter showing no formation of DNA-protein complex. The last two lanes contain the same concentration of unphosphorylated or phosphorylated ArcA^{WT} and the *sdhC* promoter as a positive control for protein activity.

V. cholerae organic hydroperoxide resistance protein OhrA (VCA1006) is an organic peroxide-specific peroxiredoxin that is important for *V. cholerae* resistance to ROS during colonization[101,146(p)]. We tested if ArcA^{C173S} affects *ohrA* expression by qPCR, in the absence or in

the presence of CHP under ArcA-activating conditions. CHP induced *ohrA* expression in WT *V. cholerae* C6706, consistent with previous findings that *ohrA* is derepressed upon oxidation from cysteine-containing regulators, OhrR and AphB [101]. However, in *arcA*^{C173S} mutants, *ohrA* expression remains low even in the presence of CHP, suggesting a lack of resistance proteins in *arcA*^{C173S} mutants to provide ROS protection (**Fig. 22A**). Based on these results, we propose that ArcA C173 plays a critical role in *V. cholerae* adaptation to the organic ROS challenge under microaerobic growth, in part by activating *ohrA* transcription when oxidized.

Although we observed an effect of ArcA on *ohrA* induction where C173S mutant failed to turn on the expression of the ROS resistance gene immediately following exposure, the C173-dependent oxidation-induction of *ohrA* transcription is not a direct regulatory effect from ArcA, as EMSAs with an *ohrA* promoter did not show any binding with either phosphorylated (**Fig. 22B**) or oxidized ArcA with $CuCl_2$, $CuSO_4$, CHP, or GSSG as oxidants *in vitro*. It is admissible that ArcA represses an intermediate regulator, a repressor of *ohrA*, in achieving a net activating effect. The apparent repressor for *ohrA* expression, OhrR (VCA1005), shares the same promoter as *ohrA*, as they are divergently transcribed with a 96bp intergenic region. Since ArcA does not bind to the *ohrA/R* promoter, included in the DNA fragment used for the EMSA experiment here, it is improbable that ArcA regulates *ohrR* transcriptionally or through competitive occupancy at the *ohrA* promoter. We speculated that ArcA regulate *ohrA* expression via intermediate regulator proteins or cellular flux of signaling molecules.

ArcA, extracellular iron, and *V. cholerae* H_2O_2 resistance

Another way ROS can manifest their bactericidal effects is by generating more reactive free-radical species from the non-radical species. Fenton chemistry describes the process of the formation of hydroxyl radicals (•OH) and hydroxide anion, from non-radical species in the presence of transition metals, most commonly in the forms of iron and copper species. *V. cholerae* iron uptake is strictly regulated to sustain the need of iron-requiring enzymes such as the heme-containing proteins, while avoiding deleterious effects of the Fenton chemistry. One of

the major regulators, the ferric uptake regulator *fur* (VC2106) has a predicted ArcA box in its promoter immediately following its -10 box. In an iron deplete environment, Fur is in its apo form, activating the machineries for iron uptake and storage; in an iron replete condition, Fur-Fe^{2+} complex represses further iron uptake, and upregulates free iron sequestering proteins[147148,149]. The predicted ArcA box in the *V. cholerae fur* promoter led us to hypothesize that ArcA acts through regulating *fur* to confer ROS resistance.

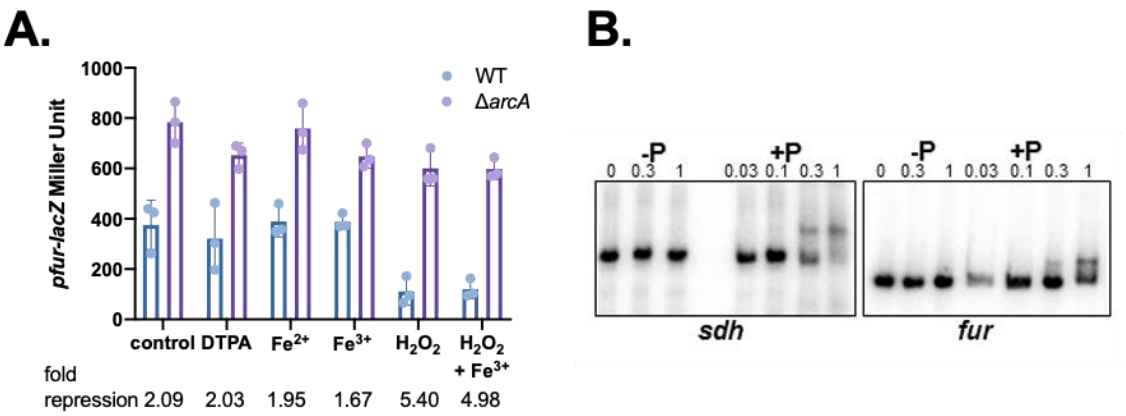

Figure 23: ArcA represses *fur* expression in *V. cholerae*, especially under ROS stress

A. The expression of *fur* as quantified by β-galactosidase activities with a *fur* promoter controlling a promoterless *lacZ* gene on a reporter plasmid under different extracellular iron and ROS conditions, with WT in blue and *ΔarcA* in purple. Fold repression is calculated as the average expression levels of *fur* as indicated by β-galactosidase activities in *ΔarcA* mutants divided by that in WT. *fur* expression is repressed by ArcA regardless of the extracellular iron and hydrogen peroxide conditions. **B.** A gel shift assay (EMSA) showing *fur* promoter binding to phosphorylated $ArcA^{WT}$, with *sdhC* promoter binding as a positive control for protein activity and sensitivity.

We constructed a transcription reporter plasmid with the promoter of *fur* leading to a promoterless *lacZ* gene on a plasmid and quantified β-galactosidase activities in *V. cholerae* C6706 WT and Δ*arcA* mutants under different iron and H_2O_2 conditions under microaerobic growth. Since rich media like LB contain unquantifiable amount of unknown iron species, we used a modified EZ rich defined media (EZRDM by Teknova) with $FeSO_4$ remitted from the recipe and glucose as a carbon source. Fe^{2+} or Fe^{3+} were supplied in the media in the forms of $FeSO_4$ or $FeCl_3$ at concentrations comparable to the original recipe when indicated. The divalent cation chelator diethylenetriaminepentaacetic acid (DTPA) was added to the modified no iron EZRDM to remove

any basal level iron that may be present due to adsorption to experimental vessels. As hypothesized, ArcA represses the expression of *fur*, regardless of iron abundance in the growth media (**Fig. 23A**). In fact, iron abundance does not affect *fur* expression, as seen by the comparable levels of *fur* expression in *V. cholerae* C6706 WT across different extracellular iron conditions (**Fig. 23A**). When challenged by H_2O_2, the ArcA-dependent repression of *fur* is exacerbated, increasing from approximately 2-fold in the absence of H_2O_2 to about 5-fold when exposed (**Fig. 23A**). This is unexpected since a H_2O_2 exposure is shown to activate *fur* transcription by OxyR in *E. coli* [150]. The co-presence of H_2O_2 and extracellular ferrous iron led to similar expression profiles as the H_2O_2 only condition (**Fig. 23A**), suggesting a more dominant role of ROS, instead of iron, in ArcA-dependent *fur* repression. Gel shift assays with a *fur* promoter further confirmed *fur* an ArcA regulated gene. Phosphorylated $ArcA^{WT}$ can form a DNA-protein complex with a *fur* promoter at the same sensitivity as a *sdhC* promoter (**Fig. 23B**), suggesting a direct repression of *fur* expression when ArcA is active.

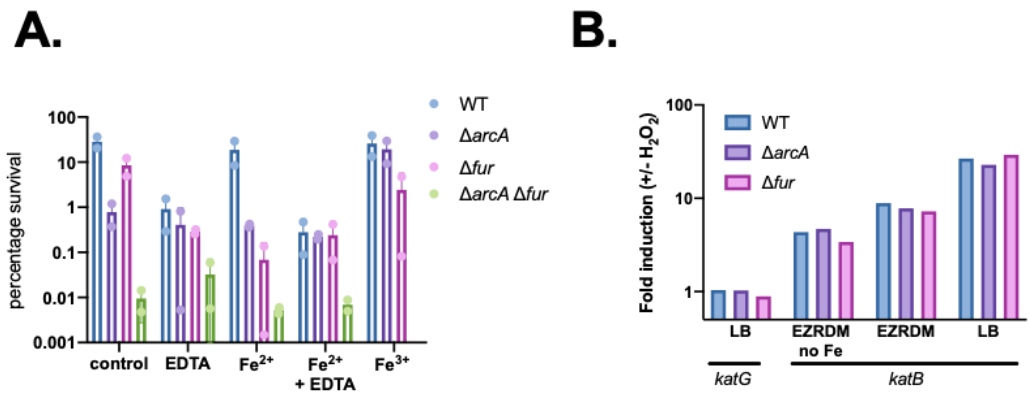

Figure 24: Iron is important for *V. cholerae* ROS resistance

A. The percentage survival of WT, *ΔarcA, Δfur* and *ΔarcAΔfur* double mutants to a H_2O_2 challenge, calculated as the CFU in the H_2O_2 treated cultures divided by those in the untreated cultures. **B.** The fold induction of catalases KatG and KatB expression quantified with the respective promoters controlling the expression of the *luxCDABE* as a reporter, arbitrary unit of luminescent is normalized to growth by OD_{600}, fold induction is calculated as the normalized luminescent signal of the H_2O_2 treated cells divided by those that were untreated.

The characterization of *fur* expression in the context of ArcA and ROS led us to hypothesize that a plethora of Fur proteins in Δ*arcA* mutants under ROS stress may be detrimental, contributing to

the higher sensitivity in Δ*arcA* mutants. We constructed Δ*arcA* Δ*fur* double mutants to test if the elimination of Fur proteins in Δ*arcA* mutants restores *V. cholerae* resistance to H_2O_2. Cells were grown microaerobically to mid-log phase in LB media supplemented with various species of iron or the divalent cation chelator ethylenediaminetetraacetic acid (EDTA) prior to the addition of H_2O_2 to the growth media. Contrary to our hypothesis, Δ*arcA* Δ*fur* double deletion mutants did not rescue the sensitivity to H_2O_2 in Δ*arcA* mutants, showing even lower survival percentages compared to the single mutants in the conditions tested (**Fig. 24A**). Nevertheless, it is worth noting that Δ*arcA* Δ*fur* double mutants are extremely sick with a severe growth defect, more so than Δ*arcA* mutants, under normal growth conditions in the absence of H_2O_2 exposure. Although we tried to challenge different strains in the same growth phase with similar OD_{600} as a reference, and survival percentages were used as a measure of sensitivity to further offset any growth discrepancies, the extent of basic metabolism defect seen in Δ*arcA* Δ*fur* double mutants may be too severe to reach a metabolic baseline for a meaningful H_2O_2 challenge.

Although not having an impact on *fur* expression, extracellular iron levels do influence *V. cholerae* resistance to H_2O_2. When extracellular divalent cations including ferrous iron were chelated by EDTA, the H_2O_2 resistance advantage seen in *V. cholerae* C6706 WT is eliminated (**Fig. 24A**). This implies important ROS resistance roles for various divalent cations, including extracellular ferrous iron as a candidate for mediating the resistance to H_2O_2 in WT. However, supplementing LB with ferrous iron showed no effect in either WT or Δ*arcA* mutants' survival percentages. In contrast, an addition of ferric iron in the rich media significantly boosts Δ*arcA* mutants' survival by about 10-fold to a WT level (**Fig. 24A**). The co-presence of H_2O_2 with extracellular iron at the concentrations tested did not aggravate the oxidative stress but proved iron essential in ameliorating the stress. *E. coli* ArcA directly activates the expression of the *feoA* operon [65], which encodes the ferrous iron transport system. Our preliminary studies of *V. cholerae feoA* expression using a *lacZ* reporter also supports a positive regulation from ArcA, with higher β-galactosidase activities indicating higher *feoA* expression in WT, despite having very low absolute miller unit

values. The exogenous supply of ferric iron in the form of $FeCl_3$ restored the survival rate in Δ*arcA* mutants, suggesting a lack of ferric iron uptake or sequestering machinery in Δ*arcA* mutants that is necessary for conferring ROS resistance.

V. cholerae has two major detoxifying enzymes for H_2O_2, catalases KatG and KatB [89]. As we see an extracellular iron-dependent effect for *V. cholerae* H_2O_2 resistance in the context of ArcA, we tested if these catalases are differentially induced in WT, Δ*arcA* and Δ*fur* mutants as a response to H_2O_2 exposure. With the *katG* and *katB* promoters transcriptionally fused to a promoterless *luxCDABE* gene encoding a luciferase, we quantified the expression of the catalases as luminescence signals normalized to cell growth measured by OD_{600}. Under the microaerobic growth conditions tested, we see high expression of *katG* in LB regardless of H_2O_2 exposure, resulting in a H_2O_2-dependent fold induction of 1 (**Fig. 24B**). In contrast, H_2O_2 exposure causes an almost 10-fold induction of *katB* expression, and even more to about 20-fold in iron rich environment such as the complete EZRDM and LB (**Fig. 24B**). Despite having a slightly lower *katB* expression level, Δ*arcA* mutants are equally capable of producing catalases in response to an H_2O_2 exposure as WT and Δ*fur* mutants.

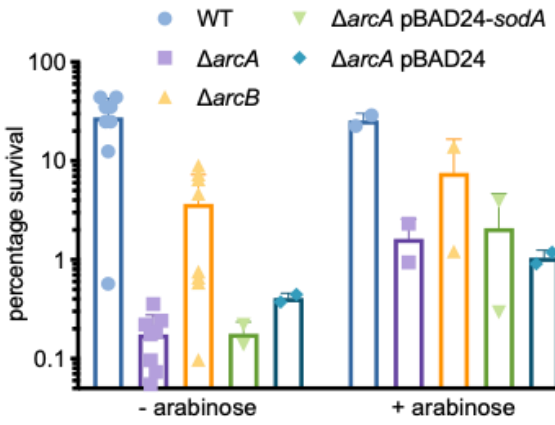

Figure 25: *ΔarcA* mutants' sensitivity to ROS is not due to a lack of SodA

An attempt to restore *ΔarcA* mutant's sensitivity to H_2O_2 by overexpressing *sodA* on a pBAD24 plasmid with an arabinose-inducible promoter. Percentage survival is calculated as the CFU in the H_2O_2 treated cultures divided by those in the untreated cultures times 100. The over expression of *sodA* did not restore *ΔarcA* mutants' sensitivity to H2O2. *ΔarcB* mutants exhibited intermediate sensitivity to H_2O_2 relative to WT and *ΔarcA* mutants.

To further elucidate the mechanism of ArcA-dependent ROS resistance, we considered superoxide dismutases as a candidate. Neither the iron-binding SodB (VC2045) nor the manganese-binding SodA (VC2694) have a predicted Vibrionaceae ArcA box in their promoter sequences. Nonetheless, in iron replete conditions, Fur bind to intracellular ferrous iron to form Fur-Fe^{2+} complexes, repressing the expression of *sodA*, which encodes the manganese binding superoxide dismutase. The Fur-Fe^{2+} complexes are prone to dissociate upon ROS exposure [151], lifting such repression in WT for SodA production. Since Δ*arcA* mutants have a higher level of *fur* expression, especially in the presence of ROS (**Fig. 23A**), it is conceivable that more Fur is present to form Fur-Fe^{2+} complexes and *sodA* expression is further repressed in Δ*arcA* mutants, leading to a lack of dismutases to cope with the extracellular oxidative stress. To test this, we supplied Δ*arcA* mutants with *sodA* on a pBAD24 plasmid with an arabinose inducible promoter that over expresses *sodA* upon arabinose induction. While the inclusion of arabinose in the LB increased survival to H_2O_2 for almost 10-fold in Δ*arcA* mutants, it is a *sodA*-independent effect. Δ*arcA* mutants and Δ*arcA* mutants carrying an empty pBAD24 vector also showed improved survival in the presence of arabinose (**Fig. 25**). Over expression of *sodA* does not help Δ*arcA* mutants in defending H_2O_2. We also tested the susceptibility of Δ*arcB* mutants to H_2O_2. Consistent to the phos-tag gel shown in Chapter 3 where Δ*arcB* mutants grown microaerobically still contain a considerable portion of phosphorylated ArcA (**Fig. 11A**), Δ*arcB* mutants are less sensitive to H_2O_2 than Δ*arcA* mutants, showing an intermediate survival rate between that of Δ*arcA* mutants and WT (**Fig. 25**).

Other attempts for elucidating the ArcA-dependent ROS resistance

The way arabinose partially restores Δ*arcA* mutants' survival to H_2O_2 (**Fig. 25**) allude to an ArcA-dependent metabolism defect critical to conferring ROS resistance. Although *V. cholerae* does not metabolize arabinose [152], we have observed Δ*arcA* mutants having a disadvantage when co-cultured with WT in MinA media grown microaerobically with glucose as a carbon source where Δ*arcA* mutants grew similarly as WT in separate tubes (**Fig. 26A**). Cell-free spent media from WT

failed to elicit such growth disadvantage in Δ*arcA* mutants, advising against a hypothetical WT toxic metabolite causing harm. Instead, impaired resource acquisition in Δ*arcA* mutants may be responsible for the growth disadvantage compared to WT. When grown in MinA media with mucin as the sole carbon source, both WT and Δ*arcA* mutants showed at least a log more CFU in 24hrs compared to using glucose, suggesting mucin as a superior carbon source for *V. cholerae* microaerobic growth (**Fig. 26B**). With a preferred carbon source, the co-culture-dependent Δ*arcA* mutants growth deficiency is ameliorated (**Fig. 26B**), further supporting the hypothesis that Δ*arcA* mutants may be lacking nutrients for ROS resistance.

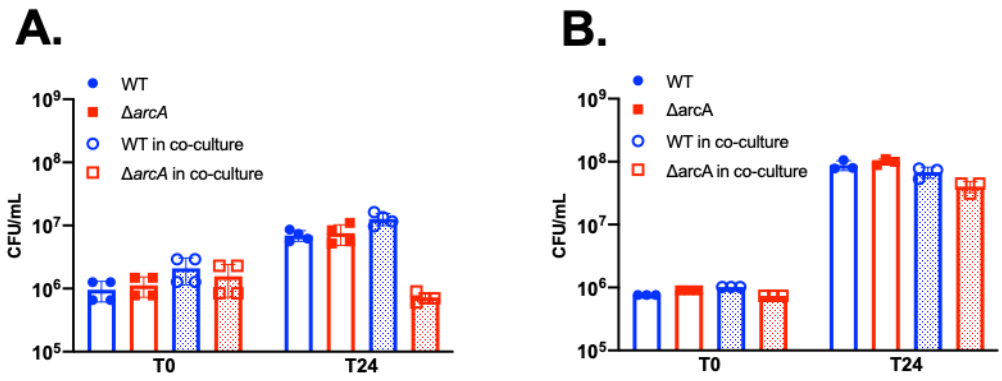

Figure 26: *ΔarcA* mutants have nutrient acquisition defects

A Quantification of CFU of WT and *ΔarcA* mutants grown in MinA media with glucose as a carbon source, separately or in a 1:1 mix. **B** Quantification of CFU of WT and *ΔarcA* mutants grown in MinA media with mucin as a carbon source, separately or in a 1:1 mix.

oppA, encoding the oligopeptide ABC transporter substrate-binding protein, is directly activated by ArcA in *E. coli* [125].When exposed to H_2O_2, *E. coli* Δ*arcA* mutants are deficient in OppA and struggle to suffice the increased need for amino acids under ROS stress [125]. We performed gel shift assays with the *V. cholerae oppA* (VC1091) promoter sequence containing a predicted Vibrionaceae ArcA site (TAACATTTTGTACAC). However, we did not observe any DNA-binding with reduced, phosphorylated, or $CuSO_4$ oxidized $ArcA^{WT}$ protein. As oxidized $ArcA^{WT}$ binding with the *sdhC* promoter is seen with GSSG as an oxidant (**Fig. 12A**), it is still possible that the *oppA* promoter specifically interact with GSSG-oxidized ArcA.

Besides the evidence that *ohrA* transcription rely on ArcA in a C173-dependent manner upon ROS exposure, the downstream ArcA-dependent cellular processes that confer ROS resistance still require more investigation. At this point we speculate that it is a combined effect of multiple ArcA-regulated genes that lead to a lack of ROS resistance gene expression and defective nutrient acquisition in Δ*arcA* mutants.

<u>*arcA* expression in the context of *V. cholerae* virulence regulation</u>

To further understand the relevant context of ArcA in a *V. cholerae* life cycle, we examined *arcA* expression in relation to the virulence regulatory cascade. With the *arcA* promoter leading to a promoterless *lacZ* gene on a plasmid, we quantified the β-galactosidase activities as expression of *arcA* in *V. cholerae* C6706 WT, Δ*arcA* mutants and various virulence regulator mutants including Δ*tcpPH*, Δ*toxT*, Δ*toxRS*, and Δ*aphB*. Cells were grown aerobically in LB to mid-log phase and then transitioned into virulence inducing condition in AKI media for standing growth to mimic an ArcA-activating condition where the virulence regulators are active.

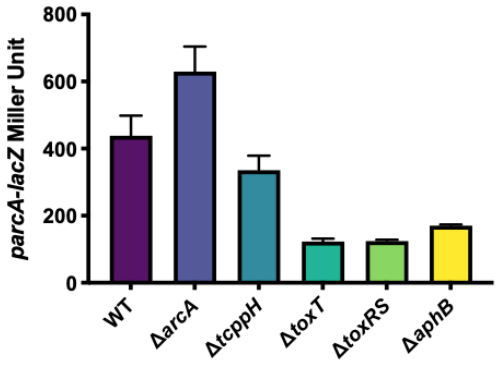

Figure 27: *V. cholerae* virulence regulation network on *arcA* expression

The expression of *arcA* as quantified by β-galactosidase activities controlled by an *arcA* promoter. Data shown is from a single experiment with two technical repeats but is representative of the general trend from more independent experiments. ArcA self-regulates, repressing the expression of itself. In the context of virulence regulatory network, *arcA* expression is affected by ToxT, ToxRS and AphB but unaffected by TcpPH.

ArcA represses the expression of itself, as *arcA* expression indicated by the arcA promoter-controlled β-galactosidase activity in Δ*arcA* mutants is elevated compared to that in WT (**Fig. 27**). TcpPH have no apparent effect on *arcA* expression, as demonstrated by the similar β-

galactosidase activity levels in Δ*tcpPH* mutants and in WT. ToxT, ToxRS, and AphB all play a role in activating *arcA* expression, as β-galactosidase activities in these mutant strains are only about a quarter of the levels in WT (**Fig. 27**). Sengupta and colleagues have described that *toxT* expression is dependent on ArcA, and here we see *arcA* expression depends on ToxT [70]. The reciprocal positive regulation between ArcA and ToxT suggest a positive feedback loop for *arcA* expression under virulence inducing conditions, which is capped by ArcA self-regulation. Since TcpPH are downstream of AphB but upstream of ToxT in the virulence regulation cascade (**Fig. 1**), the AphB-dependent yet TcpPH-independent *arcA* expression seen in the condition tested is suggestive of a ToxT-independent link between AphB and ArcA, suggesting an additional connection of ArcA to *V. cholerae* virulence under microaerobiosis. It is possible that ToxT, ToxRS and AphB's close association to a microaerobiosis lifestyle led *V. cholerae* to associate the presence of these virulence regulating proteins to a need for ArcA, the regulator to transition the cell into microaerobiosis.

Concluding remarks and open questions

In this study, we have identified *V. cholerae* ArcA as a reversibly oxidizable cysteine-containing protein, among many others, in a proteomic detection of oxidized thiols in ROS-challenged *V. cholerae* by mass spec. The ArcA cysteine residues identified, C173 and C233, are the only two cysteine residues in ArcA, both in the C-terminal DNA-binding domain. The susceptibility of these cysteine residues to reversible oxidation are validated by western blot analysis of *V. cholerae* whole cell lysates containing overexpressed ArcA, subsequent to AMS-labeling targeted at oxidized thiols. To isolate the cysteine oxidation-dependent functions of ArcA from the rest of ArcA functions, we investigated various phenotypes of the cysteine to serine mutants, $arcA^{C173S}$ and $arcA^{C233S}$, which lack the reactive thiol side chain and therefore unresponsive to the respective cysteine-dependent oxidation. A C233S mutation generally causes a Δ*arcA* mutant-like phenotype, suggesting an essential role, likely structural, for this cysteine residue at the far C-terminus of ArcA. A C173S mutation does not affect ArcA functions under normal ArcA-activating conditions, yet renders ArcA unfunctional under ROS exposure, as seen in the defective survival

of *in vitro* ROS challenge and the colonization disadvantage during colonization of ROS-rich mouse guts. Transcriptional analysis of an ArcA repressed gene *sdhC* showed that $ArcA^{C173S}$ failed to repress *sdhC* expression in the presence of extracellular ROS while $ArcA^{WT}$ largely maintained repression under the same stress.

We further investigated the molecular mechanism through which ArcA respond to oxidative stress while maintaining regulatory functions. Biochemical analysis revealed that ArcA phosphorylation is jeopardized in the presence of extracellular ROS. *In vitro* phosphorylation by small molecule donor carbamoyl phosphate and oxidation by GSSG both independently enable ArcA's binding to DNA fragments encompassing a predicted Vibrionaceae ArcA box, a 15bp motif containing two direct repeats separated by a 10bp center-to-center distance. Similarly, in a bacterial two hybrid system, increased ArcA-ArcA interactions are shown under an ArcA-stimulating microaerobic condition or under ROS exposure in an otherwise non-stimulating aerobic condition in a C173-dependent manner. Non-reducing SDS-PAGE analysis of *V. cholerae* cell lysates containing His_6-tagged ArcA revealed that ArcA forms an intramolecular disulfide bond when *V. cholerae* is challenged by extracellular ROS. C173 plays an important role in occluding the formation of an intermolecular disulfide bond via C233, upon its formation leads to an unfunctional conformation of ArcA. We propose that oxidation by extracellular ROS drives the formation of intramolecular disulfide bond between C173 and C233, which induces an ArcA conformation such that multiple ArcA monomers interact and collectively bind to the promoters of ArcA regulated genes.

In conclusion, our data provides a mechanism through which ArcA's regulatory functions remain active under oxidative stress. Preliminary results in *S. enterica* and a high conservation of C173 in many ArcA homologs in different bacteria suggest a wide application of this mechanism beyond *V. cholerae*. This work provides evidence to explain how the response regulator ArcA

directly respond to oxidative stress that eventually result in ROS resistance. However, the attempts at elucidating the downstream cellular responses solicited by oxidized ArcA failed to directly tie ArcA-dependent ROS resistance to any specific process. We are intrigued by the oxidant specificity shown by ArcA, with *arcA*^{C173S} mutants being more sensitive to CHP than to H_2O_2 and purified ArcA only responding to GSSG as an oxidant *in vitro*. Complex unknown cellular processes are involved to distinguish the nuances between different oxidative stresses. Our results motivate studies of glutathionylation as a post-translational modification signal in *V. cholerae* oxidative stress response. We are also curious if the relatively unique genetic organization of *V. cholerae arcA* and *arcB* genes in a tail-to-tail formation is indicative of special evolutionary pressures associated with the dynamic lifestyle of *V. cholerae*.

To respond to external stresses with the limited resources available, bacteria are constantly faced with costly decisions. In the case of ArcA, when exposed to ROS in an otherwise activating condition, such as inside a host intestine with host and microbiome-derived ROS, it is dangerous to mistake an oxidative stress as an aerobic growth condition. The cysteine-mediated redox response in a separate domain from the aspartate-mediated activation from ArcB phosphorylation provides an additional channel of signal perception to inform ArcA activities. Our work establishes ArcA as a thiol-dependent transcriptional regulator that is involved in conferring ROS resistance in *V. cholerae*, and possibly in other bacteria. The dual signal perception, accepting oxidation or phosphorylation as an activating signal, allows ArcA to couple multiple important global transitions that require simultaneous regulation, such as ROS resistance and transition into microaerobiosis, with maximal synchronization and minimal compromises.

Chapter 5: Methods and Materials

Growth conditions

V. cholerae El Tor C6706 was used as the wild type strain in this study. Strains were streaked out from frozen (-80°C) glycerol stocks to grow on 1.5% LB agar plates containing appropriate antibiotics overnight at 37°C. Colonies were scraped off for resuspension in 0.8% (w/v) saline to optical density (OD_{600}) of around 1. Colony morphology were observed by spotting 5μl of 10-fold serially diluted cell resuspension on LB agar plates with or without 1μg/ml of toluidine blue (TB) incubated overnight at 37°C. Growth are evaluated under aerobic growth in LB with 200rpm shaking for aeration, or under virulent-inducing microaerobic condition with standing growth in AKI medium (1.5%(w/v) bacto-peptone, 0.4% (w/v) yeast extract, 0.5% (w/v) NaCl) supplemented with freshly made filter sterilized $NaHCO_3$ at a final concentration of 0.3%. Cultures of *V. cholerae* were propagated at 37°C and with appropriate antibiotics and inducers when necessary, at final concentrations of 100μg/ml for streptomycin, 100μg/ml for spectinomycin, 50μg/ml for kanamycin, 2μg/ml for chloramphenicol, 100μg/ml for ampicillin, 0.1% for arabinose and 0.5mM for IPTG. CFU in bacterial cell cultures were enumerated by spotting 5μl of 10-fold serially diluted cultures in 0.8% (w/v) saline on LB agar plates incubated overnight at 37°C.

Strain construction

Disruption of *arcA* (VC2368) was constructed by inserting a kanamycin resistance cassette by a pWM91-based suicide plasmid with a *sacB* counter selection protocol [153]. Specifically, in both C6706 *lacZ* and C6706 WT backgrounds, the chromosomal *arcA* gene was disrupted by a 795nt PCR fragment of a kanamycin cassette with its own promoter from the pBBR1MCS2 in the opposite orientation of *arcA*, replacing the 352nd-369th bases of the 717nt gene. For complementation, the sequence of *arcA*, with its upstream promoter region, was inserted in the *lacZ* locus on the chromosome in a C6706 *arcA::kan lacZ*+ background on a pJL1-based plasmid by a double cross-over recombination [154]. The native *arcA* promoter, followed by $arcA^{C173S}$, $arcA^{C233S}$, $arcA^{C173SC233S}$, or $arcA^{D54A}$, were put on the *lacZ* locus (VC2338) on the chromosome to construct the ArcA variant strains. The point mutation fragments were subcloned from pSRKTc

plasmids containing the promoterless *arcA* constructs to the pJL-1-based plasmids with StuI and NotI as restriction sites with the addition of 400nt upstream sequences encompassing the native promoter. Disruption of *arcB* (VC2369) by a spectinomycin resistance cassette was constructed by the MuGent method with chitin-induced *V. cholerae* natural competence [155]. Plasmids were propagated in DH5α λpir or pir2 and introduced to *V. cholerae* by electroporation or by conjugation with SM10λpir as a donor when feasible.

Disruption of *Salmonella enterica* serovar Typhimurium SL1344 was done with a P22 transduction of kanamycin resistant LT2 *arcA* (STM4598) lysate. LT2 *arcA::kan* was obtained by electroporating PCR fragments of a kanamycin cassette from pKD4 flanked by the *arcA* genetic neighborhood into *Salmonella enterica* serovar Typhimurium LT2 containing a pKD46 as previously described [156]. pACYC117 plasmid was digested with BamHI and HindIII to insert the *Salmonella arcA*^{WT} *or arcA*^{C173S} sequence following the *Salmonella arcA* promoter that disrupts the kanamycin resistance cassette on pACYC117, resulting in an ampicillin resistant plasmid for complementation in SL1344 *arcA::kan*. Strains, plasmids, and primers in this work are listed in **Table 2**, **Table 3**, and **Table 4** in the Appendix, respectively.

Proteomic profiling of cysteine-based reversible modification mass spectrometry

Vibrio cholerae El tor C6706 WT cells were grown *in vitro* under virulence induction conditions, namely, cells grown overnight aerobically at 30C to saturation were inoculated at 1:10,000 into 4ml AKI media supplemented with 0.3% NaHCO3 and grown standing for 4hrs. The cells were then challenged by 50uM CHP for 1hr with aeration. The proteomic profiling of cysteine-based reversible modification was carried out following [157(p)]. Briefly, the cell cultures were pelleted and then resuspended in 300ul lysis buffer (250mM HEPES, pH7.0, 6M Urea, 1mM EDTA, 0.1mM neocuproine, 1% v/v SDS) with 100mM freshly made NEM and incubated in the dark at 37C for 1hr at 850rpm. After removal of excess NEM by acetone precipitation, the samples were treated with 10mM DTT for 1hr at 37C with 850rpm shaking in the dark. Excess DTT was removed by another acetone precipitation and the pellets were rinsed by 500ul of cold acetone and air dried

for 2min before being resuspended in 120ul of enrichment coupling buffer (50mM HEPES and 1mM EDTA, pH 7.5) supplemented with 2.4ul of 10% SDS. Samples were then loaded onto the preconditioned thiopropyl Sepharose 6B resin[157], with 10mg of resin in coupling buffer with roughly 100ul volume in a pierce spin column (Thermo fisher scientific, Rockford, IL). The resin column is thoroughly washed three times with 500ul of each of the enrichment washing buffers in the following order: 1) 8M Urea; 2) 2M NaCl; 3) 80% (v/v) CAN and 1% v/v TFA; 4) 25mM HEPES. Replace both the top cap and bottom plug of the column after the last wash, then spin at 1000xg for 10sec. [concentration] of trypsin was added to allow min digestion of the protein into peptides. 30ul of 25mM NH4HCO3 buffer containing 20mM of DTT was added to the resin column and mixed with a pipette tip and incubated at RT with shaking at 850rpm for 10min to elute thiol containing peptides. The eluted peptides were collected with a 1500xg spin for 1min with both top cap and bottom plug removed. Samples were treated in DAB buffer (6M Urea, 250mM HEPES pH7.0, 10mM EDTA, 0.5% w/v SDS) supplemented with 100mM iodoacetamide for 1hr at 25C with 850rpm shaking. Samples were submitted to LC-MS/MS (FTMS) to identify a 57Da shift signifying a carbamidomethyl modification on a cysteine residue. Peptides were identified by SEQUEST HT and MASCOT. The reported hits have a high confidence score from analysis by either one or both software.

Thiol-labeling by 4-acetamido-4'-maleimidylstillbene-2,2'-disulfonic acid (ASM)

V. cholerae C6706 containing a T7 polymerase on a pTara plasmid and pET41-His_6-$ArcA^{var}$ were grown in 2ml LB media containing 2μg/ml chloramphenicol and 50μg/ml kanamycin for plasmid maintenance. After 2hrs of growth at 37°C with aeration, 0.1% arabinose were added to allow induction of ArcA variants overexpression for another 2hrs with aeration. The culture is switched to standing growth at 37°C to mimic the virulence-inducing microaerobic condition with 1/5 final volume of 5x AKI media included in the culture to constitute a 1x AKI in LB media, in the absence or in the presence of CHP. Thiol labeling of oxidized cysteine residues were performed on acidify collected samples precipitated with a final 10% TCA. The protocol of Wholey and Jakob was then followed with 0.5kDa ASM as the modifying agent[158]. Briefly, after adding 10% TCA to samples

and a 30min incubation on ice, samples were centrifuged at 13,000rom for 30min at 4°C, Pellets were then rinsed with 100μl of 10% TCA, and centrifuged at 13,000rpm for 20min at 4°C. Then 100μl of 5% TCA were used to rinse the pellet again, followed by a spin and the remainder of TCA were aspirated without disturbing the pellet. The pellets were resuspended in 50μl DAB buffer (6M Urea, 250mM HEPES pH7.0, 10mM EDTA, 0.5% (w/v) SDS) supplemented with freshly made 100mM NEM to irreversibly alkylate all *in vivo* reduced thiols. Samples were incubated for 30min at 55°C with 850rpm shaking, followed by another TCA precipitation to remove excess NEM. After rinsing the pellet by 50μl 20%TCA, 100μl of 10% TCA, and 100μl of 5% TCA, all remaining TCA was removed without disturbing the pellet. The pellets were then resuspended in 50μl DAB buffer supplemented with 10mM DTT to reduce all *in vivo* oxidized cysteine residues at 37°C for 1hr with 850rpm shaking. Excess DTT was removed by another TCA precipitation and rinses. The resulting pellet were then resuspended in 20μl of labeling buffer (6M Urea, 50mM Tris pH7.5, 2% w/v SDS, 20mM ASM).

Scanning the *V. cholerae* C6706 genome for ArcA regulated genes

The position weight matrix reported by Ravcheev and colleagues[69] was linearly transformed by the nucleic acid frequencies in *V. cholerae* El tor, approximately 0.262 for adenine and thymine, and 0.238 for cytosine and guanine. The resulting probability matrix is put in MEME version 4 FIMO search with input genomes AE003852 for chromosome I and AE003853 for chromosome II of *V. cholerae* O1 N16961.

Quantification of transcription of *sdhC*, *ohrA*, *fur*, *katG*, *katB*, *feoA* and *arcA*

The *psdhC*-lacZ plasmid reporter (pYTZ104) was constructed by cloning *sdhC* promoter DNA into a promoterless *lacZ* transcriptional reporter plasmid pAH6[159]. *V. cholerae* WT, Δ*arcA* and *arcA*^{C173S} mutants containing *psdhC-lacZ* reporters were streaked out for heavy streaks on LB agar plates containing 2μg/ml chloramphenicol to grow at 37°C overnight. Cells were scraped off of the plate and resuspended in 0.8%(w/v) saline to inoculate at 1:100 into AKI media supplemented with freshly made $NaHCO_3$ containing 2μg/ml chloramphenicol to grow standing

for approximately 3 hours. Final concentrations of 60μM-80μM CHP were added to the cultures to generate a ~90% killing effect in the respective strains, determined by serial dilution for CFU enumeration. Samples that were in this range were retained in the final analysis for β-galactosidase activity quantification, normalized to per million CFU in respective samples.

qPCR for *ohrA* expression was done with cell lysates that were grown under the virulence inducing conditions for 2.5hrs with or without 1hr of 60μM CHP exposure. qPCR primers were designed such that around 100bp sequence in the transcript are amplified. Two regions in the 16S RNA were amplified as internal references. RNA was extracted using a Qiagen RNeasy Mini kit. A DNA cleanup was followed using Ambion Turbo DNA-free kit DNase Treatment and removal reagents (AM1907). cDNA synthesis was carried out with Biorad iScript cDNA synthesis kit (Cat. 170-8890). The Genecopoeia All-in-One qPCR mix (Cat. AOPR-1000) was used to set up the qPCR reaction run on a Biorad iCycler CFX-96 with the following program: 95°C, 10'; [95°C, 10''; 55°C, 20'', 72°C 15''] x40; 72-95°C, 0.5C/unit time, 6''/unit time for melting curve, 25C, 30''.

β-galactosidase activities were quantified for *fur, feoA,* and *arcA* expression in miller units. pAH6-based plasmids were constructed such that approximately 1000bp upstream of a target gene, i.e., *fur*, *feoA* and *arcA* were ligated by XbaI and SalI to control the expression of a *lacZ* gene. *V. cholerae* strains containing the reporter plasmids are grown in media supplemented with 2μg/ml chloramphenicol before assayed for β-galactosidase activities as described before. *fur* expression was characterized in EZ rich defined media (EZRDM) by Teknova (Cat. M2105) or modified EZRDM with iron remitted from the recipe in sterile plastic vessels to minimize exogenous iron from adsorption. For *arcA* expression, cells were inoculated at 1:500 from saturated overnight cultures or 1:250 for Δ*arcA* mutants to account for growth defect in LB media supplemented with 100μg/ml streptomycin and 2μg/ml chloramphenicol to grow at 37°C with 200rpm shaking for 2 hours. The cells were then pelleted and resuspended in equal volume of AKI supplemented with

the same antibiotics to incubate standing at 37°C for another hour. The resulting cultures in AKI were then assayed for β-galactosidase activities.

Expression of *katG* and *katB* were quantified as luminescence signal intensity normalized to OD_{600} as described before[160].

***in vitro* CHP killing assays**

V. cholerae cells streaked out from -80°C storage were grown on LB agar plate overnight at 37°C and washed once in 1x M9 salts before resuspended in 1x M9 salts to an OD_{600} of 1. Cell resuspension of each strain were introduced into AKI supplemented with freshly made filter sterilized $NaHCO_3$ to a final concentration of 0.3% at a 1:300 dilution in 2ml screw top vials to create a more anoxic microaerobic growth condition. Cells are incubated at 37°C until OD_{600} reaches 0.1, around 2hrs, then challenged by 60μM CHP for 1hr in the screw top vials. Bacterial cultures are then enumerated for CFU on LB agar plates.

***in vitro* H_2O_2 challenge**

V. cholerae C6706 WT, Δ*arcA*, $arcA^{WT}$, $arcA^{C173S}$, $arcA^{C233S}$, $arcA^{C173SC233S}$ were grown overnight at 37°C with 200rpm aeration to saturation. The saturated cultures were inoculated at 1:250 for Δ*arcA* and 1:500 for the other strains in LB to grow standing with ambient atmosphere for 3hrs at 37°C. After 3hrs of growth, cells are challenged with 300μM H_2O_2 for 1hr before serial dilution for CFU enumeration on LB agar plates. Similar H_2O_2 challenges were done with mid-log cells grown in AKI supplemented with 0.3% $NaHCO_3$, EZRDM or in MinA media supplemented with a final concentration of 0.2% glucose and 0.2% casamino acids in the anaerobic chamber.

V. cholerae C6706 WT, Δ*arcA*, Δ*arcB*, and *sodA* complementation on a pBAD24 plasmid were inoculated at 1:500 for WT and 1:250 for the mutants to grow standing in LB with or without a final concentration of 0.1% arabinose to induce overexpression of SodA. After 3hrs of growth and

protein induction, cells are challenged with 300μM H_2O_2 for 1hr before serial dilution for CFU enumeration on LB agar plates.

Electrophoretic Mobility Shift assays (EMSA)

His_6-ArcA variant proteins were expressed in BL21(DE3) cells and purified on nickel columns according to the manufacturer's instruction (Qiangen Cat. 30210). PCR products of a roughly 300bp region in the *sdhC* promoter containing the predicted ArcA box were digested by HindIII and end-labeled with α-^{32}P dATP. Binding reactions contained purified protein at 0.1-1.5μM concentrations were incubated with 0.1ng of DNA in a EMSA bind buffer (60mM Tris-Cl, pH7.5, 100ug/ml BSA, 5% glycerol, 10mM MgCl2, 20mM KCl, and 1mM DTT) at 30°C for 20min. *In vitro* phosphorylation was carried out with 10-30μM protein with 20mM carbamoyl phosphate (Santa Cruz) in phosphorylation buffer (50mM Tris-Cl, pH7.5, 50mM KCl, 20mM MgCl2, 17mM DTT, 10ug/ml BSA) at 30°C for 30min, with a stoichiometry of 1-part 10x phosphorylation buffer, 1-part 10x carbamoyl phosphate and 8-parts purified protein. Mock reaction was setup in the same reaction buffer as the phosphorylation reaction except adding Milli-Q water instead of carbamoyl phosphate. Oxidation is carried out with protein samples that have DTT removed by dialysis, with 30mM of freshly prepared GSSG at 30°C for 1hr, with a stoichiometry of 1-part oxidant and 1-part purified protein. The EMSA bind buffer for the oxidized samples excluded the 1mM DTT to ensure the oxidized state of proteins. Prior to *in vitro* modification reactions, His-tags were cleaved off by an overnight (>16hr) thrombin digestion with 1U thrombin per 100μg protein at 4°C and verified by SDS-PAGE followed by Coomassie staining. Beside GSSG, other oxidants include $CuSO_4$, $CuCl_2$, CHP, and H_2O_2 at varying oxidant concentrations ranging from 1μM to hundreds of mM. Roughly 300bp region in the *fur* and *oppA* promoters containing a predicted ArcA box were also used in EMSAs with EcoRI sites flanking the fragments for end-labeling by α-^{32}P dATP.

***V. cholerae* colonization in mouse models**

All animal experiments were performed in strict accordance with the animal protocols that were approved by the IACUC of the University of Pennsylvania. The streptomycin-treated adult mouse

model was used to examine *V. cholerae* ROS resistance *in vivo* as previously described with gut ROS mitigation by the antioxidant, N-acetyl cysteine (NAC) [101]. Six-week-old CD-1 mice were provided with drinking water with or without 1% (w/v) NAC for one week. 0.5% (w/v) streptomycin and 0.5% (w/v) Stevia were included in the drinking water for the remainder of the experiment. Two days after streptomycin treatment, saturated liquid LB cultures of each of the two strains (WT and mutant) were mixed at a 1:1 ratio to a total of 10E8 CFU bacteria in 100μl LB media and intragastrically administered to each mouse within 20min of neutralizing its stomach acid by 50μl of 10% (w/v) $NaHCO_3$ by oral gavage. Input CFU of both WT and mutant in the mix were obtained by enumerating the cell culture mix used to inoculate the mice immediately after infection. Fecal pellets were collected in days subsequent to infection for enumeration of bacterial counts. At 6 days post infection, mice were sacrificed, and the small intestine fragments were homogenized for enumeration of bacterial counts. In an infant mouse colonization experiment, 4- to 6-day-old CD-1 mice are infected with *V. cholerae* via oral gavage after separation from mother mouse for 2hrs. A total of 1E6 CFU of 1:1 mix of mutant and WT *V. cholerae* C6706 from overnight saturated LB liquid cultures were administered perorally to the mouse using fine plastic tubing (BD Cat.427401) attached to a tuberkulin syringe. Mice are monitored for signs of distress such as altered behavior and abdominal breathing then placed on tissue paper in a small beaker. The beaker is placed in a 30°C incubator along with a container of water to provide humidity. 12hrs after infection, the mice are sacrificed and the small intestine between the stomach and the cecum is recovered and homogenized in 5ml of LB media. The homogenate is diluted for enumeration of bacterial counts on LB agar plates.

Bacterial Two Hybrid system (BacTH)

E. coli BTH101 are co-transformed with a pKT25 derived plasmid and a pUT18c derived plasmid using the TSS competent methods [161]. pKT25 carrying $arcA^{WT}$ was paired with pUT18c carrying either $arcA^{WT}$ or $arcA^{C173S}$. pKT25 carrying the coding sequence for the yeast transcription factor GCN4 containing a leucine zipper was paired with pUT18c plasmid carrying the same sequence as a positive control for protein interactions. pKT25 and pUT18c vectors are co-transformed for a

negative control strain. Transformants were selected on LB agar plates containing kanamycin and ampicillin. After overnight incubation at 37°C, multiple transformant colonies are inoculated to LB liquid media containing kanamycin and ampicillin to grow overnight at 37°C with 200rpm shaking to saturation. These saturated cultures were then used to set up growth in a 96-well block in LB media containing appropriate antibiotics to grow shaking until cells reached mid-log phase. Next, the 96-well block either continued to be shaken for an aerobic growth condition or was switched to standing with 1x AKI media included in the culture to mimic a virulence inducing microaerobic growth condition. For ROS exposure, a final concentration of 250μM CHP and 2.5mM H_2O_2 mix were included in the shaking culture for 1hr to induce protein interactions. The resulting cells were lysed by Popculture reagents (Millipore Cat. 71092) prior to β-galactosidase assays. β-galactosidase activities were then measured in a 96-well plate as previously described [162].

Protein purification

An overnight culture of *E. coli* BL21(DE3) transformed with a pET41 derived plasmids containing N-terminally His_6-tagged ArcA variant was used to inoculate at 1:100 into 500ml of LB containing kanamycin in 3L flat bottom flasks. After growth at 37°C with 200rpm shaking for approximately 2hrs, the mid-exponential phase culture was induced with a final concentration of 0.5mM IPTG and switched to 16°C 200rpm shaking for an additional 16hrs for optimized soluble target protein production. Cells were harvested from the culture by centrifugation with a F12-6x500 LEX rotor in a Sorvall LYNX 4000 Superspeed centrifuge (Thermo Fisher) at 4248 rcf for 20min at 4°C. The pellet was stored at -20°C if not immediately proceeded to the next steps. Cell pellets were resuspended in 5ml Ni-NTA bind buffer (50mM NaH_2PO_4, pH 8.0; 300mM NaCl; 10mM imidazole). The cell resuspension is sonicated on ice with 10 second durations five times with 10 second intervals. The cell lysate is centrifuged for 10min at 27,000 rcf at 4°C to pellet cell debris. The cleared lysate is loaded on pre-equilibrated Ni-NTA agarose (Qiagen Cat. 30210) column with 2ml of bed volume at room tempearture. Following the lysate, 10ml of Ni-NTA bind buffer and 10ml of Ni-NTA wash buffer (50mM NaH_2PO_4, pH8.0, 300mM NaCl, 20mM imidazole) are

subsequently applied to the column. Protein was eluted in 1ml fractions in Ni-NTA elution buffer (50mM NaH_2PO_4, pH 8.0, 300mM NaCl, 300mM imidazole). Fractions were analyzed by standard SDS-PAGE to confirm elution of protein. Pooled fractions of ArcA variants were buffer exchanged overnight at 4°C with sample buffer (10mM Tris-Cl pH7.5, 200mM NaCl, 1% glycerol) for a subsequent size exclusion purification. The Ni-NTA purified protein in sample buffer were passed through a 0.22μm filter before loaded onto an AKTA purifier system (GE) with a HiLoad 16/600 Supderdex 200 PG column equilibrated with sample buffer for size exclusion purification. Fractions containing ArcA as indicated by the elution chromatograph and confirmed by SDS-PAGE analysis were pooled and concentrated using Amicon Ultra-4 10K columns (Millipore Cat. UFC801008) per manufacturer's instructions. Final concentrations of 20% glycerol and 10mM DTT were included for storage at -20°C.

Non-reducing SDS-PAGE analysis for ArcA variants

V. cholerae El tor (C6706) with pTara and pET41-*his*$_6$-*arcA*^{WT}, *arcA*^{C173S}, *arcA*^{C233S}, or *arcA*^{C173SC233S} were streaked out for single colonies on LB agar plate containing kanamycin and chloramphenicol to grow overnight at 37°C. A single colony (~1x10^6 CFU/ml) is inoculated into 1.5ml of LB supplemented with kanamycin and chloramphenicol to grow shaking at 37°C for 2hrs, arabinose was added to a final concentration of 0.1% to induce the expression of protein for 2hrs. The culture is switched to standing growth at 37°C to mimic the virulence-inducing microaerobic condition with 1/5 final volume of 5x AKI media included in the culture to constitute a 1x AKI in LB media, in the absence or in the presence of a ROS mix at a final concentration of 50μM of CHP and 500μM of H_2O_2, and in the absence or in the presence of BME. After 3hrs of standing incubation at 37°C, equivalent number of cells according to OD_{600} were spun down and resuspended in Popculture reagents (Millipore Cat. 71092) to allow cell lysis. Samples were mixed 5:1 with 6x SDS non-reducing loading dye (0.3M Tris-Cl, pH7.0, 10% (w/v) SDS, 30% glycerol, 0.06% bromophenol blue) and separated on 12% poly-acrylamide gels. Electrophoresis was performed at room temperature alongside Pageruler pre-stained protein ladder (Thermo

Fisher Cat.26616) with SDS running buffer (25mM Tris, 192mM glycine, 3mM SDS, pH8.3) until the 25kDa pre-stained band reached the bottom of the gel to allow maximal separation of different ArcA variant species under oxidation.

in vitro oxidation of purified His_6-ArcA variants was done with a 1:1 mix of 40μM His_6-ArcA variant proteins in sample buffer with 60mM freshly made GSSG dissolved in Milli-Q water. The mock treatment is a 1:1 mix of protein with Milli-Q water. Phosphorylation reaction was set up per EMSA phosphorylation.

ArcA sequence comparisons

V. cholerae ArcA protein sequence (NCBI accession: WP_09547195.1) was blasted against available protein references in the non-redundant protein sequences in NCBI blastp, excluding *Vibrio cholerae* (taxid 666). 389 ArcA homologs with 100% coverage were detected at a 66% identity cutoff. Among these 15 representative sequences were manually curated for a shortlist with amino acid sequences retrieved in fasta formats for an alignment. A subset of the short list is used for the TREND analysis for the *arcA* genetic neighborhood comparison [143]. A rootless tree with *Pseudoalteromonas sp. T1lg22* ArcA, which is 66% identical to *V. cholerae* ArcA, as an outgroup is generated by MEGA5 using the neighbor-joining algorithm. The amino acid sequences around residues 54, 173 and 233 are examined for conservation of aspartate residue and cysteine residues.

The *E. coli* (NCBI accession: NP_418818.1) and *V. cholerae* ArcA C-terminal DNA binding domains, residues 119-238, were compared to that of representative PhoB/OmpR family RRs: PhoP (PBD ID: 5ED4), KdpE (4KNY), PmrA (4S04), RstA (4NHJ), BaeR (4B09), RitR (5U8K), and PhoB (1GXP). The amino acid sequences were aligned using the Clustal omega (1.2.4) multiple sequence alignment tool.

Phos-tag SDS-PAGE

Mn-based phos-tag SDS-polyacrylamide gels were prepared within 3hrs of use. The resolving gel contains 10% acrylamide and 20μM phos-tag reagent (NARD Cat. AAL-107) and 20μM $MnCl_2$. The phos-tag reagent was dissolved in 100μl of methanol and subsequently diluted with 3.2ml distilled water to constitute a 5mM stock solution and stored at 4°C per manufacturer's instruction. Freshly made 30% ammonium persulfate (APS) is used to ensure proper polymerization of the cation-containing gel. *V. cholerae* C6706 WT with a pTara plasmid encoding the T7 polymerase that over expresses His_6-$ArcA^{WT}$ on a pET41 plasmid were grown under microaerobic conditions in the absence or in the presence of an ROS mixture of 50μM CHP and 500μM H2O2 for 3hrs following 2hrs of induction of protein expression with 0.1% arabinose included in the media. Cell lysates were then immediately lysed by Popculture and mixed with 4x reducing loading buffer onto a freshly made Mn-based phos-tag gel. Proteins are separated by electrophoresis at a constant voltage of 160V for approximately 1hr at room temperature, then transferred to a PVDF membrane with EDTA supplemented transfer buffer for subsequent western blot.

A gradient of carbamoyl phosphate (0, 0.5, 2.5, 12.5, 20, or 40mM final concentrations) was incubated with reduced or oxidized $ArcA^{WT}$ on water buffered heat block (Labnet Accublock) at 30°C for 30min. The mock and oxidation reaction prior to phosphorylation was done at 30°C for 1hr with 0 or 60mM GSSG mixed 1:1 with 36μM $ArcA^{WT}$. 2, 10, 20, 40, 60, or 80μM final concentration of CHP were exposed to $ArcA^{WT}$ phosphorylated at a final concentration of 200mM carbamoyl phosphate at 30°C for 30min.

Intracellular Glutathione quantification

V. cholerae cells were grown on LB agar plate overnight at 37°C and resuspended in AKI media to an OD_{600} of 1. The cell resuspension is diluted at 1:100 into 50ml of AKI supplemented with freshly made filter sterilized $NaHCO_3$ to a final concentration of 0.3% in a falcon tube to grow at 37°C standing for 2hrs. The cell culture is then exposed to none or 60μM of CHP at 37°C for 30min. The culture is pelleted at 4°C with 17,000 rcf for 5min, resuspend in 1ml 0.8% (w/v) saline

to wash away excess CHP, and pelleted again at room temperature for 3min. The pellet is resuspended in 200μl of Milli-Q water and sonicated in Branson 1210 ultrasonic cleaner for 10min. Total and oxidized glutathione in the lysates are quantified using the GSH/GSSG-Glo assay (Promega Cat. V6611) following manufacturer's instructions. Luminescence was taken with clear flat bottom white polystyrene 96 well microplates on Synergy HT plate reader. Data are collected from three independent experiments.

Ultracentrifugation analysis

Purified His_6-tagged $ArcA^{WT}$ protein is oxidized, phosphorylated, or mock treated as described for EMSA. Briefly, 75μl of 54μM His_6-tagged $ArcA^{WT}$ is mixed with 75μl of Milli-Q water for mock reaction, or 75μl of 60mM GSSG for oxidation. 150μl of $ArcA^{WT}$ protein reaction solution is first subject to a 17,000 rcf spinning in a tabletop centrifuge at 4°C for 30min, then 140μl of the supernatant is transferred to an ultracentrifuge polycarbonate tube (Beckman Cat. 343776) to spin at 109,000 rcf in a Beckman Coulter Optima TLX Ultracentrifuge with a TLA120.1 rotor at 4°C for 30min. The protein concentration in each sample at each step are determined by Bradford assays using BSA as a standard. Percentage soluble is calculated by the protein concentration in the supernatant after each spin divided by the initial unspun protein concentration immediately following the (mock) treatment.

Size exclusion chromatography

Purified His_6-tagged $ArcA^{WT}$ after oxidation, phosphorylation, or mock treatment are analyzed by an AKTA Pure chromatography system with a Superose 6 Increase 10/300 column at a 0.5ml/min system flow rate with sample buffer (10mM Tris-Cl, 200mM NaCl, 1% glycerol, pH 7.5) for a total volume of 30ml. 30μg of protein in a 200μl volume (5.6μM) were loaded. Similar results were obtained using an AKTA Purifier chromatography system with a HiLoad 16/600 Superdex 200 PG column at 0.5ml/min flow rate for a total volume of 120ml where approximately 1mg of protein in a 4ml volume (9.3μM) were loaded.

***Salmonella in vitro* CHP challenge**

Salmonella enterica serovar Typhimurium SL1344 were streaked out on an 1.5% LB agar plate containing 100μg/ml ampicillin for single colonies. A single colony of each strain, SL1344 WT with pACYC117 vector, SL1344 Δ*arcA* with pACYC117 vector, pACYC117-*arcA*^{WT} or pACYC117-*arcA*^{C173S}, were confirmed for their respective colony sizes (WT and complementation strain big, Δ*arcA* and *arcA*^{C173S} mutants small) and inoculated to LB media supplemented with 100μg/ml streptomycin and 100μg/ml ampicillin to grow to saturation at 37°C with 200rpm aeration overnight. The overnight culture is diluted 1:40 in LB supplemented with 130μM NaCl, 100μg/ml streptomycin and 100μg/ml ampicillin and grown standing at 37°C for 3hrs. After the 3hr virulence induction, cultures from a single tube were divided in half and 0 or 200μM final concentrations of CHP was added to each part and mixed well. CFU was determined after another hour of static incubation at 37°C. Survival percentage of each strain was calculated by the CFU in the CHP present sample divided by that in the CHP absent sample. Data was collected from three biological repeats.

***Salmonella* Caco-2 Infection**

Salmonella enterica serovar Typhimurium SL1344 WT with pACYC117 vector, SL1344 ΔarcA with pACYC117 vector, pACYC117-*arcA*^{WT} or pACYC117-*arcA*^{C173S} were induced for virulence expression as described in the *Salmonella in vitro* CHP challenge. After the 3hr virulence induction, cells were spun down at 8000rpm for 3min, washed in PBS once before resuspending in 500μl PBS. OD_{600} were determined for each strain to calculate for a multiplicity of infection (moi) of 20 for 2x10E5 Caco-2 cells per well on a 48-well plate in antibiotics free fresh FBS medium changed 1hr before infection. An input CFU was determined by serial dilution of this bacterial cell resuspension to confirm the calculated moi. 100μg/ml gentamycin were added 30 minutes prior to harvesting to eliminate extracellular *Salmonella*. Intracellular bacterial counts were evaluated at 30min, 1hr, 2hr and 4hr post infection. Briefly, supernatant was discarded, and the adhered Caco-2 cells were washed with PBS for five times. 200μl of 0.2% Triton X-100 in PBS was added to each well for 1hr of incubation at RT before collected in an Eppendorf tube. An

additional 800μl of PBS was used to wash the empty wells and combined with the lysed cells. The resulting cell lysate was used for enumeration of CFU at respective timepoints. Data was collected from three infections.

***in vitro* co-culturing of WT and *arcA* mutants in MinA media**

Δ*arcA* mutants (*lacZ*-) and WT (*lacZ*+) cells were grown on an LB plate overnight and resuspended in 0.8% (w/v) saline to similar OD_{600}. The cells were introduced to fresh media either individually, or as a 1:1 mix at a total dilution of 1:1000. Cultures were incubated at 37°C standing. MinA media (46mM K_2HPO_4, 33mM KH_2PO_4, 7.5mM $(NH_4)_2SO_4$, 1.7mM sodium citrate, 1mM $MgSO_4$) was supplied with a final concentration of 0.2% glucose or 0.5% (w/v) of mucin. Sterile mucin was prepared by submerging mucin in 99% ethanol and a complete evaporation of the ethanol in a covered-ventilated vessel on a 60°C heat block. CFU in the input and after 24hr incubation were determined by serial dilution and tilting 10ul of each dilution on an LB agar plate containing 40μg/ml X-gal.

Appendix

Table 1: Mass spec hit summary

Accession #	Gene name	Description	# of unique C oxidation
translation			
Q9KP07	rpsD	30S ribosomal protein S4	1
Q9KNZ8	rpsH	30S ribosomal protein S8	1
Q9KUF0	rpsI	30S ribosomal protein S9	1
Q9KUZ9	rpsL	30S ribosomal protein S12	2
Q9KNZ3	rpsQ	30S ribosomal protein S17	1
Q9KV32	rplJ	50S ribosomal protein L10	1
Q9KP02	rpmD	50S ribosomal protein L30	1
Q9KNQ2	rpmE	50S ribosomal protein L31	4
O68845	rpmI	50S ribosomal protein L35	1
Q9KPM5	fusA2	Elongation factor G 2	2
Q9KUZ6	tufB	Elongation factor Tu-B	3
energy metabolism			
Q9KPJ9	arcA	Aerobic respiration control response regulator ArcA	2
Q9KPF6	lpd	Dihydrolipoyl dehydrogenase	2
Q9KNH5	atpD	ATP synthase subunit beta	1
P0C6Q3	pgk	Phosphoglycerate kinase	1
Q9KT07	ackA1	Acetate kinase 1	2
Q9KQH9	fabF	3-oxoacyl-[acyl-carrier-protein] synthase 2	1
Q9KQY1	VC_1866	Formate acetyltransferase	1
Q9KTA8	VC_0995	PTS system, N-acetylglucosamine-specific IIABC component	1
Q9KQI5	VC_2013	PTS system, glucose specific IIBC component	1
Q9KQG5	VC_2033	Aldehyde-alcohol dehydrogenase	1
redox homeostasis			
Q9KV51	VC_0306	Thioredoxin	2
others			
Q9KRJ1	VC_1649	Trypsin, putative	1
Q9KNR7	groL1	60 kDa chaperonin 1	1
H9L4Q5	VC_0409	MSHA pilin protein MshA	1
Q9KUV4	VC_0408	MSHA pilin protein MshB	1

Table 2: Bacterial strains

Strain	Description	Source or reference
Escherichia coli		
DH5α λpir	λpir lysogen of DH5α	Zhu lab stock
pir2	F- Δ*lac169*, *rpoS*(Am), *robA1*, *creC510*, *hsdR514*, *endA*, *recA1*, *uidA*(Δ*MluI)::pir*	Goulian lab stock (Invitrogen)
XL1-Blue	*recA1, endA1, gyrA96, thi-1, hsdR17, supE44, relA1, lac* [F' *proAB lacI^{q}ZΔM15 Tn10*]	Goulian lab stock (Stratagene)
SM10 λpir	*thi thr leu tonA lacY supE recA::* RP4-2-TC::Mu λ*pir*, KanR	Zhu lab stock
BL21 (DE3)	F$^-$ *ompT hsdS$_B$* (r_B^-, m_B^-) *gal dcm* (DE3)	Zhu lab stock
BL21 (DE3) pYTZ105	BL21(DE3) His$_6$-ArcA^{WT} expression strain	This work
BL21 (DE3) pYTZ105.1	BL21(DE3) His$_6$-ArcA^{C173S} expression strain	This work
BL21 (DE3) pYTZ105.2	BL21(DE3) His$_6$-ArcA^{C233S} expression strain	This work
BL21 (DE3) pYTZ105.3	BL21(DE3) His$_6$-ArcA^{C173SC233S} expression strain	This work
BL21 (DE3) pYTZ105.4	BL21(DE3) His$_6$-ArcA^{D54A} expression strain	This work
BTH101	*F-, cyaA-99, araD139, galE15, galK16, rpsL1 (Strr), hsdR2, mcrA1, mcrB1*	BacTH [142]
BTH101 GCN4-GCN4	BHT101 with pKT25-GCN4 and pUT18c-GCN4	BacTH [142]
BTH101 vector	BHT101 with pKT25 and pUT18c vectors	BacTH [142]
BTH101 ArcA^{WT}-ArcA^{WT}	BTH101 with pYTZ116 and pYTZ117	This work
BTH101 ArcA^{WT}-ArcA^{C173S}	BTH101 with pYTZ116 and pYTZ117.1	This work
Vibrio cholerae		
C6706 WT	*V. cholerae* serovar O1 biotype El tor	Joelsson et al., 2006 [163]
C6706 Δ*lacZ*	*lacZ::ptcpA-sh ble*	Liu et al., 2008 [164]
Δ*arcA*	C6706 *arcA (VC2368)::kan lacZ::ptcpA-sh ble*	This work
Δ*arcA lacZ+*	C6706 *arcA (VC2368)::kan*	This work
arcA^{WT}	C6706 *arcA::kan lacZ::arcA^{WT}*	This work
arcA^{C173S}	C6706 *arcA::kan lacZ::arcA^{C173S}*	This work
arcA^{C233S}	C6706 *arcA::kan lacZ::arcA^{C233S}*	This work
arcA^{C173SC233S}	C6706 *arcA::kan lacZ::arcA^{C173SC233S}*	This work
arcA^{D54A}	C6706 *arcA::kan lacZ::arcA^{D54A}*	This work
Δ*arcB*	C6706 *arcB::spc lacZ::ptcpA-sh ble*	This work
C6706 WT pTara pYTZ105	T7 RNA polymerase His$_6$-ArcA^{WT} *V. cholerae* expression strain	This work
C6706 WT pTara pYTZ105.1	T7 RNA polymerase His$_6$-ArcA^{C173S} *V. cholerae* expression strain	This work
C6706 WT pTara pYTZ105.2	T7 RNA polymerase His$_6$-ArcA^{C233S} *V. cholerae* expression strain	This work

C6706 WT pTara pYTZ105.3	T7 RNA polymerase His_6-$ArcA^{C173SC233S}$ *V. cholerae* expression strain	This work
C6706 WT pTara pYTZ105.3	T7 RNA polymerase His_6-$ArcA^{D54A}$ *V. cholerae* expression strain	This work
∆*arcB* pTara pYTZ105	T7 RNA polymerase His_6-$ArcA^{WT}$ *V. cholerae* ∆*arcB* expression strain	This work
WT pYTZ104	*sdhC* expression *lacZ* reporter plasmid in a C6706 *lacZ::ptcpA sh ble* background	This work
∆*arcA* pYTZ104	*sdhC* expression *lacZ* reporter plasmid in a C6706 *arcA::kan lacZ::ptcpA-sh ble* background	This work
$arcA^{C173S}$ pYTZ104	*sdhC* expression *lacZ* reporter plasmid in a C6706 *arcA::kan lacZ::*$arcA^{C173S}$ background	This work
WT pYTZ204	*fur* expression *lacZ* reporter plasmid in a C6706 *lacZ::ptcpA-sh ble* background	This work
∆*arcA* pYTZ204	*fur* expression *lacZ* reporter plasmid in a C6706 *arcA::kan lacZ::ptcpA-sh ble* background	This work
∆*fur* (lacZ-)	in frame clean deletion of *fur* in a C6706 *lacZ::ptcpA sh ble* background	This work
∆*arcA* ∆fur	in frame clean deletion of fur in C6706 *arcA::kan lacZ::ptcpA-sh ble* background	This work
WT p*katG-lux*	*katG* expression *luxCDABE* reporter plasmid in a C6706 *lacZ::ptcpA sh ble* background	This work
∆*arcA* p*katG-lux*	*katG* expression *luxCDABE* reporter plasmid in a C6706 *arcA::kan lacZ::ptcpA-sh ble* background	This work
∆fur p*katG-lux*	*katG* expression *luxCDABE* reporter plasmid in a C6706 ∆fur background	This work
WT p*katB-lux*	*katB* expression *luxCDABE* reporter plasmid in a C6706 *lacZ::ptcpA sh ble* background	This work
∆*arcA* p*katB-lux*	*katB* expression *luxCDABE* reporter plasmid in a C6706 *arcA::kan lacZ::ptcpA-sh ble* background	This work
∆fur p*katB-lux*	*katB* expression *luxCDABE* reporter plasmid in a C6706 ∆fur background	This work
∆*arcA* pBAD24	C6706 *arcA::kan lacZ::ptcpA-sh ble* with a pBAD24 vector	This work
∆*arcA* pYTZ115	C6706 *arcA::kan lacZ::ptcpA-sh ble* with pBAD24-*sodA*	This work
WT pYTZ103	*feoA* expression *lacZ* reporter plasmid in a C6706 *lacZ::ptcpA-sh ble* background	This work
∆*arcA* pYTZ103	*feoA* expression *lacZ* reporter plasmid in a C6706 *arcA::kan lacZ::ptcpA-sh ble* background	This work
WT pYTZ205	*arcA* expression *lacZ* reporter plasmid in a C6706 *lacZ::ptcpA-sh ble* background	This work
∆*arcA* pYTZ205	*arcA* expression *lacZ* reporter plasmid in a C6706 *arcA::kan lacZ::ptcpA-sh ble* background	This work

Δ*tcpPH* pYTZ205	*arcA* expression l*acZ* reporter plasmid in a C6706 *tcpPH lacZ::ptcpA-sh ble* background	This work
Δ*toxT* pYTZ205	*arcA* expression *lacZ* reporter plasmid in a C6706 *toxT lacZ::ptcpA-sh ble* background	This work
Δ*toxRS* pYTZ205	*arcA* expression *lacZ* reporter plasmid in a C6706 *toxRS lacZ::ptcpA-sh ble* background	This work
Δ*aphB* pYTZ205	*arcA* expression *lacZ* reporter plasmid in a C6706 *aphB lacZ::ptcpA-sh ble* background	This work
Δ*arcA*(KanS)	C6706 with a truncated chromosomal *arcA* (VC2368), kanamycin sensitive	Zhu lab unpublished
Δ*arcA*(KanS) pTara pYTZ105	T7 RNA polymerase His_6-$ArcA^{WT}$ *V. cholerae* expression strain in an arcA KanS background	This work
Salmonella enterica serovar Typhimurium		
LT2 pKD46	avirulent laboratory strain (*rpoS* mutant), with a temperature sensitive plasmid (AmpR) for recombination	Datsenkko & Wanner, 2000 [156]
LT2 *arcA::Kan*	*arcA* (STM4598) KO in LT2	This work
SL1344 WT	virulent laboratory strain (*hisG* mutant) SopE+	Reyes Ruiz et al., 2017 [165]
SL1344 *arcA::Kan*	$P22_{vir}$(LT2 *arcA::Kan*) x SL1344 WT	This work
SL1344 *arcA::Kan* pYTZ210	SL1344 *arcA::Kan* with pACYC117-*parcA-*$arcA^{WT}$	This work
SL1344 *arcA::Kan* pYTZ210.1	SL1344 *arcA::Kan* pACYC117-*parcA-*$arcA^{C173S}$	This work

Table 3: Plasmids

Plasmid	Description	Source or reference
pWM91	R6K vector with *oriR oriT lacZ tetAR sacB*, AmpR	Metcalf et al., 1996 [153]
pYTZ101	pWM91-*arcA* suicide plasmid to disrupt chromosomal *arcA* (VC2368)	This work
pWM91-*fur*	suicide plasmid to disrupt chromosomal *fur* (VC2106)	Zhu lab unpublished
pTara	pACYC184-based plasmid with an AraBAD promoter regulated T7 RNA polymerase (from pAR1217), CmR	Addgene
pET41	*plac*, TEV, Thrombin cleavage sites, N-terminal His_6 expression vector, KanR	Mo et al., 2018 [166]
pYTZ105	pET41-His_6-$ArcA^{WT}$	This work
pYTZ105.1	pET41-His_6-$ArcA^{C173S}$	This work
pYTZ105.2	pET41-His_6-$ArcA^{C233S}$	This work
pYTZ105.3	pET41-His_6-$ArcA^{C173SC233S}$	This work
pYTZ105.4	pET41-His_6-$ArcA^{D54A}$	This work
pJL1	R6K ori, *sacB, lacZ(Vc)::MCS*, AmpR	Zhu lab stock
pYTZ111	pJL1-*parcA*-$arcA^{WT}$	This work
pYTZ112	pJL1-*parcA*-$arcA^{C173S}$	This work
pYTZ113	pJL1-*parcA*-$arcA^{C233S}$	This work
pYTZ114	pJL1-*parcA*-$arcA^{C173SC233S}$	This work
pYTZ118.2	pJL1-*parcA*-$arcA^{D54A}$	This work
pAH6	pACYC184 ori, promoterless *lacZ*, CmR	Hsiao et al., 2006 [167]
pYTZ104	pAH6-1024bp of *sdhC* upstream sequence-*lacZ*	This work
pYTZ204	pAH6-*pfur-lacZ*	This work
pYTZ205	pAH6-*parcA-lacZ*	This work
pYTZ103	pAH6-*pfeoA-lacZ*	This work
pKT25	MCS for C-term translational fusion to T25 ORF on a pSU40 derivative, KanR	BacTH [142]
pUT18c	MCS for C-term translational fusion to T18 ORF on a pUC19 derivative, AmpR	BacTH [142]
pKT25-GCN4	yeast transcription factor GCN4 containing a leucine zipper for protein interaction on pKT25	BacTH [142]
pUT18c-GCN4	yeast transcription factor GCN4 containing a leucine zipper for protein interaction on pUT18c	BacTH [142]
pYTZ116	pKT25-$arcA^{WT}$	This work
pYTZ116.1	pKT25-$arcA^{C173S}$	This work
pYTZ117	pUT18c-$arcA^{WT}$	This work
pYTZ117.1	pUT18c-$arcA^{C173S}$	This work
pBAD24	arabinose inducible promoter, AmpR	Guzman et al., 1995 [168]

pYTZ115	pBAD24-*sodA* (VC2694)	This work
p*katB-luxCDABE*	pBBRlux backbone *katB* (VC1585) promoter-*luxCDABE*, CmR	Xia et al., 2017 [160]
p*katG-luxCDABE*	pBBRlux backbone *katG* (VC1560) promoter-*luxCDABE*, CmR	Xia et al., 2017 [160]
pACYC117	Multi-copy number cloning vector, KanR AmpR	Zhu lab stock
pYTZ210	pACYC117-*Salmonella parcA-arcA*^{WT}, AmpR	This work
pYTZ210.1	pACYC117-*Salmonella parcA-arcA*^{C173S}, AmpR	This work
pKD4	template plasmid for kanamycin resistance cassette for recombination in LT2 to knockout *arcA* (STM4598)	Datsenkko & Wanner, 2000 [156]
pSRKTc	pBBR1MCS-3-derived broad-host-range expression vector, p*lac, lacI*^{q}, *lacZ*α+, TetR	Khan et al., 2008 [169]
pSRKTc-*arcA*^{WT}	*arcA* (VC2368) on pSRKTc	Zhu lab unpublished
pSRKTc-*arcA*^{C173S}	*arcA*^{C173S} (TGT to AGC mutation) on pSRKTc	Zhu lab unpublished
pSRKTc-*arcA*^{C233S}	*arcA*^{C233S} (TGT to AGC mutation) on pSRKTc	Zhu lab unpublished
pSRKTc-*arcA*^{C173SC233S}	*arcA*^{C173SC233S} (TGT to AGC mutation at respective loci) on pSRKTc	Zhu lab unpublished

Table 4: Primers

Primer	Sequence	Resulting construct or purpose
arcA5upFW	GGCGAATTGGGTACCGGGCCCCCCCAACTCTCTTCAAACCAGTGAAAATGAGC	pYTZ101 (*arcA::kan* by Gibson cloning inserted to pWM91)
arcA5upRV	AAATGACCGACCACAAGTTACGTGCGCGAAT	pYTZ101 (*arcA::kan* by Gibson cloning inserted to pWM91)
KmrFW	GCACGTAACTTGTGGTCGGTCATTTCGAACCCC	pYTZ101 (*arcA::kan* by Gibson cloning inserted to pWM91)
KmrRV	TGAGCGGCTCAACAAAGAGAAAGCAGGTAGCTTGCAGT	pYTZ101 (*arcA::kan* by Gibson cloning inserted to pWM91)
arcA3dnFW	TGCTTTCTCTTTGTTGAGCCGCTCAATGCATG	pYTZ101 (*arcA::kan* by Gibson cloning inserted to pWM91)
arcA3dnRV	GGTGGCGGCCGCTCTAGAACTAGTGTTTATCGGTAGCGGCGGTGCG	pYTZ101 (*arcA::kan* by Gibson cloning inserted to pWM91)
StuI400arcA5	CGAGGCCTCAGTAAAATGGCCAATTTACTGG	insert with a StuI site followed by 400 bp of *arcA* upstream sequences (native promoter) for chromosomal complementation with pJL1 derived plasmids
arcA3NotI	CGGCGGCCGCTTAATCTTCTAAATCACC	*arcA* sequence including stop codon followed by a NotI site for chromosomal complementation with pJL1 derived plasmids
parcA5 (f1 For)	GGGGATTGGTACCGCCAGTAAAATGGCCAATTTACTGGCT	amplify native *arcA* promoter from *V. cholerae* genome for pJL1 based plasmids
parcA3 (f1 Rev)	GGTTTGCATTAGCGTTACCTAAACTTG	amplify native *arcA* promoter from *V. cholerae* genome for pJL1 based plasmids
arcA3 (f2 For)	TTGGTACCAGATCTTAATTAAGGTTAATCTTCTAAATCACCACAGAAGC	PCR fragment for Gibson assembly for pJL1 based plasmids from pSRKTc subcloning
arcA5 (f2 Rev)	GTAACGCTAATGCAAACCCCGCAGA	PCR fragment for Gibson assembly for pJL1 based plasmids from pSRKTc subcloning
arcA3C2S (f2 for')	TTGGTACCAGATCTTAATTAAGGTTAATCTTCTAAATCACCGCTGAAGC	PCR fragment for Gibson assembly for pJL1 based plasmids from pSRKTc subcloning
pJL1seqFW	GATGAGCCGACTTTCCAA	sequencing primer to confirm insert sequences on a pJL1 derived plasmid
pJL1seqRV	TCGACCCGCGCATACATC	sequencing primer to confirm insert sequences on a pJL1 derived plasmid
pJL1StuIparcA5FOR1	TTGGTACCAGATCTTAATTAAGGCCTCAGTAAAATGGCCAATTTACTGGCTTTTCA	pYTZ118.2 (pJL1-*arcA*^{D54A})

pYTZ118.2REV1	GCAGGTTGATGGCCATAATCACCAA	pYTZ118.2 (pJL1-*arcA*^{D54A})
pYTZ118.2FOR2	GATTATGGCCATCAACCTGCCAGGA	pYTZ118.2 (pJL1-*arcA*^{D54A})
pJL1arcA3NotIREV2	GAATCGGGGATTGGTACCGCGGCCGCTTAATCTTCTAAATCACCACAGAAGCGGT	pYTZ118.2 (pJL1-*arcA*^{D54A})
lacZ insertion sequencing NotI	TTTGGTCGCTCGGCAATG	sequencing primer to confirm pJL1 insert on genome
lacZ insertion StuI sequencing	GATGGGTCGCGCTGTTTC	sequencing primer to confirm pJL1 insert on genome
arcB F1	CAACTGGTGAACACCATAGG	*arcB::spec* by MuGent
arcB R1	GTCGACGGATCCCCGGAATCATTCACTGCTCCGTCAGATAAAG	*arcB::spec* by MuGent
arcB F2	GAAGCAGCTCCAGCCTACACAAGCAAACGCAAAGCAG	*arcB::spec* by MuGent
arcB R2	CTCGCATCCCTTCCTCCAAA	*arcB::spec* by MuGent
ABD123	ATTCCGGGGATCCGTCGAC	MuGent primers for introducing antibiotics cassettes
ABD124	TGTAGGCTGGAGCTGCTTC	MuGent primers for introducing antibiotics cassettes
arcB check	TTCTTTTATATCTAATTAGA	primer to check MuGent *arcB::spec* on chromosome
arcA-3NdeI-TEV	GGCCATATGGAGAACCTCTACTTCCAATCGATGCAAACCCCGCAGATCC	PCR insert with 3 random bases for NdeI cleavage for pET41 derived plasmids for His_6-tag ArcA variants
arcA3-XhoI	GTCTCGAGTTAATCTTCTAAATCACC	PCR insert for pET41 derived plasmids for His-tagged ArcA variants
sdhClacZ-SalI	GAGTCGACGGCTTGCTCACTCAGCTCC	pYTZ104 (pAH6 derived *psdhC-lacZ* reporter plasmid)
sdhClacZ-XbaI	GATCTAGAGGCAAACATCATGTGCAGG	pYTZ104 (pAH6 derived *psdhC-lacZ* reporter plasmid)
feoAlacZ-XbaI	GATCTAGAGTCGTTAAATGAGGTTCGC	pYTZ103 (pAH6 derived *pfeoA-lacZ* reporter plasmid)
feoAlacZ-SalI	ATGTCGACGTGACAATTTCATAGAGG	pYTZ103 (pAH6 derived *pfeoA-lacZ* reporter plasmid)
fur-SalI	TGGTCGACTGACATATACTTTCCTG	pYTZ204 (pAH6 derived *pfur-lacZ* reporter plasmid)
fur-XbaI	GCTCTAGACAGGGAAGCATTTATCGC	pYTZ204 (pAH6 derived *pfur-lacZ* reporter plasmid)
arcA_SalI	ATGTCGACTTGCTCGTCTTCGACGAT	pYTZ205 (pAH6 derived *parcA-lacZ* reporter plasmid)
arcA-XbaI	CCTCTAGACGATCAAGCATTGCTGTA	pYTZ205 (pAH6 derived *parcA-lacZ* reporter plasmid)
pKT25-ArcA-EcoRI	ATGAATTCTTAATCTTCTAAATCACC	pYTZ116 and pYTZ117 derived plasmids for BacTH
pKT25-ArcA-XbaI	GGTCTAGAGATGCAAACCCCGCAGATCC	pYTZ116 and pYTZ117 derived plasmids for BacTH
pUT18c sequencing	TGCCGGGAGCAGACA	pUT18c sequencing to confirm correct insert

sdhC EMSA1 HindIII	GCAAAGCTTTTGCAGTCCGTATAGTGA	HindIII site 5' to a ~300bp of sdhC promoter
sdhC EMSA2 HindIII	GCAAAGCTTATTGCTGAGATCGGAAAG	HindIII site 3' to a ~300bp of sdhC promoter
fur_EMSA	ATGAATTCGCCGTCTACCTGCATCTC	EcoRI site 5' to a *fur* promoter sequence
fur EMSA2	ATGAATTCCAAAATGGAGGCCAAGA	EcoRI site 3' to a *fur* promoter sequence
oppA EMSA1	GCGAATTCAGATTGATAGGCTTGAAGGAGGC	EcoRI site 5' to an *oppA* promoter sequence
oppA EMSA2	GCGAATTCAACAGACTATCCTCTTTGG	EcoRI site 3' to an *oppA* promoter sequence
Fur Check 5F	GTAAGAGCACTTTGTTCAG	PCR primer to confirm chromosomal *fur* deletion
Fur Check R3	CGGTGCGGATTTCCCAAC	PCR primer to confirm chromosomal *fur* deletion
sodA-EcoRI	ATGAATTCATGCTATCCGCCTTGCTGA	pYTZ115 (pBAD24-*sodA*)
sodA-HindIII	GAAAGCTTCCCTTCTGATGATTTACG	pYTZ115 (pBAD24-*sodA*)
5'pcr	GGCAGGTCAGGGACTTTTGT	*arcA* (STM4598) KO in LT2
3'pcr	AAGAAACAGCCAGTAAGAAT	*arcA* (STM4598) KO in LT2
5'+P1	ACTTCCTGTTTCGATTTAGTTGGCAATTTAGGTAGCAAAC GTGTAGGCTGGAGCTGCTTC	*arcA* (STM4598) KO in LT2
3'+P2	AACTTACCGGCTGTTTTTACAGTTTGGCGCCTGGGCCGAA CATATGAATATCCTCCTTAG	*arcA* (STM4598) KO in LT2
SLarcA5BamHI	GCCGGATCCTACGTCTTAGCCTGTTATG	pYTZ210 and pYTZ210.1 inserts (with native SL1344 *arcA* promoter) PCR primers using synthesized fragment (Genewiz) as template
SLarcA3HindIII	GGCAAGCTTGGCCGAATTAATCCTGC	pYTZ210 and pYTZ210.1 inserts (with native SL1344 *arcA* promoter) PCR primers using synthesized fragment (Genewiz) as template
ohrAqPCRF	CAAAAGAGATGGGTGGAAGC	*ohrA* qPCR primer
ohrAqPCRR	GAAAAGCAAGCAGCATAGCC	*ohrA* qPCR primer
16S60bpcontrol Fw	CGGTAATACGGAGGGTGCAA	16s RNA qPCR primer for internal control
16S60bpcontrol Rv	CACCTGCATGCGCTTTACG	16s RNA qPCR primer for internal control
16S-C6706-For	GTGTAGCGGTGAAATGCGTAG	16s RNA qPCR primer for internal control
16S-C6706-RT	TAGGGCACAACCTCCAAGTAG	16s RNA qPCR primer for internal control

BIBLIOGRAPHY

1. Escobar LE, Ryan SJ, Stewart-Ibarra AM, et al. A global map of suitability for coastal Vibrio cholerae under current and future climate conditions. *Acta Trop*. 2015;149:202-211. doi:10.1016/j.actatropica.2015.05.028

2. Datta PP, Bhadra RK. Cold Shock Response and Major Cold Shock Proteins of Vibrio cholerae. *Appl Environ Microbiol*. 2003;69(11):6361-6369. doi:10.1128/AEM.69.11.6361-6369.2003

3. Faruque SM, Albert MJ, Mekalanos JJ. Epidemiology, Genetics, and Ecology of ToxigenicVibrio cholerae. *Microbiol Mol Biol Rev*. Published online 1998. doi:10.1128/mmbr.62.4.1301-1314.1998

4. Gupta S, Chowdhury R. Bile affects production of virulence factors and motility of Vibrio cholerae. *Infect Immun*. Published online 1997. doi:10.1128/iai.65.3.1131-1134.1997

5. Schuhmacher DA, Klose KE. Environmental signals modulate ToxT-dependent virulence factor expression in Vibrio cholerae. *J Bacteriol*. Published online 1999. doi:10.1128/jb.181.5.1508-1514.1999

6. Kovacikova G, Lin W, Skorupski K. The LysR-type virulence activator AphB regulates the expression of genes in Vibrio cholerae in response to low pH and anaerobiosis. *J Bacteriol*. 2010;192(16):4181-4191. doi:10.1128/JB.00193-10

7. Midgett CR, Almagro-Moreno S, Pellegrini M, Taylor RK, Skorupski K, Kull FJ. Bile salts and alkaline pH reciprocally modulate the interaction between the periplasmic domains of Vibrio cholerae ToxR and ToxS. *Mol Microbiol*. Published online 2017. doi:10.1111/mmi.13699

8. Chatterjee A, Dutta PK, Chowdhury R. Effect of fatty acids and cholesterol present in bile on expression of virulence factors and motility of Vibrio cholerae. *Infect Immun*. Published online 2007. doi:10.1128/IAI.01435-06

9. Lowden MJ, Skorupski K, Pellegrini M, Chiorazzo MG, Taylor RK, Kull FJ. Structure of Vibrio cholerae ToxT reveals a mechanism for fatty acid regulation of virulence genes. *Proc Natl Acad Sci U S A*. Published online 2010. doi:10.1073/pnas.0915021107

10. Abuaita BH, Withey JH. Bicarbonate Induces Vibrio cholerae virulence gene expression by enhancing ToxT activity. *Infect Immun*. 2009;77(9):4111-4120. doi:10.1128/IAI.00409-09

11. Acosta N, Pukatzki S, Raivio TL. The Vibrio cholerae Cpx envelope stress response senses and mediates adaptation to low iron. *J Bacteriol*. 2015;197(2):262-276. doi:10.1128/JB.01957-14

12. Acosta N, Pukatzki S, Raivio TL. The Cpx system regulates virulence gene expression in Vibrio cholerae. *Infect Immun*. 2015;83(6):2396-2408. doi:10.1128/IAI.03056-14

13. Scott Merrell D, Bailey C, Kaper JB, Camilli A. The ToxR-mediated organic acid tolerance response of vibrio cholerae requires OmpU. *J Bacteriol*. Published online 2001. doi:10.1128/JB.183.9.2746-2754.2001

14. DiRita VJ, Parsot C, Jander G, Mekalanos JJ. Regulatory cascade controls virulence in Vibrio cholerae. *Proc Natl Acad Sci U S A*. Published online 1991. doi:10.1073/pnas.88.12.5403

15. Higgins DE, DiRita VJ. Transcriptional control of toxT, a regulatory gene in the ToxR regulon of Vibrio cholerae. *Mol Microbiol*. Published online 1994. doi:10.1111/j.1365-2958.1994.tb01263.x

16. Miller VL, DiRita VJ, Mekalanos JJ. Identification of toxS, a regulatory gene whose product enhances ToxR-mediated activation of the cholera toxin promoter. *J Bacteriol*. Published online 1989. doi:10.1128/jb.171.3.1288-1293.1989

17. Yang M, Liu Z, Hughes C, et al. Bile salt-induced intermolecular disulfide bond formation activates Vibrio cholerae virulence. *Proc Natl Acad Sci U A*. 2013;110(6):2348-2353. doi:10.1073/pnas.1218039110

18. Morgan SJ, French EL, Thomson JJ, Seaborn CP, Shively CA, Krukonis ES. Formation of an Intramolecular Periplasmic Disulfide Bond in TcpP Protects TcpP and TcpH from Degradation in Vibrio cholerae. *J Bacteriol*. 2016;198(3):498-509. doi:10.1128/JB.00338-15

19. Almagro-Moreno S, Root MZ, Taylor RK. Role of ToxS in the proteolytic cascade of virulence regulator ToxR in Vibrio cholerae. *Mol Microbiol*. 2015;98(5):963-976. doi:10.1111/mmi.13170

20. Goss TJ, Seaborn CP, Gray MD, Krukonis ES. Identification of the TcpP-binding site in the toxT promoter of Vibrio cholerae and the role of ToxR in TcpP-mediated activation. *Infect Immun*. 2010;78(10):4122-4133. doi:10.1128/IAI.00566-10

21. Krukonis ES, Yu RR, Dirita VJ. The Vibrio cholerae ToxR/TcpP/ToxT virulence cascade: distinct roles for two membrane-localized transcriptional activators on a single promoter. *Mol Microbiol*. 2000;38(1):67-84.

22. Fan F, Liu Z, Jabeen N, Birdwell LD, Zhu J, Kan B. Enhanced interaction of Vibrio cholerae virulence regulators TcpP and ToxR under oxygen-limiting conditions. *Infect Immun*. 2014;82(4):1676-1682. doi:10.1128/IAI.01377-13

23. Kovacikova G, Skorupski K. A Vibrio cholerae LysR homolog, AphB, cooperates with AphA at the tcpPH promoter to activate expression of the ToxR virulence cascade. *J Bacteriol*. Published online 1999. doi:10.1128/jb.181.14.4250-4256.1999

24. Liu Z, Yang M, Peterfreund GL, et al. Vibrio cholerae anaerobic induction of virulence gene expression is controlled by thiol-based switches of virulence regulator AphB. *Proc Natl Acad Sci U A*. 2011;108(2):810-815. doi:10.1073/pnas.1014640108

25. Taylor JL, de Silva RS, Kovacikova G, et al. The crystal structure of AphB, a virulence gene activator from Vibrio cholerae, reveals residues that influence its response to oxygen and pH. *Mol Microbiol*. Published online 2012. doi:10.1111/j.1365-2958.2011.07919.x

26. Kovacikova G, Lin W, Skorupski K. The virulence activator AphA links quorum sensing to pathogenesis and physiology in Vibrio cholerae by repressing the expression of a penicillin amidase gene on the small chromosome. *J Bacteriol*. Published online 2003. doi:10.1128/JB.185.16.4825-4836.2003

27. Kovacikova G, Skorupski K. Regulation of virulence gene expression in Vibrio cholerae by quorum sensing: HapR functions at the aphA promoter. *Mol Microbiol*. Published online 2002. doi:10.1046/j.1365-2958.2002.03229.x

28. Kovacikova G, Skorupski K. Overlapping binding sites for the virulence gene regulators AphA, AphB and cAMP-CRP at the Vibrio cholerae TcpPH promoter. *Mol Microbiol*. Published online 2001. doi:10.1046/j.1365-2958.2001.02518.x

29. Abuaita BH, Withey JH. Bicarbonate Induces Vibrio cholerae Virulence Gene Expression by Enhancing ToxT Activity. *Infect Immun*. 2009;77(9):4111-4120. doi:10.1128/IAI.00409-09

30. Abuaita BH, Withey JH. Termination of Vibrio cholerae virulence gene expression is mediated by proteolysis of the major virulence activator, ToxT. *Mol Microbiol*. 2011;81(6):1640-1653. doi:10.1111/j.1365-2958.2011.07798.x

31. Abd H, Weintraub A, Sandstrom G. Intracellular survival and replication of Vibrio cholerae O139 in aquatic free-living amoebae. *Env Microbiol*. 2005;7(7):1003-1008. doi:10.1111/j.1462-2920.2005.00771.x

32. Espinoza-Vergara G, Hoque MM, McDougald D, Noorian P. The Impact of Protozoan Predation on the Pathogenicity of Vibrio cholerae. *Front Microbiol*. Published online 2020. doi:10.3389/fmicb.2020.00017

33. Faruque SM, Mekalanos JJ. Phage-bacterial interactions in the evolution of toxigenic Vibrio cholerae. *Virulence*. Published online 2012. doi:10.4161/viru.22351

34. Long RA, Rowley DC, Zamora E, Liu J, Bartlett DH, Azam F. Antagonistic interactions among marine bacteria impede the proliferation of Vibrio cholerae. *Appl Env Microbiol*. 2005;71(12):8531-8536. doi:10.1128/AEM.71.12.8531-8536.2005

35. West AH, Stock AM. Histidine kinases and response regulator proteins in two-component signaling systems. *Trends Biochem Sci*. 2001;26(6):369-376.

36. Teschler JK, Cheng AT, Yildiz FH. The two-component signal transduction system VxrAB positively regulates Vibrio cholerae biofilm formation. *J Bacteriol*. Published online 2017. doi:10.1128/JB.00139-17

37. Sultan SZ, Silva AJ, Benitez JA. The PhoB regulatory system modulates biofilm formation and stress response in El Tor biotype Vibrio cholerae. *FEMS Microbiol Lett*. Published online 2010. doi:10.1111/j.1574-6968.2009.01837.x

38. Herrera CM, Crofts AA, Henderson JC, Pingali SC, Davies BW, Trent MS. The Vibrio cholerae VprA-VprB Two-Component System Controls Virulence through Endotoxin Modification. Taylor RK, ed. *mBio*. 2014;5(6):e02283-14. doi:10.1128/mBio.02283-14

39. Slamti L, Waldor MK. Genetic analysis of activation of the Vibrio cholerae Cpx pathway. *J Bacteriol*. Published online 2009. doi:10.1128/JB.00406-09

40. Taylor DL, Renee Bina X, Slamti L, Waldor MK, Bina JE. Reciprocal regulation of resistance-nodulation-division efflux systems and the Cpx two-component system in vibrio cholerae. *Infect Immun*. Published online 2014. doi:10.1128/IAI.00025-14

41. Laub MT, Goulian M. Specificity in Two-Component Signal Transduction Pathways. *Annu Rev Genet*. 2007;41(1):121-145. doi:10.1146/annurev.genet.41.042007.170548

42. Capra EJ, Perchuk BS, Skerker JM, Laub MT. Adaptive Mutations that Prevent Crosstalk Enable the Expansion of Paralogous Signaling Protein Families. *Cell*. 2012;150(1):222-232. doi:10.1016/j.cell.2012.05.033

43. Wang H, Ayala JC, Benitez JA, Silva AJ. RNA-Seq Analysis Identifies New Genes Regulated by the Histone-Like Nucleoid Structuring Protein (H-NS) Affecting Vibrio cholerae Virulence, Stress Response and Chemotaxis. *PLOS ONE*. 2015;10(2):e0118295. doi:10.1371/journal.pone.0118295

44. Lee SH, Angelichio MJ, Mekalanos JJ, Camilli A. Nucleotide Sequence and Spatiotemporal Expression of the Vibrio cholerae vieSAB Genes during Infection. *J Bacteriol*. 1998;180(9):2298-2305. doi:10.1128/JB.180.9.2298-2305.1998

45. Martinez-Wilson HF, Tamayo R, Tischler AD, Lazinski DW, Camilli A. The Vibrio cholerae Hybrid Sensor Kinase VieS Contributes to Motility and Biofilm Regulation by Altering the Cyclic Diguanylate Level. *J Bacteriol*. 2008;190(19):6439-6447. doi:10.1128/JB.00541-08

46. Dey AK, Bhagat A, Chowdhury R. Host Cell Contact Induces Expression of Virulence Factors and VieA, a Cyclic di-GMP Phosphodiesterase, in Vibrio cholerae. *J Bacteriol*. 2013;195(9):2004-2010. doi:10.1128/JB.02127-12

47. Tischler AD, Camilli A. Cyclic diguanylate (c-di-GMP) regulates Vibrio cholerae biofilm formation: c-di-GMP regulates V. cholerae biofilm. *Mol Microbiol*. 2004;53(3):857-869. doi:10.1111/j.1365-2958.2004.04155.x

48. Tamayo R, Patimalla B, Camilli A. Growth in a Biofilm Induces a Hyperinfectious Phenotype in Vibrio cholerae. *Infect Immun*. 2010;78(8):3560-3569. doi:10.1128/IAI.00048-10

49. Seper A, Fengler VHI, Roier S, et al. Extracellular nucleases and extracellular DNA play important roles in *Vibrio cholerae* biofilm formation. *Mol Microbiol*. 2011;82(4):1015-1037. doi:10.1111/j.1365-2958.2011.07867.x

50. Mitchell SL, Ismail AM, Kenrick SA, Camilli A. The VieB auxiliary protein negatively regulates the VieSA signal transduction system in Vibrio cholerae. *BMC Microbiol*. 2015;15(1):59. doi:10.1186/s12866-015-0387-7

51. Tamplin ML, Gauzens AL, Huq A, Sack DA, Colwell RR. Attachment of Vibrio cholerae serogroup O1 to zooplankton and phytoplankton of Bangladesh waters. *Appl Env Microbiol*. 1990;56(6):1977-1980.

52. Merrell DS, Butler SM, Qadri F, et al. Host-induced epidemic spread of the cholera bacterium. *Nature*. 2002;417(6889):642-645. doi:10.1038/nature00778

53. Shukla BN, Singh D V, Sanyal SC. Attachment of non-culturable toxigenic Vibrio cholerae O1 and non-O1 and Aeromonas spp. to the aquatic arthropod Gerris spinolae and plants in the River Ganga, Varanasi. *FEMS Immunol Med Microbiol*. 1995;12(2):113-120. doi:10.1111/j.1574-695X.1995.tb00182.x

54. Wang J, Yan M, Gao H, Lu X, Kan B. Vibrio cholerae Colonization of Soft-Shelled Turtles. *Appl Env Microbiol*. 2017;83(14). doi:10.1128/AEM.00713-17

55. Huq A, Small EB, West PA, Huq MI, Rahman R, Colwell RR. Ecological relationships between Vibrio cholerae and planktonic crustacean copepods. *Appl Env Microbiol*. 1983;45(1):275-283.

56. Li X, Roseman S. The chitinolytic cascade in Vibrios is regulated by chitin oligosaccharides and a two-component chitin catabolic sensor/kinase. *Proc Natl Acad Sci*. 2004;101(2):627-631. doi:10.1073/pnas.0307645100

57. Chourashi R, Mondal M, Sinha R, et al. Role of a sensor histidine kinase ChiS of Vibrio cholerae in pathogenesis. *Int J Med Microbiol*. 2016;306(8):657-665. doi:10.1016/j.ijmm.2016.09.003

58. Klancher CA, Yamamoto S, Dalia TN, Dalia AB. ChiS is a noncanonical DNA-binding hybrid sensor kinase that directly regulates the chitin utilization program in Vibrio cholerae. *bioRxiv*. Published online 2020. doi:10.1101/2020.01.10.902320

59. Li X, Roseman S. The chitinolytic cascade in Vibrios is regulated by chitin oligosaccharides and a two-component chitin catabolic sensor/kinase. *Proc Natl Acad Sci U A*. 2004;101(2):627-631. doi:10.1073/pnas.0307645100

60. Bekker M, Alexeeva S, Laan W, Sawers G, Teixeira de Mattos J, Hellingwerf K. The ArcBA two-component system of Escherichia coli is regulated by the redox state of both the ubiquinone and the menaquinone pool. *J Bacteriol*. 2010;192(3):746-754. doi:10.1128/JB.01156-09

61. Malpica R, Sandoval GR, Rodriguez C, Franco B, Georgellis D. Signaling by the arc two-component system provides a link between the redox state of the quinone pool and gene expression. *Antioxid Redox Signal*. 2006;8(5-6):781-795. doi:10.1089/ars.2006.8.781

62. Malpica R, Franco B, Rodriguez C, Kwon O, Georgellis D. Identification of a quinone-sensitive redox switch in the ArcB sensor kinase. *Proc Natl Acad Sci U A*. 2004;101(36):13318-13323. doi:10.1073/pnas.0403064101

63. Alvarez AF, Rodriguez C, Georgellis D. Ubiquinone and Menaquinone Electron Carriers Represent the Yin and Yang in the Redox Regulation of the ArcB Sensor Kinase. *J Bacteriol*. 2013;195(13):3054-3061. doi:10.1128/JB.00406-13

64. Kan B, Habibi H, Schmid M, et al. Proteome comparison of Vibrio cholerae cultured in aerobic and anaerobic conditions. *Proteomics*. 2004;4(10):3061-3067. doi:10.1002/pmic.200400944

65. Park DM, Akhtar MS, Ansari AZ, Landick R, Kiley PJ. The Bacterial Response Regulator ArcA Uses a Diverse Binding Site Architecture to Regulate Carbon Oxidation Globally. *PLoS Genet*. Published online 2013. doi:10.1371/journal.pgen.1003839

66. Nobechi K. CONTRIBUTIONS TO THE KNOWLEDGE OF VIBRIO CHOLERAE I. FERMENTATION OF CARBOHYDRATES AND POLYATOMIC ALCOHOLS BY VIBRIO CHOLERAE. *J Bacteriol*. 1925;10(3):197-215. doi:10.1128/JB.10.3.197-215.1925

67. Lee K-M, Park Y, Bari W, et al. Activation of Cholera Toxin Production by Anaerobic Respiration of Trimethylamine N-oxide in *Vibrio cholerae*. *J Biol Chem*. 2012;287(47):39742-39752. doi:10.1074/jbc.M112.394932

68. Hiremath G, Hyakutake A, Yamamoto K, et al. Hypoxia-induced localization of chemotaxis-related signaling proteins in Vibrio cholerae. *Mol Microbiol*. 2015;95(5):780-790. doi:10.1111/mmi.12887

69. Ravcheev DA, Gerasimova AV, Mironov AA, Gelfand MS. Comparative genomic analysis of regulation of anaerobic respiration in ten genomes from three families of gamma-proteobacteria (Enterobacteriaceae, Pasteurellaceae, Vibrionaceae). *BMC Genomics*. 2007;8(1):54. doi:10.1186/1471-2164-8-54

70. Sengupta N, Paul K, Chowdhury R. The global regulator ArcA modulates expression of virulence factors in Vibrio cholerae. *Infect Immun*. 2003;71(10):5583-5589. doi:10.1128/iai.71.10.5583-5589.2003

71. Kadir K, Nelson KL. Sunlight mediated inactivation mechanisms of Enterococcus faecalis and Escherichia coli in clear water versus waste stabilization pond water. *Water Res*. 2014;50:307-317. doi:10.1016/j.watres.2013.10.046

72. Babior BM. The NADPH oxidase of endothelial cells. *IUBMB Life*. 2000;50(4-5):267-269. doi:10.1080/713803730

73. Singh SP, Rastogi RP, Hader DP, Sinha RP. Temporal dynamics of ROS biogenesis under simulated solar radiation in the cyanobacterium Anabaena variabilis PCC 7937. *Protoplasma*. 2014;251(5):1223-1230. doi:10.1007/s00709-014-0630-3

74. Pattison DI, Davies MJ. Actions of ultraviolet light on cellular structures. *EXS*. Published online 2006. doi:10.1007/3-7643-7378-4_6

75. Imlay JA. Where in the world do bacteria experience oxidative stress? *Environ Microbiol*. Published online 2019. doi:10.1111/1462-2920.14445

76. Payne SM, Mey AR, Wyckoff EE. Vibrio Iron Transport: Evolutionary Adaptation to Life in Multiple Environments. *Microbiol Mol Biol Rev*. Published online 2016. doi:10.1128/mmbr.00046-15

77. Kettle AJ, Winterbourn CC. Myeloperoxidase: A key regulator of neutrophil oxidant product. *Redox Rep*. Published online 1997. doi:10.1080/13510002.1997.11747085

78. Gutteridge JM, Halliwell B. The measurement and mechanism of lipid peroxidation in biological systems. *Trends Biochem Sci*. 1990;15(4):129-135. doi:10.1016/0968-0004(90)90206-q

79. Imlay JA, Linn S. DNA damage and oxygen radical toxicity. *Science*. 1988;240(4857):1302-1309. doi:10.1126/science.3287616

80. Lesser MP. Oxidative stress in marine environments: biochemistry and physiological ecology. *Annu Rev Physiol*. 2006;68:253-278. doi:10.1146/annurev.physiol.68.040104.110001

81. Tretyakova NY, Groehler A th, Ji S. DNA-Protein Cross-Links: Formation, Structural Identities, and Biological Outcomes. *Acc Chem Res*. 2015;48(6):1631-1644. doi:10.1021/acs.accounts.5b00056

82. Sanchez-Alberola N, Campoy S, Barbé J, Erill I. Analysis of the SOS response of Vibrio and other bacteria with multiple chromosomes. *BMC Genomics*. Published online 2012. doi:10.1186/1471-2164-13-58

83. Krin E, Pierlé SA, Sismeiro O, et al. Expansion of the SOS regulon of Vibrio cholerae through extensive transcriptome analysis and experimental validation. *BMC Genomics*. Published online 2018. doi:10.1186/s12864-018-4716-8

84. Baharoglu Z, Mazel D. Vibrio cholerae triggers SOS and mutagenesis in response to a wide range of antibiotics: A route towards multiresistance. *Antimicrob Agents Chemother*. Published online 2011. doi:10.1128/AAC.01549-10

85. Yan LJ. Analysis of oxidative modification of proteins. *Curr Protoc Protein Sci*. 2009;Chapter 14:Unit 14 4. doi:10.1002/0471140864.ps1404s55

86. Pattison DI, Davies MJ. Absolute rate constants for the reaction of hypochlorous acid with protein side chains and peptide bonds. *Chem Res Toxicol*. Published online 2001. doi:10.1021/tx0155451

87. Prasad S, Gupta SC, Tyagi AK. Reactive oxygen species (ROS) and cancer: Role of antioxidative nutraceuticals. *Cancer Lett*. Published online 2017. doi:10.1016/j.canlet.2016.03.042

88. Xia X, Larios-Valencia J, Liu Z, et al. OxyR-activated expression of Dps is important for Vibrio cholerae oxidative stress resistance and pathogenesis. *PLoS One*. 2017;12(2):e0171201. doi:10.1371/journal.pone.0171201

89. Wang H, Chen S, Zhang J, et al. Catalases promote resistance of oxidative stress in Vibrio cholerae. *PLoS One*. 2012;7(12):e53383. doi:10.1371/journal.pone.0053383

90. Wang H, Naseer N, Chen Y, et al. OxyR2 modulates OxyR1 activity and Vibrio cholerae oxidative stress response. *Infect Immun*. Published online 2017. doi:10.1128/IAI.00929-16

91. Jiang H-H, Zhou Y, Liu M, et al. Vibrio cholerae Virulence Activator ToxR Regulates Manganese Transport and Resistance to Reactive Oxygen Species. *Infect Immun*. 2020;88(3). doi:10.1128/IAI.00944-19

92. Wang H, Xing X, Wang J, et al. Hypermutation-induced in vivo oxidative stress resistance enhances Vibrio cholerae host adaptation. *PLoS Pathog*. 2018;14(10):e1007413. doi:10.1371/journal.ppat.1007413

93. Bhatnagar A, Bandyopadhyay D. Characterization of cysteine thiol modifications based on protein microenvironments and local secondary structures. *Proteins Struct Funct Bioinforma*. Published online 2018. doi:10.1002/prot.25424

94. Braun M, Thöny-Meyer L. Cytochrome c maturation and the physiological role of c-type cytochromes in Vibrio cholerae. *J Bacteriol*. Published online 2005. doi:10.1128/JB.187.17.5996-6004.2005

95. Mukhopadhyay R, Chacón KN, Jarvis JM, Talipov MR, Yukl ET. Structural insights into the mechanism of oxidative activation of heme-free H-NOX from Vibrio cholerae. *Biochem J*. Published online 2020. doi:10.1042/BCJ20200124

96. Guo Y, Iavarone AT, Cooper MM, Marletta MA. Mapping the H-NOX/HK Binding Interface in Vibrio cholerae by Hydrogen/Deuterium Exchange Mass Spectrometry. *Biochemistry*. Published online 2018. doi:10.1021/acs.biochem.8b00027

97. Plate L, Marletta MA. Nitric Oxide Modulates Bacterial Biofilm Formation through a Multicomponent Cyclic-di-GMP Signaling Network. *Mol Cell*. Published online 2012. doi:10.1016/j.molcel.2012.03.023

98. Hillion M, Antelmann H. Thiol-based redox switches in prokaryotes. *Biol Chem*. 2015;396(5):415-444. doi:10.1515/hsz-2015-0102

99. Antelmann H, Helmann JD. Thiol-based redox switches and gene regulation. *Antioxid Redox Signal*. 2011;14(6):1049-1063. doi:10.1089/ars.2010.3400

100. Poole LB, Karplus PA, Claiborne A. Protein sulfenic acids in redox signaling. *Annu Rev Pharmacol Toxicol*. 2004;44:325-347. doi:10.1146/annurev.pharmtox.44.101802.121735

101. Liu Z, Wang H, Zhou Z, et al. Thiol-based switch mechanism of virulence regulator AphB modulates oxidative stress response in Vibrio cholerae. *Mol Microbiol*. 2016;102(5):939-949. doi:10.1111/mmi.13524

102. Liu Z, Wang H, Zhou Z, et al. Differential Thiol-Based Switches Jump-Start Vibrio cholerae Pathogenesis. *Cell Rep*. 2016;14(2):347-354. doi:10.1016/j.celrep.2015.12.038

103. Choi HJ, Kim SJ, Mukhopadhyay P, et al. Structural basis of the redox switch in the OxyR transcription factor. *Cell*. Published online 2001. doi:10.1016/S0092-8674(01)00300-2

104. Zheng M, Åslund F, Storz G. Activation of the OxyR transcription factor by reversible disulfide bond formation. *Science*. Published online 1998. doi:10.1126/science.279.5357.1718

105. Liu Z, Yang M, Peterfreund GL, et al. Vibrio cholerae anaerobic induction of virulence gene expression is controlled by thiol-based switches of virulence regulator AphB. *Proc Natl Acad Sci*. 2011;108(2):810-815. doi:10.1073/pnas.1014640108

106. Ezraty B, Gennaris A, Barras F, Collet J-F. Oxidative stress, protein damage and repair in bacteria. *Nat Rev Microbiol*. 2017;15(7):385-396. doi:10.1038/nrmicro.2017.26

107. Lowther WT, Haynes AC. Reduction of Cysteine Sulfinic Acid in Eukaryotic, Typical 2-Cys Peroxiredoxins by Sulfiredoxin. *Antioxid Redox Signal*. 2011;15(1):99-109. doi:10.1089/ars.2010.3564

108. Stamler JS, Lamas S, Fang FC. Nitrosylation. *Cell*. 2001;106(6):675-683. doi:10.1016/S0092-8674(01)00495-0

109. Wong CM, Marcocci L, Liu L, Suzuki YJ. Cell Signaling by Protein Carbonylation and Decarbonylation. *Antioxid Redox Signal*. 2010;12(3):393-404. doi:10.1089/ars.2009.2805

110. Thomas JA, Park E-M, Chai Y-C, Brooks R, Rokutan K, Johnston RB. S-Thiolation of Protein Sulfhydryls. In: Witmer CM, Snyder RR, Jollow DJ, Kalf GF, Kocsis JJ, Sipes IG, eds. *Biological Reactive Intermediates IV*. Vol 283. Advances in Experimental Medicine and Biology. Springer New York; 1991:95-103. doi:10.1007/978-1-4684-5877-0_10

111. Loi VV, Rossius M, Antelmann H. Redox regulation by reversible protein S-thiolation in bacteria. *Front Microbiol*. 2015;6. doi:10.3389/fmicb.2015.00187

112. Antelmann H, Helmann JD. Thiol-Based Redox Switches and Gene Regulation. *Antioxid Redox Signal*. 2011;14(6):1049-1063. doi:10.1089/ars.2010.3400

113. Hillion M, Antelmann H. Thiol-based redox switches in prokaryotes. *Biol Chem*. 2015;396(5):415-444. doi:10.1515/hsz-2015-0102

114. Gupta A, Fuentes SM, Grove A. Redox-Sensitive MarR Homologue BifR from *Burkholderia thailandensis* Regulates Biofilm Formation. *Biochemistry*. 2017;56(17):2315-2327. doi:10.1021/acs.biochem.7b00103

115. Sun F, Liang H, Kong X, et al. Quorum-sensing agr mediates bacterial oxidation response via an intramolecular disulfide redox switch in the response regulator AgrA. *Proc Natl Acad Sci*. 2012;109(23):9095-9100. doi:10.1073/pnas.1200603109

116. Glanville DG, Han L, Maule AF, et al. RitR is an archetype for a novel family of redox sensors in the streptococci that has evolved from two-component response regulators and is required for pneumococcal colonization. Orihuela CJ, ed. *PLOS Pathog*. 2018;14(5):e1007052. doi:10.1371/journal.ppat.1007052

117. Ulijasz AT, Andes DR, Glasner JD, Weisblum B. Regulation of Iron Transport in Streptococcus pneumoniae by RitR, an Orphan Response Regulator. *J Bacteriol*. 2004;186(23):8123-8136. doi:10.1128/JB.186.23.8123-8136.2004

118. Szabo A, Langer T, Schroder H, Flanagan J, Bukau B, Hartl FU. The ATP hydrolysis-dependent reaction cycle of the Escherichia coli Hsp70 system DnaK, DnaJ, and GrpE. *Proc Natl Acad Sci*. 1994;91(22):10345-10349. doi:10.1073/pnas.91.22.10345

119. Zhang H, Yang J, Wu S, Gong W, Chen C, Perrett S. Glutathionylation of the Bacterial Hsp70 Chaperone DnaK Provides a Link between Oxidative Stress and the Heat Shock Response. *J Biol Chem*. 2016;291(13):6967-6981. doi:10.1074/jbc.M115.673608

120. Leichert LI, Gehrke F, Gudiseva HV, et al. Quantifying changes in the thiol redox proteome upon oxidative stress in vivo. *Proc Natl Acad Sci*. 2008;105(24):8197-8202. doi:10.1073/pnas.0707723105

121. Buxton RS, Drury LS, Curtis CAM. Dye Sensitivity Correlated with Envelope Protein Changes in dye (sfrA) Mutants of Escherichia coli K12 Defective in the Expression of the Sex Factor F. *Microbiology*. 1983;129(11):3363-3370. doi:10.1099/00221287-129-11-3363

122. Tuite EM, Kelly JM. New trends in photobiology. *J Photochem Photobiol B*. 1993;21(2-3):103-124. doi:10.1016/1011-1344(93)80173-7

123. Alvarez AF, Malpica R, Contreras M, Escamilla E, Georgellis D. Cytochrome d But Not Cytochrome o Rescues the Toluidine Blue Growth Sensitivity of arc Mutants of Escherichia coli. *J Bacteriol*. 2010;192(2):391-399. doi:10.1128/JB.00881-09

124. Pardo-Esté C, Hidalgo AA, Aguirre C, et al. The ArcAB two-component regulatory system promotes resistance to reactive oxygen species and systemic infection by Salmonella Typhimurium. Gerlach RG, ed. *PLOS ONE*. 2018;13(9):e0203497. doi:10.1371/journal.pone.0203497

125. Loui C, Chang AC, Lu S. Role of the ArcAB two-component system in the resistance of Escherichia coli to reactive oxygen stress. *BMC Microbiol*. 2009;9(1):183. doi:10.1186/1471-2180-9-183

126. Morales EH, Collao B, Desai PT, et al. Probing the ArcA regulon under aerobic/ROS conditions in Salmonella enterica serovar Typhimurium. *BMC Genomics*. 2013;14(1):626. doi:10.1186/1471-2164-14-626

127. Lasaro M, Liu Z, Bishar R, et al. Escherichia coli Isolate for Studying Colonization of the Mouse Intestine and Its Application to Two-Component Signaling Knockouts. *J Bacteriol*. 2014;196(9):1723-1732. doi:10.1128/JB.01296-13

128. Fu Y, Waldor MK, Mekalanos JJ. Tn-Seq Analysis of Vibrio cholerae Intestinal Colonization Reveals a Role for T6SS-Mediated Antibacterial Activity in the Host. *Cell Host Microbe*. 2013;14(6):652-663. doi:10.1016/j.chom.2013.11.001

129. Matson JS. Infant Mouse Model of Vibrio cholerae Infection and Colonization. In: Sikora AE, ed. *Vibrio Cholerae*. Vol 1839. Methods in Molecular Biology. Springer New York; 2018:147-152. doi:10.1007/978-1-4939-8685-9_13

130. Ouellette AJ, Greco RM, James M, Frederick D, Naftilan J, Fallon JT. Developmental regulation of cryptdin, a corticostatin/defensin precursor mRNA in mouse small intestinal crypt epithelium. *J Cell Biol*. 1989;108(5):1687-1695. doi:10.1083/jcb.108.5.1687

131. Gao R, Bouillet S, Stock AM. Structural Basis of Response Regulator Function. *Annu Rev Microbiol*. 2019;73(1):175-197. doi:10.1146/annurev-micro-020518-115931

132. Solà M, Gomis-Rüth FX, Serrano L, González A, Coll M. Three-dimensional crystal structure of the transcription factor PhoB receiver domain 1 1Edited by R. Huber. *J Mol Biol*. 1999;285(2):675-687. doi:10.1006/jmbi.1998.2326

133. Robinson VL, Wu T, Stock AM. Structural Analysis of the Domain Interface in DrrB, a Response Regulator of the OmpR/PhoB Subfamily. *J Bacteriol*. 2003;185(14):4186-4194. doi:10.1128/JB.185.14.4186-4194.2003

134. Toro-Roman A, Mack TR, Stock AM. Structural Analysis and Solution Studies of the Activated Regulatory Domain of the Response Regulator ArcA: A Symmetric Dimer Mediated by the α4-β5-α5 Face. *J Mol Biol*. 2005;349(1):11-26. doi:10.1016/j.jmb.2005.03.059

135. Gao R, Mack TR, Stock AM. Bacterial response regulators: versatile regulatory strategies from common domains. *Trends Biochem Sci*. 2007;32(5):225-234. doi:10.1016/j.tibs.2007.03.002

136. Maule AF, Wright DP, Weiner JJ, et al. The Aspartate-Less Receiver (ALR) Domains: Distribution, Structure and Function. Zhang G, ed. *PLOS Pathog*. 2015;11(4):e1004795. doi:10.1371/journal.ppat.1004795

137. Jeon Y, Lee YS, Han JS, Kim JB, Hwang DS. Multimerization of Phosphorylated and Non-phosphorylated ArcA Is Necessary for the Response Regulator Function of the Arc Two-component Signal Transduction System. *J Biol Chem*. 2001;276(44):40873-40879. doi:10.1074/jbc.M104855200

138. Park DM, Akhtar MdS, Ansari AZ, Landick R, Kiley PJ. The Bacterial Response Regulator ArcA Uses a Diverse Binding Site Architecture to Regulate Carbon Oxidation Globally. Burkholder WF, ed. *PLoS Genet*. 2013;9(10):e1003839. doi:10.1371/journal.pgen.1003839

139. Lynch AS, Lin EC. Transcriptional control mediated by the ArcA two-component response regulator protein of Escherichia coli: characterization of DNA binding at target promoters. *J Bacteriol*. 1996;178(21):6238-6249. doi:10.1128/JB.178.21.6238-6249.1996

140. Kinoshita E, Kinoshita-Kikuta E, Koike T. Separation and detection of large phosphoproteins using Phos-tag SDS-PAGE. *Nat Protoc*. 2009;4(10):1513-1521. doi:10.1038/nprot.2009.154

141. Cabezas CE, Laulié AM, Briones AC, et al. Activation of regulator ArcA in the presence of hypochlorite in Salmonella enterica serovar Typhimurium. *Biochimie*. 2021;180:178-185. doi:10.1016/j.biochi.2020.11.009

142. Karimova G, Pidoux J, Ullmann A, Ladant D. A bacterial two-hybrid system based on a reconstituted signal transduction pathway. *Proc Natl Acad Sci*. 1998;95(10):5752-5756. doi:10.1073/pnas.95.10.5752

143. Gumerov VM, Zhulin IB. TREND: a platform for exploring protein function in prokaryotes based on phylogenetic, domain architecture and gene neighborhood analyses. *Nucleic Acids Res*. 2020;48(W1):W72-W76. doi:10.1093/nar/gkaa243

144. Galán JE, Curtiss R. Expression of Salmonella typhimurium genes required for invasion is regulated by changes in DNA supercoiling. *Infect Immun*. 1990;58(6):1879-1885. doi:10.1128/IAI.58.6.1879-1885.1990

145. Guerrero P, Collao B, Álvarez R, et al. Salmonella enterica serovar Typhimurium BaeSR two-component system positively regulates sodA in response to ciprofloxacin. *Microbiology*. 2013;159(Pt_10):2049-2057. doi:10.1099/mic.0.066787-0

146. Dubbs JM, Mongkolsuk S. Peroxide-Sensing Transcriptional Regulators in Bacteria. *J Bacteriol*. 2012;194(20):5495-5503. doi:10.1128/JB.00304-12

147. Mey AR, Wyckoff EE, Kanukurthy V, Fisher CR, Payne SM. Iron and Fur Regulation in Vibrio cholerae and the Role of Fur in Virulence. *Infect Immun*. 2005;73(12):8167-8178. doi:10.1128/IAI.73.12.8167-8178.2005

148. Davies BW, Bogard RW, Mekalanos JJ. Mapping the regulon of Vibrio cholerae ferric uptake regulator expands its known network of gene regulation. *Proc Natl Acad Sci*. 2011;108(30):12467-12472. doi:10.1073/pnas.1107894108

149. Bagg A, Neilands JB. Ferric uptake regulation protein acts as a repressor, employing iron(II) as a cofactor to bind the operator of an iron transport operon in Escherichia coli. *Biochemistry*. 1987;26(17):5471-5477. doi:10.1021/bi00391a039

150. Zheng M, Doan B, Schneider TD, Storz G. OxyR and SoxRS regulation of fur. *J Bacteriol*. 1999;181(15):4639-4643. doi:10.1128/JB.181.15.4639-4643.1999

151. Varghese S, Wu A, Park S, Imlay KRC, Imlay JA. Submicromolar hydrogen peroxide disrupts the ability of Fur protein to control free-iron levels in Escherichia coli. *Mol Microbiol*. 2007;64(3):822-830. doi:10.1111/j.1365-2958.2007.05701.x

152. Kaper JB, Morris JG, Levine MM. Cholera. *Clin Microbiol Rev*. 1995;8(1):48-86. doi:10.1128/CMR.8.1.48-86.1995

153. Metcalf WW, Jiang W, Daniels LL, Kim SK, Haldimann A, Wanner BL. Conditionally replicative and conjugative plasmids carrying lacZ alpha for cloning, mutagenesis, and allele replacement in bacteria. *Plasmid*. 1996;35(1):1-13. doi:10.1006/plas.1996.0001

154. Hsiao A, Toscano K, Zhu J. Post-transcriptional cross-talk between pro- and anti-colonization pili biosynthesis systems in Vibrio cholerae: Pili biosynthesis systems in Vibrio cholerae. *Mol Microbiol*. 2007;67(4):849-860. doi:10.1111/j.1365-2958.2007.06091.x

155. Dalia AB, McDonough E, Camilli A. Multiplex genome editing by natural transformation. *Proc Natl Acad Sci*. 2014;111(24):8937-8942. doi:10.1073/pnas.1406478111

156. Datsenko KA, Wanner BL. One-step inactivation of chromosomal genes in Escherichia coli K-12 using PCR products. *Proc Natl Acad Sci U S A*. 2000;97(12):6640-6645. doi:10.1073/pnas.120163297

157. Guo J, Gaffrey MJ, Su D, et al. Resin-assisted enrichment of thiols as a general strategy for proteomic profiling of cysteine-based reversible modifications. *Nat Protoc*. 2014;9(1):64-75. doi:10.1038/nprot.2013.161

158. Wholey W-Y, Jakob U. Hsp33 confers bleach resistance by protecting elongation factor Tu against oxidative degradation in Vibrio cholerae: Elongation factor EF-Tu - a central target protein of Hsp33. *Mol Microbiol*. 2012;83(5):981-991. doi:10.1111/j.1365-2958.2012.07982.x

159. Hsiao A, Xu X, Kan B, Kulkarni RV, Zhu J. Direct Regulation by the Vibrio cholerae Regulator ToxT To Modulate Colonization and Anticolonization Pilus Expression. *Infect Immun*. 2009;77(4):1383-1388. doi:10.1128/IAI.01156-08

160. Xia X, Larios-Valencia J, Liu Z, et al. OxyR-activated expression of Dps is important for Vibrio cholerae oxidative stress resistance and pathogenesis. Volkert MR, ed. *PLOS ONE*. 2017;12(2):e0171201. doi:10.1371/journal.pone.0171201

161. Chung CT, Miller RH. [43] Preparation and storage of competent Escherichia coli cells. In: *Methods in Enzymology*. Vol 218. Elsevier; 1993:621-627. doi:10.1016/0076-6879(93)18045-E

162. Thibodeau SA, Fang R, Joung JK. High-throughput β-galactosidase assay for bacterial cell-based reporter systems. *BioTechniques*. 2004;36(3):410-415. doi:10.2144/04363BM07

163. Joelsson A, Liu Z, Zhu J. Genetic and phenotypic diversity of quorum-sensing systems in clinical and environmental isolates of Vibrio cholerae. *Infect Immun*. 2006;74(2):1141-1147. doi:10.1128/IAI.74.2.1141-1147.2006

164. Liu Z, Miyashiro T, Tsou A, Hsiao A, Goulian M, Zhu J. Mucosal penetration primes Vibrio cholerae for host colonization by repressing quorum sensing. *Proc Natl Acad Sci U S A*. 2008;105(28):9769-9774. doi:10.1073/pnas.0802241105

165. Reyes Ruiz VM, Ramirez J, Naseer N, et al. Broad detection of bacterial type III secretion system and flagellin proteins by the human NAIP/NLRC4 inflammasome. *Proc Natl Acad Sci*. 2017;114(50):13242-13247. doi:10.1073/pnas.1710433114

166. Mo CY, Culyba MJ, Selwood T, et al. Inhibitors of LexA Autoproteolysis and the Bacterial SOS Response Discovered by an Academic–Industry Partnership. *ACS Infect Dis*. 2018;4(3):349-359. doi:10.1021/acsinfecdis.7b00122

167. Hsiao A, Liu Z, Joelsson A, Zhu J. Vibrio cholerae virulence regulator-coordinated evasion of host immunity. *Proc Natl Acad Sci*. 2006;103(39):14542-14547. doi:10.1073/pnas.0604650103

168. Guzman LM, Belin D, Carson MJ, Beckwith J. Tight regulation, modulation, and high-level expression by vectors containing the arabinose PBAD promoter. *J Bacteriol*. 1995;177(14):4121-4130. doi:10.1128/JB.177.14.4121-4130.1995

169. Khan SR, Gaines J, Roop RM, Farrand SK. Broad-Host-Range Expression Vectors with Tightly Regulated Promoters and Their Use To Examine the Influence of TraR and TraM Expression on Ti Plasmid Quorum Sensing. *Appl Environ Microbiol*. 2008;74(16):5053-5062. doi:10.1128/AEM.01098-08